INVESTIGATING THE SEMILEPTONIC B TO $K_1(1270, 1400)$ DECAYS IN QCD SUM RULES

A THESIS SUBMITTED TO
THE GRADUATE SCHOOL OF NATURAL AND APPLIED SCIENCES
OF
MIDDLE EAST TECHNICAL UNIVERSITY

BY

HÜSEYİN DAĞ

IN PARTIAL FULFILLMENT OF THE REQUIREMENTS
FOR
THE DEGREE OF DOCTOR OF PHILOSOPHY
IN
PHYSICS

FEBRUARY 2010

Approval of the thesis:

INVESTIGATING THE SEMILEPTONIC B TO $K_1(1270, 1400)$ DECAYS IN QCD SUM RULES

submitted by **HÜSEYİN DAĞ** in partial fulfillment of the requirements for the degree of **Doctor of Philosophy in Physics Department, Middle East Technical University** by,

Prof. Dr. Canan Özgen
Dean, Graduate School of **Natural and Applied Sciences** ________________

Prof. Dr. Sinan Bilikmen
Head of Department, **Physics** ________________

Prof. Dr. Mehmet T. Zeyrek
Supervisor, **Physics Department, METU** ________________

Examining Committee Members:

Prof. Dr. Müge Boz Evinay
Department of Physics Engineering, Hacettepe University ________________

Prof. Dr. Mehmet T. Zeyrek
Department of Physics, METU ________________

Prof. Dr. Ali Ulvi Yılmazer
Department of Physics Engineering, Ankara University ________________

Prof. Dr. Meltem Serin
Department of Physics, METU ________________

Assoc. Prof. Dr. Altuğ Özpineci
Department of Physics, METU ________________

Date: ________________

I hereby declare that all information in this document has been obtained and presented in accordance with academic rules and ethical conduct. I also declare that, as required by these rules and conduct, I have fully cited and referenced all material and results that are not original to this work.

Name, Last Name: HÜSEYİN DAĞ

Signature :

ABSTRACT

INVESTIGATING THE SEMILEPTONIC B TO $K_1(1270, 1400)$ DECAYS IN QCD SUM RULES

Dağ, Hüseyin

Ph.D., Department of Physics

Supervisor : Prof. Dr. Mehmet T. Zeyrek

February 2010, 83 pages

Quantum Chromodynamics(QCD) is part of the Standard Model(SM) that describes the interaction of fundamental particles. In QCD, due to the fact that strong coupling constant is large at low energies, perturbative approaches do not work. For this reason, non-perturbative approaches have to be used for studying the properties of hadrons. Among several non-perturbative approaches, QCD sum rules is one of the reliable methods which is applied to understand the properties of hadrons and their interactions.

In this thesis, the semileptonic rare decays of B meson to $K_1(1270)$ and $K_1(1400)$ are analyzed in the framework of three point QCD sum rules approach. The $B \to K_1(1270, 1400)\ell^+\ell^-$ decays are significant flavor changing neutral current (FCNC) decays of the B meson, since FCNC processes are forbidden at tree level at SM. These decays are sensitive to the new physics beyond SM. The radiative $B \to K_1(1270)\gamma$ decay is observed experimentally. Although semileptonic $B \to K_1(1270, 1400)$ decays are still not observed, they are expected to be observed at future B factories. These decays happens at the quark level with $b \to s\ell^+\ell^-$

transition, providing new opportunities for calculating CKM matrix elements: V_{tb} and V_{ts}.

Applying three point QCD sum rules to $B \rightarrow K_1(1270, 1400)\ell^+\ell^-$ decays is tricky, due to the fact that the $K_1(1270)$ and $K_1(1400)$ states are the mixtures of ideal ${}^3P_1(K_1^A)$ and ${}^1P_1(K_1^B)$ orbital angular momentum states. First, by taking axial vector and tensor current definitions for K_1 mesons, the transition form factors of $B \rightarrow K_{1A}\ell^+\ell^-$ and $B \rightarrow K_{1B}\ell^+\ell^-$ are calculated. Then using the definitions for K_1 mixing, the transition form factors of $B \rightarrow K_1(1270, 1400)\ell^+\ell^-$ decays are obtained. The results of these form factors are used to estimate the branching ratio of B meson into $K_1(1270)$ and $K_1(1400)$. The results obtained for form factors and branching fractions are also compared with the ones in the literature.

Keywords: Non-perturbative approaches, QCD sum rules, form factors, B meson.

ÖZ

QCD TOPLAMA KURALLARI ÇERÇEVESİNDE B MEZONUNUN YARI LEPTONİK $K_1(1270, 1400)$ GEÇİŞLERİNİN İNCELENMESİ

Dağ, Hüseyin

Doktora, Fizik Bölümü

Tez Yöneticisi : Prof. Dr. Mehmet Zeyrek

Şubat 2010, 83 sayfa

Kuvantum Renk Dinamiği(KRD), temel parçacık etkieşmelerini açıklayan Standart Model'in(SM) bir parçasıdır. KRD'de kuvvetli etkileşim kuplaj sabitinin düşük enerjilerde büyük olmasından dolayı, hadronlar ve özellikleri tedirgemeli yaklaşımlar ile çalışılamamaktadır. Bu sebeple hadronlar incelenirken tedirgemesiz yaklaşımlar kullanılmalıdır. Kuantum renk dinamiği (KRD) toplam kuralları, diğer tedirgemesiz yaklaşımlar arasında güvenilirliği olan bir metod olarak, hadronların özellikleri ve etkileşmelerinin çalışılmasında kullanılmaktadır.

Bu tezde B mesonunun yarı leptonik ve nadir gorulen $K_1(1270)$ ve $K_1(1400)$ geçişleri, üç nokta KRD toplama kuralları yaklaşımı kullanılarak hesaplandı. $B \to K_1(1270, 1400)\ell^+\ell^-$ geçişleri, B mezonun çeşni değiştiren nötür akımlar vasıtasıyla gerçekleştirdiği geçişler arasında önemli bir yer tutar ve standart model ötesi teorilerin etkilerinin gözlemlenmesi açısından önem arzetmektedir. Ayrıca bu geçişler KRD de ağaç seviyesinde görülmemektedirler. Tüm bunlara ilave olarak, $B \to K_1(1270)\gamma$ geçişleri deneysel olarak gözlemlenmiş olmasına rağmen $B \to K_1(1270)\ell^+\ell^-$ ve $B \to K_1(1400)\ell^+\ell^-$ henüz gözlemlenmemişlerdir. Bu geçişleri

gelecekteki B mezon üreteçlerinde gözlemlenmeleri beklenmektedir. Bu geçişler kuark seviyesinde $b \to s\ell^+\ell^-$ geçişi ile açıklanmakta olup, CKM matrix elemanlarından V_{tb} ve V_{ts} nin anlaşılmaları açısından da önem arz etmektedirler.

KRD toplama kuralları kullanılarak $B \to K_1(1270, 1400)\ell^+\ell^-$ bozunumlarını çalışmak incelikli bir uygulamadır. Çünkü $K_1(1270)$ ve $K_1(1400)$ aksiyel vektör mezonları aslında ideal $^3P_1(K_1^A)$ ve $^1P_1(K_1^B)$ açısal momentum durumlarının karışımlarından oluşmaktadırlar. Dolayısı ile KRD toplama kurallarında aksiyel vector ve tensör akımları kullanılarak iki ayrı ilişkilendirici fonksiyonu hesaplanmalıdır. Bu hesaplar sonucunda önce $B \to K_{1A}\ell^+\ell^-$ ve $B \to K_{1B}\ell^+\ell^-$ bozunumlarının bozunum katsayıları ve ardından karışım tanımı kullanılarak $B \to K_1\ (1270, 1400)\ell^+\ell^-$ geçişlerinin bozunum katsayıları bulunmuştur. Bu bozunum katsayıları kullanılarak bu geçişlerin oranları hesaplanmış ve literatürdeki değerlerle karşılaştırılmıştır.

Anahtar Kelimeler: tedirgemesiz yaklaşımlar, KRD toplama kuralları, yapı faktörleri, B mezonu.

to my family

ACKNOWLEDGMENTS

I am deeply thankful to my supervisor Prof. Dr. Mehmet T. Zeyrek, not only for his guidance, help and support during this thesis but also for accepting me as a Ph. D. student and encouraging me with his friendly and wise attitude. I also thank to Prof. Dr. Takhmasib M. Aliev, for introducing an interesting problem and his helps.

I specially thank to Assoc. Prof. Dr. Altuğ Özpineci, for his guidance, for his endless efforts for teaching, and for the invaluable scientific discussions. He became a mentor to me during these PhD. I thank to Assist. Prof Dr. Güray Erkol for very useful discussions on general philosophy of QCD sum rules. I also thank to Assist. Prof. Dr. Kazem Azizi for the useful tips and discussions.

I finally but not lastly, thank to my family, for every sacrifice that they made at every stage of my life.

Very special thanks is for A. Çağıl, for supporting me at every stage of this PhD, for sharing her splendid scientific view, and mostly for making life bearable to me when things get really challenging.

TABLE OF CONTENTS

LIST OF TABLES

TABLES

LIST OF FIGURES

FIGURES

CHAPTER 1

INTRODUCTION

The Standard Model (SM), which is a $SU(3)_c \otimes SU(2)_L \otimes U(1)_Y$ gauge theory of electroweak and the strong interactions, explains the experimental data with a good consistency. However it should be extended to explain problems like unification, hierarchy problem, origin of matter in the universe, and so on. In SM, fundamental particles are leptons and quarks which interact through the exchange of gauge bosons. These gauge bosons are: gluons mediating strong force, $W^{\pm}$ and Z^0 bosons mediating weak force and the photon A_μ mediating electromagnetic force.

Quantum chromodynamics (QCD) is the theory of the strong interactions and it describes the strong interactions of quarks and gluons. In QCD, it is believed that the potential energy between quarks does not vanish when the distance between them is increased, the energy required to separate them also increases, due to the gluons connecting them. This phenomena is called confinement. Due to confinement, quarks are bound into hadrons. On the other hand, for very high energies, or very short distances, quarks move almost free. This phenomena is called as asymptotic freedom. These two phenomenons characterize the behavior of QCD. At large energies (or short distances) perturbation theory can be used. On the other hand, for low energies (or large separations), such as the hadronic scales, due to the value of the effective strong coupling constant, perturbation theory does not work. In this regime, a non-perturbative approach is needed.

Some non-perturbative methods can be listed as: QCD sum rules and light cone QCD sum rules(LCQSR)[1, 2, 3, 4, 5, 6], the lattice QCD[7], heavy quark effective theory(HQET)[8], covariant light-front quark model[9], QCD factorization[10], low energy effective theory(LEET)[11], chiral perturbation theory(ChPT)[12], and AdS-QCD or the so called holographic QCD[13]. Among these methods, the main advantage of QCD sum rules is that it is based on fundamental QCD lagrangian. In QCD sum rules, hadrons are interpreted by their model independent interpolating currents. The QCD sum rules are discussed in many reviews [4, 5, 6, 14, 15, 16, 17, 18, 19, 20, 21, 22, 23] emphasizing the various aspects of the method.

In this thesis, the semileptonic $B \to K_1(1270, 1400)\ell^+\ell^-$ decays are analyzed. These decays are characteristic flavor changing neutral current (FCNC) decays of B meson which are forbidden at tree level and occur only at loop level. These decays are good candidates for searching new physics (NP) beyond SM or the modifications on the SM. Some of these rare FCNC decays of B meson; radiative and semileptonic decays into a vector or an axial vector meson, such as $B \to K^*(892)\gamma$ [24, 25, 26], $B \to K_1(1270, 1400)\gamma$[27] and $B \to K^{0*}(892)e^+e^-(\mu^+\mu^-)$[28, 29] have been observed. For the channel $B \to K^*(892)\ell^+\ell^-$, the measurement of isospin and forward backward asymmetries at BaBar are also reported[30, 31, 32]. The radiative decays of B meson to $K_1(1270, 1400)$ axial vector meson states are also observed at Belle[33]. The semileptonic decay modes $B \to K_1(1270, 1400)\ell^+\ell^-$ have not been observed yet, but are expected to be observed in forthcoming pp and e^+e^- accelerators, such as LHC[34, 35] and SuperB[36]. Recently, some studies on $B \to K_1(1270, 1400)\ell^+\ell^-$ decays have been made[37, 38, 39, 40, 41, 42, 43, 44, 45].

In chapter 2, the QCD sum rules method is reviewed following Refs. [20, 21, 22]. First a general derivation for QCD sum rules is discussed using a two point correlator function. Then, three point QCD sum rules is discussed.

In chapter 3, the properties of axial vector K_1 mesons are analyzed. In section 2.1, the classification of mesons in terms of their quantum numbers is reviewed. In section 2.2, the mixing between K_1 states is described. And also in this section, application of QCD sum rules to K_1 mesons is discussed.

In chapter 4, the semileptonic $B \to K_1(1270, 1400)\ell^+\ell^-$ decays are examined in the framework of three-point QCD sum rules. Since, the $K_1(1270, 1400)$ states are combination of $K_{1(A,B)}$ states, firstly, sum rules for the form factors of $B \to K_{1(A,B)}\ell^+\ell^-$ decays are derived. From these sum rules, the q^2 dependance of form factors of $B \to K_1(1270, 1400)\ell^+\ell^-$ decays are obtained. Using these results, the branching fractions to e^+e^-, $\mu^+\mu^-$ and $\tau^+\tau^-$ leptonic final states are estimated. Chapter 5 includes the summary and conclusions.

CHAPTER 2

QCD SUM RULES

2.1 Introduction

The QCD sum rules, proposed in 1979 by Shifman, Vainsthein and Zakharov (SVZ)[1], is one of the most applicable tools in studying the properties of hadrons. Among other non-perturbative methods, the main power of QCD sum rules approach and its extensions is the analyticity of the methods. In this method a connection between the low energy processes and the non-trivial QCD vacuum via quark ($\langle \bar{q}q \rangle$), quark-gluon ($\langle \bar{q}\sigma Gq \rangle$), gluon ($\langle g^2G^2 \rangle$) and other higher order condensates is established.

In QCD sum rules approach, hadrons are represented by their interpolating quark currents. The main object of QCDSR is the correlation of these interpolating currents. This correlator is calculated both in terms of hadronic properties and also using operator product expansion(OPE), where the short and long distance quark gluon interactions are separated.

The short distance interactions are calculated using QCD perturbation theory and the long distance interactions are parameterized in terms of vacuum condensates. In general, calculating the correlation function within the framework of OPE is called the QCD or the theoretical side of the correlation function.

In this method, the correlation function is also calculated by inserting a complete set of hadronic states, where hadrons are treated as point-like objects characterized by their hadronic properties such as leptonic decay constants and masses. This hadronic approach in calculating the correlation function is commonly named as the phenomenological or physical side of the calculations.

The results of these two representations of the correlation function, i.e., the QCD side and the phenomenological side, is matched via dispersion relation and the sum rules are found. From these sum rules, the physical quantities of the hadrons such as form factors, decay constants and the masses can be achieved.

In this chapter, the basics of the QCD sum rules approach are reviewed following references [20, 21, 22]. Some missing intermediate steps and detailed calculations can be found in [22].

2.2 The QCD Sum Rules Approach

2.2.1 The Correlation Function

In studying QCD, it is commonly believed that the QCD lagrangian explains properties of hadrons and hadronic processes and is given by

$$\mathcal{L}_{QCD} = -\frac{1}{4}G^a_{\mu\nu}G^{a\mu\nu} + \sum_q \bar{\psi}_q(i\not{D} - m_q)\psi_q, \tag{2.1}$$

where $G^a_{\mu\nu}$ is the gluon field-strength tensor and ψ_q are the quark fields with different flavors $q = u, d, c, s, t, b$. The QCD lagrangian in Eq.2.1 is applicable either within the frame work of perturbation theory or some non-perturbative approaches. The perturbation theory is applicable only when the effective quark-gluon coupling $\alpha_s = g_s^2/4\pi$ is small. For studying the QCD dynamics at distances of the order of hadron size, i.e., $R_{hadr} \sim 1/\Lambda_{QCD}$, an expansion in terms of α_s and so the perturbation theory is not applicable. Calculation in these large separations are done by non-perturbative approaches like QCD sum rules.

In QCD sum rules, the processes are considered with no initial and final hadrons, i.e., quarks are injected in QCD vacuum at the space time point $x = 0$ and their space-time evolution is studied. This is described by the main object of the QCD sum rules approach, which is the correlation function (or alternatively correlator):

$$\Pi(q^2) = i\int d^4x\, e^{iq\cdot x}\langle 0|\, \mathcal{T}\{j(x)\bar{j}(0)\}\, |0\rangle, \tag{2.2}$$

where q is the momentum of the quarks, $j(x)$ is the quark current that injects quarks into the QCD vacuum at point x and $\mathcal{T}$ is the time ordering operator which acts as

$$\mathcal{T}\{j(x)\bar{j}(0)\} = \Theta(x-0)\,j(x)\bar{j}(0) + C\Theta(0-x)\bar{j}(0)\,j(x) \tag{2.3}$$

where $\Theta(x)$ is the unit step function and $C = +1(-1)$ for bosonic(fermionic) operators. The correlation function in Eq. 2.2 is called the two point correlation function and leads to the mass sum rules.

The q^2 behavior of the correlator is the starting point of the QCD sum rules. The correlator in Eq.2.2 is an analytic function of q^2 defined at both positive(timelike) and negative(spacelike) values of q^2. For $q^2 > 0$, the quarks move to larger spatial distances and for sufficiently large positive values of q^2 they start to form hadrons. In this regime, the correlator in Eq. 2.2 is calculated in terms of hadron language. These calculations are called the phenomenological or the physical part of the QCD sum rules. For large and negative values of q^2 i.e., $\Lambda^2_{QCD} << Q^2 \equiv -q^2$, the main contribution to correlator comes from short spatial distances and short times[20]. Therefore, in this regime the correlator can be calculated in terms of quarks and gluons interacting with QCD vacuum.

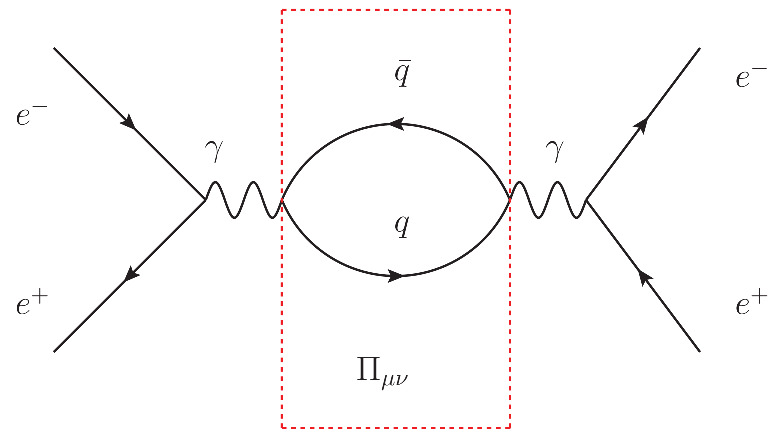

Figure 2.1: The quark-antiquark creation and annihilation at electron scattering processes. This propagation can be considered as a representation for the propagator $\Pi_{\mu\nu}$.

The correlator functions are not completely hypothetical configurations. They are realized in nature when a quark-antiquark pair is produced and absorbed by an external source[20]. For instance, at an electron electron scattering process, such quark-antiquark pairs are produced and absorbed by a virtual photon. The intermediate propagation of the quark antiquark pair may be considered as the correlation function, when it is taken separately as in Fig.2.1. In this case the correlator function should carry the Lorentz indices of the incoming and outgoing virtual photon.

2.2.2 The Phenomenological Side

In this subsection, the representation of the correlator function in terms of hadronic states in the $q^2 > 0$ regime will be analyzed. The correlator function in Eq. 2.2, can be saturated by inserting the complete set of hadronic states which has the same quantum numbers of the interpolating currents. The correlator can be written as

$$\Pi(q^2) = i\int d^4x\, e^{iq\cdot x}\langle 0|\,\mathcal{T}\{j(x)\,\mathbb{1}\,\bar{j}(0)\}\,|0\rangle, \tag{2.4}$$

where the unitary operator can be written as

$$\begin{aligned}\mathbb{1} &= \sum_h |h\rangle\langle h| \\ &= |0\rangle\langle 0| + \sum_h \int \frac{d^4k}{(2\pi)^4} 2\pi\delta(k^2 - m_h^2)|h(k)\rangle\langle h(k)| + \text{higher states},\end{aligned} \tag{2.5}$$

where $h(k)$ is the hadron with mass m_h and momentum k. Inserting Eq.2.5 in 2.4 gives

$$\begin{aligned}\Pi(q^2) = i\int d^4x\, e^{iq\cdot x}\{ & \\ & \langle 0|j(x)|0\rangle\langle 0|\bar{j}(0)|0\rangle\Theta(x_0) + \langle 0|\bar{j}(0)|0\rangle\langle 0|j(x)|0\rangle\Theta(-x_0) \\ & + \int \frac{d^4k}{(2\pi)^4}\sum_h \Theta(k_0)2\pi\delta(k^2 - m_h^2)[\langle 0|j(x)|h(k)\rangle\langle h(k)|\bar{j}(0)|0\rangle\Theta(x_0) \\ & \quad +\langle 0|\bar{j}(0)|h(k)\rangle\langle h(k)|j(x)|0\rangle\Theta(-x_0)]\}.\end{aligned} \tag{2.6}$$

The first two terms in Eq.2.6 vanish since the matrix elements $\langle 0|j(x)|0\rangle$ and $\langle 0|\bar{j}(0)|0\rangle$ are zero[1]. The matrix elements $\langle 0|\bar{j}(x)|h(k)\rangle$ and $\langle h(k)|j(x)|0\rangle$ are calculated by inserting the evolution of the operator $j(x)$ as

$$\begin{aligned}\langle 0|j(x)|h(k)\rangle &= \langle 0|e^{-iPx}j(0)e^{iPx}|h(k)\rangle \\ &= \langle 0|j(0)e^{ikx}|h(k)\rangle = e^{ikx}\langle 0|j(0)|h(k)\rangle, \\ \langle h(k)|j(x)|0\rangle &= e^{-ikx}\langle h(k)|j(0)|0\rangle,\end{aligned} \tag{2.7}$$

[1] If the current $j(x)$ has the quantum numbers of the vacuum, then these matrix elements might not be zero. But in this case, the integral will be proportional to $(2pi)^2 delta^4(q)$ which is zero if q is different from zero.

the correlator takes the form

$$\begin{aligned}\Pi(q^2) &= i\int d^4x\, e^{iq\cdot x}\{\int \frac{d^4k}{(2\pi)^4}\sum_h \Theta(k_0)2\pi\delta(k^2-m_h^2) \\ &\quad [e^{ikx}\langle 0|j(0)|h(k)\rangle\langle h(k)|\bar{j}(0)|0\rangle\Theta(x_0) \\ &\quad +e^{-ikx}\langle 0|\bar{j}(0)|h(k)\rangle\langle h(k)|j(0)|0\rangle\Theta(-x_0)]\}. \end{aligned} \tag{2.8}$$

When the integrals with respect to $\overrightarrow{k}$ and $\overrightarrow{x}$ are evaluated, Eq.2.8 becomes

$$\begin{aligned}\Pi(q^2) &= i\sum_h \int_0^\infty dk_0\delta(k_0^2-E_h^2)\int dx_0 \\ &\quad [e^{i(q_0+k_0)x_0}\langle 0|j(0)|h(k_0,-\overrightarrow{q})\rangle\langle h(k_0,-\overrightarrow{q})|\bar{j}(0)|0\rangle\Theta(x_0) \\ &\quad +e^{-i(k_0-p_0)x_0}\langle 0|\bar{j}(0)|h(k_0,\overrightarrow{q})\rangle\langle h(k_0,\overrightarrow{q})|j(0)|0\rangle\Theta(-x_0)]. \end{aligned} \tag{2.9}$$

The last two integrals in Eq. 2.9 are taken as follows. The integral with respect to k_0 is simply handled by using the delta function property

$$\delta(f(x)) = \sum_{x_0}\frac{\delta(x-x_0)}{|f'(x_0)|}, \tag{2.10}$$

where $f(x_0) = 0$ and $f' = \frac{df}{dx}$. The second integral with respect to x_0 is taken by adding a small imaginary part to E_h to assure convergence, i.e., $E_h \to E_h + i\epsilon$. These calculations yield

$$\Pi(q^2) = i2\pi\sum_h\left[\frac{|\langle 0|j(0)|h(-\overrightarrow{q})\rangle|^2}{2E_h(-\overrightarrow{q})\left(q_0+E_h(-\overrightarrow{q})+i\epsilon\right)} + \frac{|\langle 0|j(0)|h(\overrightarrow{q})\rangle|^2}{2E_h(\overrightarrow{q})\left(q_0-E_h(\overrightarrow{q})-i\epsilon\right)}\right]. \tag{2.11}$$

For $q^2 > 0$, there exist a frame in which $\overrightarrow{q} = 0$. So the numerators of the two terms in Eq. 2.11 are equal and can be added. Finally, by taking $\epsilon \to 0$, the correlator is found as

$$\Pi(q^2) = \sum_h\frac{|\langle 0|j(0)|h(\overrightarrow{q})\rangle|^2}{q^2-m_h^2} + \dots\ . \tag{2.12}$$

In Eq. 2.12, the sum goes over all possible hadronic states, i.e. the full hadronic tower, and each individual state h contributes to the correlation function. In terms of these states a more compact and useful notation can be introduced as

$$\Pi(q^2) = \frac{f_H^2}{q^2-m_H^2} + \Pi^h(q^2), \tag{2.13}$$

where H is the ground state hadron (or hadron with the smallest mass that can be created by current j), $f_H \equiv \langle 0|j(0)|H(q)\rangle$ is the leptonic decay constant, $\Pi^h(q^2)$ denotes the contributions of the higher states and continuum.

2.2.3 The QCD side and the Operator Product Expansion

The correlation function in Eq. 2.2 can also be calculated in terms of quarks, gluons and their interactions with QCD vacuum in the region: $-q^2 = Q^2 >> \Lambda^2_{QCD}$, the so called deep Euclidean region. This is done by using operator product expansion (OPE) which states that the time ordered product of two currents at different points can be expanded as the sum of local operators with space time coefficients as

$$T\{j(x)\bar{j}(0)\} = \sum_d C_d(x^2) O_d, \tag{2.14}$$

where, $C_d(x^2)$ are Wilson coefficients and O_d are a set of local operators ordered according to their dimensions(d). In QCD sum rules, the vacuum expectation value of Eq. 2.14 is needed. Since vacuum is colorless, gauge and Lorentz invariant, only colorless, gauge and Lorentz invariant operators can contribute. In QCD there are no colorless, gauge and Lorentz invariant operators with dimensions $d = 1, 2$. The operators up to $d = 6$ can be listed as

$$\begin{aligned}
O_0 &= \mathbb{1}, \\
O_3 &= \bar{\psi}\psi, \\
O_4 &= G^a_{\mu\nu} G^{a\mu\nu}, \\
O_5 &= \bar{\psi}\sigma_{\mu\nu}\frac{\lambda^a}{2} G^{a\mu\nu}\psi\,, \\
O_6^{\psi} &= (\bar{\psi}\Gamma\psi)(\bar{\psi}\Gamma\psi)\,, \\
O_6^{G} &= f_{abc} G^a_{\mu\nu} G^{b\,\nu}_{\sigma} G^{c\sigma\mu},
\end{aligned} \tag{2.15}$$

where ψ is the wave function of any quark field, Γ and Γ' denote the various combinations of Lorentz and color matrices. In terms of OPE, the correlator in Eq. 2.2 takes the form

$$\Pi^{OPE}(q^2) = \sum_d C_d(x^2)\langle O_d\rangle. \tag{2.16}$$

For $d = 0$, the coefficient $C_0(x^2)$ associated with the perturbative contributions to the correlator. For $d = 3, 4, ...,$ the operators $\langle O_d\rangle \equiv \langle 0|O_d|0\rangle$ form a set of vacuum condensates which parameterize the non-perturbative effects.

In order to calculate the Wilson coefficients, the current $j(x)$ in the definition of the correlation function in Eq. 2.2 should be known. For a general current of the form

$$j(x) = \bar{q}'(x) i\Gamma q(x) \tag{2.17}$$

where $q = u, d, s$ is one of the light quarks, $q' = b, c, t$ is one of the heavy quarks, and Γ is the matrix carrying Lorentz indices. The current defined in Eq. 2.17 creates the hadron $H \equiv \bar{q}q'$ and the excited states carrying the same quantum numbers of H.

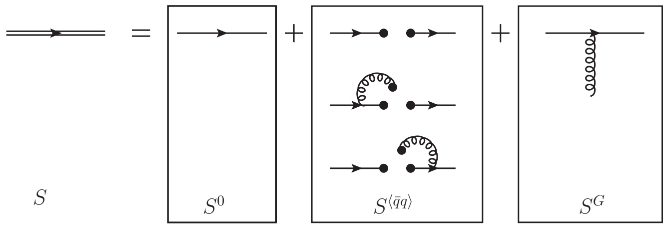

Figure 2.2: Diagrammatic representation of the full quark propagator. For $q = b, c, t$, the second term $S^{\langle\bar{q}q\rangle}$ vanish.

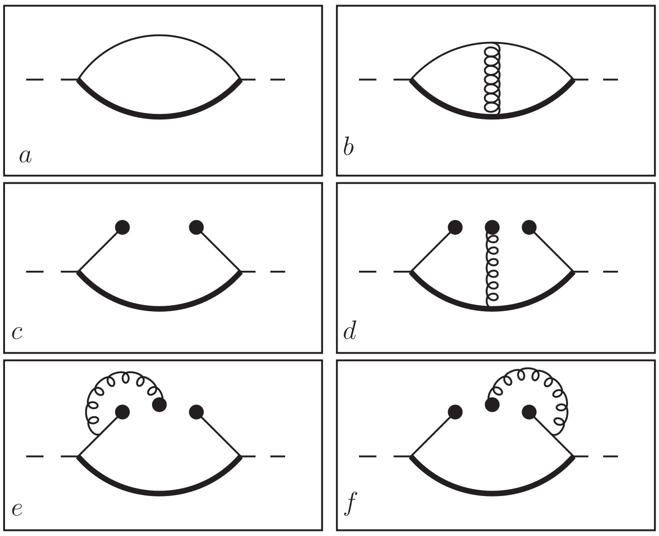

Figure 2.3: The Feynman diagram representations of the operators contributing the correlator $\Pi(q^2)$. The dashed lines denote the currents, thin(thick) solid lines denote the light(heavy) quark, and the spirals correspond to soft gluons.

The Wilson coefficients in Eq. 2.16 can be calculated either one-by-one, or more elegantly, by introducing the full quark propagator with both perturbative and non-perturbative contributions which is defined as

$$iS_q^{ab}(x-y) = \langle 0|\mathcal{T}\bar{q}^a(x)q^b(y)|0\rangle \tag{2.18}$$

where a, b are the color indices. The full quark propagator can be written in terms of perturbative and non-perturbative contributions as

$$S_q^{ab}(x) = S_q^{0,ab}(x) + S_q^{\langle\bar{q}q\rangle,ab}(x) + S_q^{G,ab}(x), \tag{2.19}$$

where

$$S_q^{0,ab}(x) = \delta^{ab}\int \frac{d^4k}{(2\pi)^4} e^{-ikx}\frac{\not{k}+m_q}{k^2-m_q^2}, \tag{2.20}$$

$$S_q^{\langle\bar{q}q\rangle,ab}(x) = i\delta^{ab}\left(\frac{\langle\bar{q}q\rangle}{12}\left(1-\frac{im_q\ \not{x}}{4}\right)+\frac{m_0^2x^2\langle\bar{q}q\rangle}{192}\left(1-\frac{im_q\ \not{x}}{6}\right)\right), \tag{2.21}$$

$$S_q^{G,ab}(x) = g_s\int \frac{d^4k}{(2\pi)^4} e^{-ikx}\left(\frac{\not{k}+m_q}{(k^2-m_q^2)^2}G^{ab}_{\mu\nu}\sigma^{\mu\nu} - \frac{1}{2(k^2-m_q^2)}x^\mu G^{ab}_{\mu\nu}\gamma^\nu\right), \tag{2.22}$$

for light quarks($q = u, d, s$). The full propagator for the heavy quarks does not have quark condensate terms, so for heavy quarks $S_{q'}^{\langle\bar{q}'q'\rangle,ab}(x) = 0$. Here the propagator in position space is given as the Fourier transform of the propagator in momentum space(Eqs. 2.20 and 2.22). The explicit expressions in position space are given and discussed in Ref. [21]. In Eq. 2.21, m_0 is defined through the relation $\langle\bar{q}\sigma Gq\rangle = m_0^2\langle\bar{q}q\rangle$. The diagrammatic representation of Eq. 2.19 is depicted in figure 2.2.

In Fig. 2.3, the OPE contributions to the correlator function is represented in a diagrammatic form. Diagrams 2.3-a and 2.3-b are perturbative contributions to the correlator, corresponding to the identity operator with $d = 0$ in the OPE. The non-perturbative contributions to the correlator are depicted in diagrams 2.3-c to 2.3-f. Diagram 2.3-c correspond to the $d = 3$ operator $\langle\bar{q}q\rangle$, quark condensate for the light quark. Diagrams 2.3-d to 2.3-f represents the contributions of the $d = 5$ operator $\langle\bar{q}\sigma Gq\rangle$. There are no diagrams for $d = 3$ contributions of the condensate $\langle\bar{q}'q'\rangle$, because the heavy quarks do not develop a condensate in vacuum due to their large mass.

Inserting the definition of the current given in Eq. 2.17, and using the Wick theorem, the correlator function in Eq. 2.2 can be written in terms of propagators as

$$\Pi^{OPE}(q^2) = -i\int d^4x e^{iqx}\mathrm{Tr}\{\Gamma S_q(x)\Gamma S_{q'}(-x)\}, \tag{2.23}$$

where color indices are not written for simplicity. The correlator in QCD side can now be written in terms of perturbative(p) and non-perturbative(n) contributions as

$$\Pi^{OPE}(q^2) = \Pi^{OPE(p)}(q^2) + \Pi^{OPE(n)}(q^2). \tag{2.24}$$

The perturbative contributions to the correlator can easily be obtained by inserting only the free quark propagators in Eq. 2.23. The perturbative part of the correlation function is found as

$$\begin{aligned}
\Pi^{OPE(p)}(q^2) &= -i\int d^4x e^{iqx}\mathrm{Tr}\{\Gamma S^0_q(x)\Gamma S^0_{q'}(-x)\}, \\
&= -i\int d^4x e^{iqx}\int\frac{d^4k_q e^{-i(k_q+q)x}}{(2\pi)^4}\int\frac{d^4k_{q'}e^{ik_{q'}x}}{(2\pi)^4} \\
&\quad \left(\frac{\mathrm{Tr}\{\Gamma(\not k_q+\not q+m_q)\Gamma(\not k_q+m_{q'})\}}{((k_q+q)^2-m_q^2)(k_q^2-m_{q'}^2)}\right) \\
&= -i\int d^4k_q\left(\frac{\mathrm{Tr}\{\Gamma(\not k_q+\not q+m_q)\Gamma(\not k_q+m_{q'})\}}{((k_q+q)^2-m_q^2)(k_q^2-m_{q'}^2)}\right),
\end{aligned} \tag{2.25}$$

where first x and then $k_{q'}$ integrals are handled. The result in Eq. 2.25 corresponds to the contributions coming from diagram 2.3-a. The contribution of diagram 2.3-b is an $O(\alpha_s)$ correction to the Wilson coefficient of the identity operator in OPE. It is numerically suppressed due to additional loop, so it is neglected as general.

The non-perturbative contributions to correlator can be calculated in two steps. The contributions of diagrams 2.3-c, 2.3-e and 2.3-f are simply

$$\Pi^{OPE(n_1)}(q^2) = i\int d^4x e^{iqx}\mathrm{Tr}\{\Gamma S_q^{\langle\bar{q}q\rangle}(x)\Gamma S^0_{q'}(-x)\}. \tag{2.26}$$

Eq. 2.26 contains both $d = 3(\langle\bar{q}q\rangle)$ and $d = 5(\langle\bar{q}\sigma Gq\rangle = m_0^2\langle\bar{q}q\rangle)$ contributions coming from the non-perturbative corrections to the light quark propagator.

The contribution of the diagram 2.3-d also corresponds to the $d = 5$ quark gluon mixed operator and calculating this contribution is not straight forward. To obtain this contribution to the non-perturbative part, $S^G_{q'}$ should be inserted into the matrix element defining the $\langle\bar{q}q\rangle$ condensate. Aforementioned contribution is obtained by

$$\Pi^{OPE(n_2)}(q^2) = i \int d^4x e^{iqx} \langle 0|\bar{q}(x)\Gamma S_{q'}^{G}(-x)\Gamma q|0\rangle. \quad (2.27)$$

After inserting the definitions of the propagators given in Eq. 2.22 into Eq. 2.27 one obtains

$$\begin{aligned}\Pi^{OPE(n_2)}(q^2) &= i \int d^4x e^{iqx} \langle 0|\bar{q}^a(x)\Gamma \\ &\left[g_s \int \frac{d^4k'}{(2\pi)^4} e^{ik'x} \left(\frac{\not{k}' + m_{q'}}{(k'^2 - m_{q'}^2)^2} G^{ab}_{\mu\nu}\sigma^{\mu\nu} - \frac{1}{2(k'^2 - m_{q'}^2)} x^{\mu} G^{ab}_{\mu\nu}\gamma^{\nu} \right) \right] \\ &\Gamma q^b|0\rangle, \end{aligned} \quad (2.28)$$

where a, b are color indices. When calculating $\Pi^{OPE(n_2)}(q^2)$, an expression for a matrix element of the form $\langle 0|\bar{q}^a(x)G^{ab}_{\mu\nu}q^b|0\rangle$ is necessary. To obtain an expression for this matrix element, the quark field is expanded around $x = 0$ as

$$q(x) = q(0) + x_{\mu}D^{\mu}q(x)|_{x=0} + \ldots \ , \quad (2.29)$$

where D^{μ} is the covariant derivative. Here, Fock-Schwinger gauge is used to write $x_{\mu}\partial^{m}u = x_{\mu}D^{\mu}$.

The first term in the expansion is proportional to σ since it is anti symmetric, and can be written as

$$\langle 0|q^b(0)_{\beta}G^{ab}_{\mu\nu}\bar{q}^a_{\alpha}|0\rangle = A(\sigma_{\mu\nu})_{\beta\alpha}, \quad (2.30)$$

where α, β are spinor and μ, ν are Lorentz indices. By multiplying both sides with $(\sigma^{\mu\nu})_{\alpha\beta}$ and taking the trace it is obtained that

$$\begin{aligned} 48A &= \langle 0|q^b(0)_{\beta}G^{ab}_{\mu\nu}\bar{q}^a_{\alpha}|0\rangle, \\ &= -\langle 0|\bar{q}^a(0)_{\beta}G^{ab}_{\mu\nu}q^b_{\alpha}|0\rangle, \\ &= -m_0^2\langle \bar{q}q\rangle. \end{aligned} \quad (2.31)$$

To obtain the second term in the expansion, the matrix element $\langle 0|q^a(0)_{\beta}G^{ab}_{\mu\nu}\overleftarrow{D_{\eta}}\bar{q}^b_{\alpha}|0\rangle$ should be written as

$$\langle 0|q^a(0)_{\beta}G^{ab}_{\mu\nu}\overleftarrow{D_{\eta}}\bar{q}^b_{\alpha}|0\rangle = B(g_{\eta\mu}\gamma_{\nu} - g_{\eta\nu}\gamma_{\mu})_{\alpha\beta}, \quad (2.32)$$

where $(g_{\eta\mu}\gamma_\nu - g_{\eta\nu}\gamma_\mu)$ is a third rank tensor antisymmetric in μ, ν. By multiplying both sides of the Eq. 2.32 with $(\gamma^\eta)_{\beta\alpha}$, and using equations of motion and Eq. 2.31 we get

$$\begin{aligned} i m_q \langle 0|\bar{q}^a(0)_\beta G^{ab}_{\mu\nu} q^b_\alpha|0\rangle &= -2iB(\sigma_{\mu\nu})_{\beta\alpha}, \\ &= i\frac{m_q m_0^2\langle\bar{q}q\rangle}{48}(\sigma_{\mu\nu})_{\beta\alpha}. \end{aligned} \tag{2.33}$$

Collecting all terms, one gets

$$\langle 0|\bar{q}^a(x) G^{ab}_{\mu\nu} q^b|0\rangle = -\frac{m_0^2\langle\bar{q}q\rangle}{48}\sigma_{\mu\nu} - \frac{m_q m_0^2\langle\bar{q}q\rangle}{96}(x_\mu\gamma_\nu - x_\nu\gamma_\mu). \tag{2.34}$$

For u and d quarks, the second term in this matrix element can be neglected.

The contribution of the diagram 2.3-d in Eq. 2.28 is also a matrix element of the form $\langle 0|\bar{q}^a(x) G^{ab}_{\mu\nu} q^b|0\rangle$, and is obtained in a similar manner. To obtain the result of Eq. 2.28, first x_μ is replaced with $-i\frac{\partial}{\partial q^\mu}$. Then integrations with respect to x which gives $\delta(q + k')$, and k' are evaluated in order. These calculations yield

$$\begin{aligned} \Pi^{OPE(n_2)}(q^2) &= i\langle 0|\bar{q}^a(x)\Gamma \\ &\quad g_s\left[\frac{-\not{q} + m_{q'}}{(q^2 - m_{q'}^2)^2} G^{ab}_{\mu\nu}\sigma^{\mu\nu} - \left(-i\frac{\partial}{\partial q^\mu}\right)\frac{1}{2(q^2 - m_{q'}^2)} G^{ab}_{\mu\nu}\gamma^\nu\right] \\ &\quad \Gamma q^b|0\rangle. \end{aligned} \tag{2.35}$$

Following the steps from Eq. 2.29 to 2.34, the matrix elements appearing in Eq. 2.35 are calculated. Then Eq. 2.35 gives

$$\begin{aligned} \Pi^{OPE(n_2)}(q^2) &= i\frac{-m_o^2\langle\bar{q}q\rangle}{48}\frac{Tr\{\Gamma(-\not{q} + m_{q'})\sigma^{\mu\nu}\Gamma\sigma_{\mu\nu}\}}{(q^2 - m_{q'}^2)^2} \\ &\quad + \frac{-m_{q'} m_o^2\langle\bar{q}q\rangle}{48}\frac{Tr\{\Gamma(\not{q})\gamma^\mu\gamma^\nu\Gamma\sigma_{\mu\nu}\}}{(q^2 - m_{q'}^2)^2}. \end{aligned} \tag{2.36}$$

In calculating the last step, only the first term in the expansion given in Eq. 2.29 is taken for simplicity. We have also used

$$\begin{aligned} \left(-i\frac{\partial}{\partial q^\mu}\right)\frac{1}{q^2 - m_{q'}^2} &= i\frac{\left(\frac{\partial(q^2 - m_{q'}^2)}{\partial q^\mu}\right)}{(q^2 - m_{q'}^2)^2} \\ &= i\frac{2q_\mu}{(q^2 - m_{q'}^2)^2}. \end{aligned} \tag{2.37}$$

Finally, the non-perturbative contributions to the correlator can be written as

$$\Pi^{OPE(n)}(q^2) = \Pi^{OPE(n_1)}(q^2) + \Pi^{OPE(n_2)}(q^2),$$

which is the sum of the contributions in Eqs. 2.26 and 2.36.

2.2.4 Dispersion Relation

Up to this point, the correlation function in Eq. 2.2, is calculated in the region $q^2 > 0$, in terms of hadrons (Eq. 2.13), and it is also calculated in the region $-q^2 = Q^2 >> \Lambda^2_{QCD}$, in terms of quarks and gluons, with perturbative and non-perturbative contributions (Eqs. 2.25, 2.26 and 2.27). Since the correlator is an analytic function of its argument q^2 everywhere in the complex plane except than on some parts of the positive real axis, it is possible to link the values of $\Pi(q^2)$ at positive values of q^2 to its values at negative values of q^2.

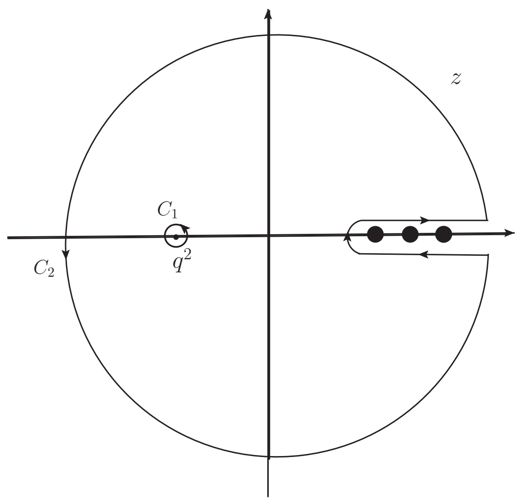

Figure 2.4: The contours in the plane of the complex variable $q^2 = z$. The contour C_1 represents the $q^2 < 0$ reference point where OPE is applied. For $q^2 > t_m$, real hadronic states are formed, which are indicated by dots.

Using the Cauchy formula for analytic functions, for the contours shown in figure 2.4, one can write

$$
\begin{aligned}
\Pi(q^2) &= \frac{1}{2i\pi}\oint_{C_1} dz\frac{\Pi(z)}{z-q^2} = \frac{1}{2i\pi}\oint_{C_2} dz\frac{\Pi(z)}{z-q^2} \\
&= \frac{1}{2i\pi}\oint_{|z|=R} dz\frac{\Pi(z)}{z-q^2} + \frac{1}{2i\pi}\int_{t_m}^{R} dz\frac{\Pi(z+i\epsilon)-\Pi(z-i\epsilon)}{z-q^2}, \qquad (2.38)
\end{aligned}
$$

where t_m is the threshold for creation of real states, and eventually the radius of the circular part of the contour C_2 will be sent to infinity, i.e., $R \to \infty$.

The integral over the circular part of the contour C_2 vanishes, if $\Pi(z)$ vanishes sufficiently fast at $|z| \to \infty$. On the other hand, if $\Pi(z)$ does not vanish, by expanding the denominator in terms of $\frac{q^2}{z}$, the integrand can be written as $\frac{\Pi(z)}{z-q^2} = \frac{\Pi(z)}{z}(1 - \frac{q^2}{z} + ...)$. And eventually for some power n' in the expansion, $\frac{\Pi(q^2)}{z^{n'}}$ would vanish sufficiently fast and the remaining terms in the expansion ($n \geq n'$) do not contribute. In this case, the terms with $n < n'$ reduces to a polynomial in q^2 in the limit $R \to \infty$. So in the limit $R \to \infty$, Eq. 2.38 reduces to

$$
\Pi(q^2) = \frac{1}{2i\pi}\oint_{C_1} dz\frac{\Pi(z)}{z-q^2} = \frac{1}{2i\pi}\int_{t_m}^{\infty} dz\frac{\Pi(z+i\epsilon)-\Pi(z-i\epsilon)}{z-q^2} + \mathcal{P}^s(q^2), \qquad (2.39)
$$

where $\mathcal{P}^s(q^2)$ is a polynomial in q^2 which is called the subtraction terms.

Using the Schwartz reflection principle which states that if $\Pi(z)$ is analytic and real over some region including the real axis when $z = q^2$ is real, then

$$
\Pi(z^*) = \Pi^*(z) = \mathrm{Re}\Pi(z) - i\mathrm{Im}\Pi(z), \qquad (2.40)
$$

the numerator of the integrand in Eq. 2.39 can be written as

$$
\begin{aligned}
\Pi(z+i\epsilon) - \Pi(z-i\epsilon) &= \Pi(z') - \Pi(z'^*) \\
&= \Pi(z') - \Pi^*(z') \\
&= (\mathrm{Re}\Pi(z') + i\mathrm{Im}\Pi(z')) - (\mathrm{Re}\Pi(z') - i\mathrm{Im}\Pi(z')) \\
&= 2i\mathrm{Im}\Pi(z') = 2i\mathrm{Im}\Pi(z+i\epsilon). \qquad (2.41)
\end{aligned}
$$

The condition to apply Eq. 2.40 is satisfied in the region $z = q^2 < t_m$. After inserting the result of Eq. 2.41 and setting $\epsilon \to 0$, Eq. 2.39 can be written as

$$
\Pi(q^2) = \int_{t_m}^{\infty} ds\frac{\rho(s)}{s-q^2} + \mathcal{P}^s(q^2), \qquad (2.42)
$$

which is called the dispersion relation, and

$$\rho(s) = \frac{\mathrm{Im}\Pi(s)}{\pi} \tag{2.43}$$

is the spectral density.

Using the dispersion relation derived in Eq. 2.43, one can link the values of $\Pi(q^2)$ for the negative values of q^2 to the $\Pi(q^2)$ for positive values of q^2. For $q^2 > 0$, using the result of Eq. 2.13, the spectral density can be written as

$$\rho(q^2) = \frac{\mathrm{Im}\Pi(q^2)}{\pi} = f_H^2 \delta(q^2 - m_H^2) + \rho^h(q^2), \tag{2.44}$$

where $\rho^h(q^2) = \frac{\mathrm{Im}\Pi^h(q^2)}{\pi}$. Inserting this relation in Eq. 2.42, one gets

$$\int_0^\infty ds \frac{\rho^{OPE}(s)}{s - q^2} = \frac{f_H^2}{q^2 - m_H^2} + \int_{s_0^h}^\infty ds \frac{\rho^h(s)}{s - q^2} + \mathcal{P}^s(q^2), \tag{2.45}$$

where s_0^h is the threshold for creation of excited states.

2.2.5 Quark Hadron Duality

In the final expression of the dispersion relation (Eq. 2.45), there is not much known about $\rho^h(q^2)$, which contains the contribution of excited states and continuum for $q^2 > 0$. Although it can not be calculated explicitly, one can approximate it by using the quark hadron duality assumption. In the deep Euclidean region, i.e., $q^2 \to -\infty$, the non-perturbative effects are suppressed and can safely be neglected. So, $\Pi(q^2) \to \Pi^{OPE(p)}(q^2)$ is valid yielding an approximation

$$\int_{s_0^h}^\infty ds \frac{\rho^h(s)}{s - q^2} = \int_{s_0}^\infty ds \frac{\rho^{OPE}(s)}{s - q^2}, \tag{2.46}$$

where s_0, which is called the continuum threshold, is a parameter to be fitted[20, 21]. After applying the quark hadron duality assumption, dispersion relation in Eq. 2.45 can be written as

$$\int_0^{s_0} ds \frac{\rho^{OPE}(s)}{s - q^2} = \frac{f_H^2}{q^2 - m_H^2} + \mathcal{P}^s(q^2). \tag{2.47}$$

2.2.6 Borel Transformations

There still exists one more step to achieve the sum rules for the physical quantities of the hadron H. In Eq. 2.47, there exist one last unknown term, which is the subtraction polynomial, that one should get rid of. Since $\mathcal{P}^s(q^2)$ is a polynomial in q^2, by taking infinitely many times derivatives with respect to q^2, the subtraction terms would be eliminated. More formally, by applying Borel transformation with respect to $Q^2 = -q^2$ to both sides of Eq. 2.47, the final form of the sum rules is found. The Borel transformation is defined as

$$\mathcal{B}_{M^2} f(q^2) = lim_{\substack{Q^2,n\to\infty \\ \frac{Q^2}{n}=M^2}} \frac{(-q^2)^n}{(n-1)!}(\frac{d}{dq^2})^{n-1} f(q^2), \tag{2.48}$$

where M^2 is the Borel transformation parameter with mass dimensions and it is usually called as the Borel mass. Any polynomial gives zero after Borel transformation. Borel transformations of some important functions are

$$\begin{aligned} \mathcal{B}_{M^2}(q^2)^k &= 0, \qquad k \geq 0 \\ \mathcal{B}_{M^2}(\frac{1}{(m^2[s]-q^2)^k}) &= \frac{1}{(k-1)!}\frac{e^{-m^2[s]/M^2}}{(M^2)^(k-1)}, \\ \mathcal{B}_{M^2}(e^{-\alpha Q^2}) &= \delta(\frac{1}{M^2}-\alpha). \end{aligned} \tag{2.49}$$

Borel transformations of more complicated functions an be found in literature[3, 19].

2.2.7 Physical Applications of QCD Sum Rules

After applying Borel transformation to Eq. 2.47, one obtains the following sum rules:

$$f_H^2 e^{-\frac{m_H^2}{M^2}} = \int_{s_m}^{s_0} ds \rho^{OPE}(s) e^{-\frac{s}{M^2}}, \tag{2.50}$$

where the lower limit of the integral is $s_m = (m_q + m_{q'})^2$[20]. In Eq. 2.50, there are two unknown parameters: the Borel mass parameter, M^2, and the continuum threshold, s_0. The continuum threshold is not completely arbitrary, being related to the energy of the excited states. The sum rules should be stable with respect to small oscillations of s_0 and in general it is taken as $(m_H + 0.3 \sim 0.7GeV)^2$[20, 21]. On the other hand, the Borel mass parameter, M^2 is completely arbitrary. It is restricted above, due to the reason that the contributions of the continuum and the contributions of the neglected higher dimensional operators stays suppressed. And also for large values of M^2, the quark hadron duality can not be trusted and exponential suppression of the higher states is reduced. The upper limit on M^2 is determined by demanding that the contributions of excited states to the sum rules remains small compared to the total dispersion integral. It is also restricted below, due to the contributions of the higher dimensional operators which are inversely proportional to the powers of M^2, should stay negligible. The lower limit on M^2 is commonly obtained by demanding that the contributions of the highest dimensional operator in the expansion is not more than a small fraction of the total result. Practically, to determine the working region of Borel parameters, one plots the desired results with respect to M^2 and searches for a region in which sum rules results are stable.

The sum rules derived in Eq. 2.50 are called the mass sum rules. In literature they are successfully applied to many problems. Given the mass m_h, the matrix element $\langle 0|j(x)|H(q)\rangle$ of the hadron H, can be directly obtained from the sum rules in Eq. 2.50.

Using the sum rules derived in Eq. 2.50, the mass m_H of the hadron H can also be obtained. To get this, one should take the derivative of Eq. 2.50 with respect to $1/M^2$, and divide it to original equation as follows:

$$
\begin{aligned}
-m_H^2 &= \frac{\frac{d\left(f_H^2 e^{-\frac{m_H^2}{M^2}}\right)}{d(1/M^2)}}{f_H^2 e^{-\frac{m_H^2}{M^2}}} \\
&= \frac{\frac{d\left(\int_{s_m}^{s_0} ds\rho^{OPE}(s)e^{-\frac{s}{M^2}}\right)}{d(1/M^2)}}{\int_{s_m}^{s_0} ds\rho^{OPE}(s)e^{-\frac{s}{M^2}}} \\
&= \frac{\int_{s_m}^{s_0} ds(-s\rho^{OPE}(s))e^{-\frac{s}{M^2}}}{\int_{s_m}^{s_0} ds\rho^{OPE}(s)e^{-\frac{s}{M^2}}}. \qquad (2.51)
\end{aligned}
$$

It should be noted that, although the mass can be obtained by taking derivatives, such manipulations usually reduce the precision of sum rules (see e.g.[49, 50]). For applications of mass sum rules to real hadrons, see e.g. [21, 46, 47, 48]. The sum rules in Eq. 2.50 is also useful to determine the value of the continuum threshold when m_H and f_H are known.

2.3 Three-Point QCD Sum Rules

The sum rules derived in previous section are called the two-point QCD or alternatively mass sum rules, and by applying them the mass and leptonic decay constant of a given hadron H can be found. On the other hand to study and obtain further properties of hadrons such as transition form factors, transition amplitudes, decay widths and branching ratios, the mass sum rules should be generalized in order to calculate hadronic matrix elements of electromagnetic and weak transitions. In this case one starts with a three-point correlator and uses double dispersion relation. For a generic decay of the form

$$H_1(p) \to H_2(p') + \mathcal{X}, \tag{2.52}$$

where $\mathcal{X}$ can be any hadron, can be $\ell^+\ell^-$, $\ell\bar{\nu}$ or $\nu\bar{\nu}$ for semileptonic decays, and is γ for radiative decays, $H_1(p)$ and $H_2(p')$ are initial and final hadronic states, and $q = p - p'$ is the momentum transferred to $\mathcal{X}$. To study the transition amplitude of the decay $H_1(p) \to H_2(p') + \mathcal{X}$, the three-point correlator can be written as

$$\Pi(p^2, p'^2; q^2) = i^2 \int\int d^4x d^4y e^{-ipx} e^{ip'y} \langle 0|\mathcal{T}\{j_2(y) j_3(0) j_1^\dagger(x)\}|0\rangle, \tag{2.53}$$

where j_3 is the operator responsible for the transition.

For positive values of p^2 and p'^2, like two-point correlators, the correlation function can be calculated by inserting complete sets of hadronic states in between the currents. Doing the straight forward calculations as described in section 2.2.2, the three-point correlator in Eq. 2.53 can be written as

$$\begin{aligned}
\Pi(p^2, p'^2; q^2) &= \sum_{i,j} \frac{\langle 0|j_1^\dagger(x)|h_i(p)\rangle\langle h_i(p)|j_3(0)|h_j(p')\rangle\langle h_j(p')|j_2(y)|0\rangle}{(p^2 - m_{h_1}^2)(p'^2 - m_{h_2}^2)} \\
&= \frac{\langle 0|j_1^\dagger(x)|H_1(p)\rangle\langle H_1(p)|j_3(0)|H_2(p')\rangle\langle H_2(p')|j_2(y)|0\rangle}{(p^2 - m_{H_1}^2)(p'^2 - m_{H_2}^2)} \\
&\quad + \Pi^h(p^2, p'^2; q^2),
\end{aligned} \tag{2.54}$$

where $H_1(H_2)$ is the hadron with the lowest mass that can be created by the interpolating current $j_1(j_2)$ and $m_{H_1}(m_{H_2})$ is its mass, and j_3 is the transition current responsable for $H_1 \to H_2$ transition. The second term in Eq. 2.54 is the contributions of the higher states and the continuum, and $\rho^h(s,s')$ is the spectral density. In contrary to Eq. 2.13, in Eq. 2.54 the imaginary part of the correlator is taken twice, first while taking the y_0 integral a small complex part is given to $E_{h_j(p')}$, and then while taking the x_0 integral a small complex part is given to $E_{h_i(p)}$, as described in section 2.2.2.

To investigate the decay $H_1(p) \to H_2(p') + X$ more deeply, one can introduce the following definitions:

$$
\begin{aligned}
j_1 &= Qi\Gamma_1\bar{q}, && (2.55)\\
j_2 &= qi\Gamma_2\bar{q}', && (2.56)\\
j_3 &= Qi\Gamma_3\bar{q}', && (2.57)
\end{aligned}
$$

where Γ_i carry Lorentz indices and can be any of the matrices: scalar($\mathbb{1}$), pseudoscalar(γ_5), vector(γ_μ), axial vector($\gamma_\mu\gamma_5$) and tensor($\sigma_{\mu\nu}$). After these definitions, the hadrons are identified as: $H_1 \equiv Q\bar{q}$ and $H_2 \equiv q'\bar{q}$. In this section q, q' are assumed to be light quarks and Q is assumed to be heavy for pedagogical reasons. The transition $H_1(p) \to H_2(p') + X$ is defined to be occur via $Q \to q' + X$ transition at quark level, and it can be described by an effective Hamiltonian. The vacuum to hadron matrix elements can be parameterized as

$$f_i = \langle h_i(p_i)|j_i|0\rangle, \qquad (2.58)$$

where f_i are called the decay constant of h_i and they are parameterized in terms of masses and momentums, and also polarizations(ϵ_μ) of hadrons, with the same Lorentz indices and parity of Γ_i. In terms of these definitions the phenomenological side of the correlator can be written as

$$
\begin{aligned}
\Pi(p^2, p'^2; q^2) &= \frac{f_1^\dagger f_2 \langle H_1(p)|j_2(0)|H_2(p')\rangle}{(p^2 - m_{H_1}^2)(p'^2 - m_{H_2}^2)}\\
&+ \Pi^h(p^2, p'^2; q^2).
\end{aligned}
$$

In calculating the first term of Eq. 2.59, if necessary, one should consider the sum over polarizations which is defined as

$$\sum_\epsilon \epsilon_\mu(k)\epsilon_\nu(k) = -g_{\mu\nu} + \frac{k_\mu k_\nu}{k^2}. \qquad (2.59)$$

In Eq. 2.59, the only unknown matrix element is $\langle H_1(p)|j_2(0)|H_2(p')\rangle$, and it is necessary for calculating the transition properties of the decay $H_1(p) \rightarrow H_2(p') + \mathcal{X}$, and it can be parameterized in terms of transition form factors.

The QCD side of the correlator can be calculated in terms of these definitions. When $p^2 << 0$ and $p'^2 << 0$, one can calculate the correlator in terms of perturbative and non-perturbative parts as described in section 2.2.3. The diagrammatic representation of perturbative and non-perturbative contributions to correlator at $p^2 << 0$ and $p'^2 << 0$ are depicted in Fig. 2.5. The perturbative contribution comes from diagram 2.5-a, and it can be calculated following section 2.2.3 from

$$\begin{aligned}\Pi^{OPE(p)}(p^2, p'^2; q^2) &= i^2 \int\int d^4x d^4y e^{-ipx} e^{ip'y} \\ &\quad \mathrm{Tr}\{\Gamma_1 S_q^0(x-y)\Gamma_2 S_{q'}^0(y)\Gamma_3 S_Q^0(-x)\}. \end{aligned} \tag{2.60}$$

The non-perturbative contributions to the correlator due to $\langle\bar{q}q\rangle$ condensate contributions to the q quark propagator comes from the diagrams 2.5-b, 2.5-c and 2.5-d, and they can be calculated from

$$\begin{aligned}\Pi^{OPE(n_1)}(p^2, p'^2; q^2) &= i^2 \int\int d^4x d^4y e^{-ipx} e^{ip'y} \\ &\quad \mathrm{Tr}\{\Gamma_1 S_q^{\langle\bar{q}q\rangle}(x-y)\Gamma_2 S_{q'}^0(y)\Gamma_3 S_Q^0(-x)\}. \end{aligned} \tag{2.61}$$

The contribution of diagrams 2.5-e and 2.5-f can be calculated following section 2.2.3 as

$$\begin{aligned}\Pi^{OPE(n_2)}(p^2, p'^2; q^2) &= i^2 \int\int d^4x d^4y e^{-ipx} e^{ip'y} \\ &\quad \Big(\langle 0|\bar{q}(x)\Gamma_2 S_{q'}^G(y)\Gamma_3 S_Q^0(-x)q|0\rangle \\ &\quad +\langle 0|\bar{q}(x)\Gamma_2 S_{q'}^0(y)\Gamma_3 S_Q^G(-x)q|0\rangle\Big). \end{aligned} \tag{2.62}$$

The contributions of the diagrams 2.5-g and 2.5-k can also be calculated from

$$\begin{aligned}\Pi^{OPE(n_1)}(p^2, p'^2; q^2) &= i^2 \int\int d^4x d^4y e^{-ipx} e^{ip'y} \\ &\quad \mathrm{Tr}\{\Gamma_1 S_q^0(x-y)\Gamma_2 S_{q'}^{\langle\bar{q}'q'\rangle}(y)\Gamma_3 S_Q^0(-x)\} \\ &\sim \frac{p'^2}{p^2 - M^2}. \end{aligned} \tag{2.63}$$

Since the result is a polynomial in p'^2, these contributions in terms of the operator $\langle \bar{q}' q' \rangle$ vanish after Borel transformation.

After calculating these contributions, the correlator in deep Euclidean region is found as

$$\begin{aligned} \Pi^{OPE}(p^2, p'^2; q^2) &= \Pi^{OPE(p)}(p^2, p'^2; q^2) \\ &+\Pi^{OPE(n_1)}(p^2, p'^2; q^2) + \Pi^{OPE(n_2)}(p^2, p'^2; q^2). \end{aligned} \tag{2.64}$$

After calculating the correlator function in both $p^2 << 0$ and $p'^2 << 0$ region, and $p^2 > 0$ and $p'^2 > 0$, following the steps described in section 2.2.4, one can get the following dispersion relation:

$$\begin{aligned} \int_0^\infty ds \int_0^\infty ds' \frac{\rho^{OPE}(s, s'; q^2)}{(s - m_{H_1}^2)(s' - m_{H_2}^2)} &= \frac{f_1^\dagger f_2 \langle H_1(p)| j_2(0) |H_2(p')\rangle}{(p^2 - m_{H_1}^2)(p'^2 - m_{H_2}^2)} \\ &+ \int_{s_0^h}^\infty ds \int_{s_0'^h}^\infty ds' \frac{\rho^h(s, s'; q^2)}{(s - m_{H_1}^2)(s' - m_{H_2}^2)} \\ &+\mathcal{P}^s(p^2, p'^2), \end{aligned} \tag{2.65}$$

where the spectral density is defined as

$$\rho^{OPE}(s, s'; q^2) = \frac{\mathrm{Im}_s \mathrm{Im}_{s'} \Pi(s, s'; q^2)}{\pi^2}. \tag{2.66}$$

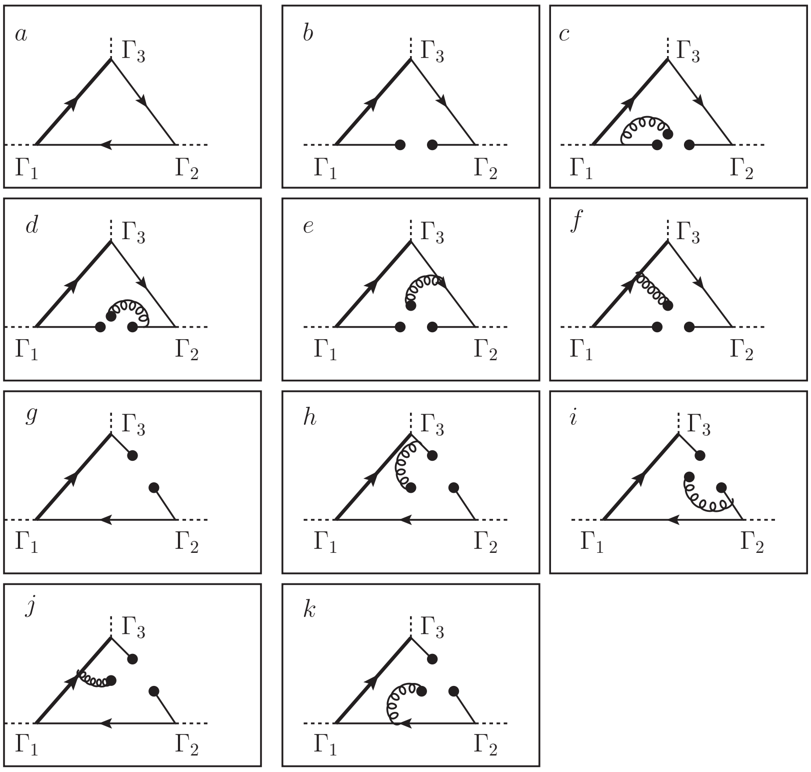

Figure 2.5: The Feynman diagram representations of the operators contributing the correlator $\Pi(q^2)$ of the decay $H_1(p) \to H_2(p') + X$. The dashed lines denote the currents, thin(thick) solid lines denote the light(heavy) quarks, and the spirals correspond to soft gluons.

In the case of three-point correlators, the local quark hadron duality in Eq. 2.46 is modified as

$$\int_{s_0}^{\infty} ds \int_{s_0'}^{\infty} ds' \frac{\rho^{OPE}(s,s';q^2)}{(s-m_{H_1}^2)(s'-m_{H_2}^2)} = \int_{s_0^h}^{\infty} ds \int_{s_0'^h}^{\infty} ds' \frac{\rho^{h}(s,s';q^2)}{(s-m_{H_1}^2)(s'-m_{H_2}^2)}, \tag{2.67}$$

where s_0 and s_0' are the continuum thresholds in p^2 and p'^2 channels. Since the subtraction terms $\mathcal{P}^s(p^2, p'^2)$ are polynomials in p^2 and p'^2, to get rid of them one should apply double Borel transformation with respect to the variables p^2 and p'^2 ($p^2 \to M_1^2, p'^2 \to M_2^2$) which is given as

$$\hat{\mathcal{B}}\left[\frac{1}{(p^2-m_1^2)^m}\frac{1}{(p'^2-m_2^2)^n}\right] \to \frac{(-1)^{m+n}e^{-m_1^2/M_1^2}e^{-m_2^2/M_2^2}}{\Gamma(m)\Gamma(n)(M_1^2)^{m-1}(M_2^2)^{n-1}}. \tag{2.68}$$

Using quark hadron duality approximation and applying double Borel transformation one ends with the following sum rules:

$$\begin{aligned} f_1^\dagger f_2\langle H_1(p)|j_2(0)|H_2(p')\rangle &= e^{m_{H_1}^2/M_1^2}e^{m_{H_2}^2/M_2^2} \\ &\quad \int_{s_m}^{s_0} ds \int_{s_m'}^{s_0'} ds' \rho^{OPE}(s,s';q^2)e^{-s/M_1^2}e^{-s'/M_2^2}, \end{aligned} \tag{2.69}$$

where the continuum thresholds s_0 and s_0', and the Borel mass parameters M_1^2 and M_2^2 are four auxiliary parameters. Their values can be determined as discussed in two-point QCD sum rules. Once the matrix element $\langle H_1(p)|j_3|H_2(p')\rangle$ is found, it can be used to study $H_1(p) \to H_2(p') + \mathcal{X}$ transition. In general the matrix element $\langle H_1(p)|j_3|H_2(p')\rangle$ can be written as the sum of some Lorentz structures. In such cases, one should calculate the expansion

$$f_1^\dagger f_2\langle H_1(p)|j_2(0)|H_2(p')\rangle = \sum_A F_A \mathbf{T}_A, \tag{2.70}$$

where $\mathbf{T}_A$ are Lorentz structures, and F_A are the called transition form factors. In this case, instead of equating the whole sum rule in Eq. 2.69, sum rules for transition form factors can be found by equating the coefficients of the Lorentz structures $\mathbf{T}_A$ on both sides of Eq. 2.69.

In applying the three-point sum rules one confronts the following problems. In the deep Euclidean region, higher dimensional operators receive multiplicative factors proportional to $\frac{Q^2}{M^2}$, hence they become more important. Thus three point sum rules are reliable when q^2 is small. Also for the decays like $H_1(p) \to H_2(p') + \mathcal{X}$, instead of the whole physical region $0 < q^2 < (m_{H_1} - m_{H_2})^2$, the three point QCD sum rules work in some region $0 < q^2 < q_c^2$, where $q_c^2 = (m_q + m_{q'})^2$. To over come this problem, the results obtained from three point QCD sum rules are plotted with respect to q^2 in the working region, i.e. $q^2 < q_c^2$, and a suitable function is fitted to sum rules results in the working region.

The second problem in applying three point QCD sum rules arises in calculating the perturbative contributions to correlator function when calculating $\Pi^{OPE(p)}(p^2, p'^2; q^2)$ in Eq. 2.60. In calculating $\Pi^{OPE(p)}(p^2, p'^2; q^2)$ (or $\rho^{OPE(p)}(s, s'; q^2)$), one has to calculate the following integral:

$$I_0(p^2, p'^2; q^2) = i \int \frac{d^4k}{(2\pi)^4} \frac{1}{((k-p)^2 - m_Q^2)((k-p')^2 - m_{q'}^2)(k^2 - m_q^2)}, \tag{2.71}$$

where m_Q, $m_{q'}$ and m_q are the quark masses, and the terms in the denominator comes from quark propagators. By applying Cutkovsky rules, which states that for $q^2 \leq 0$ the contributions to the integral in Eq. 2.71 comes from Landau type singularities, hence the terms in the denominator can be replaced by delta functions, i.e. $\frac{1}{k^2 - m^2} \to 2\pi i \delta(p^2 - m^2)$. Using Cutkovsky rules, Eq. 2.71 becomes

$$I_0(p^2, p'^2; q^2 \leq 0) = i \int \frac{d^4k}{(2\pi)^4} (2\pi i)^3 \delta((k-p)^2 - m_Q^2) \delta((k-p')^2 - m_{q'}^2) \delta(k^2 - m_q^2), \tag{2.72}$$

which can be calculated straight forward. But the results of the sum rules are needed in the region $0 < q^2 < (m_{H_1} - m_{H_2})^2$. However the I_0 integral in Eq. 2.71 receives contributions from non-Landau type singularities when $q^2 > 0$[51]. Even if these contributions are small, they reduces the reliability of the QCD sum rules results.

One alternative way to solve this problem is using the analyticity of the correlation function. Instead of finding a fit function in the region $0 < q^2 < q_c^2$, one can plot the results of the sum rules in the region $q^2 < 0$, and finds a fit function coinciding with the sum rules results where there are no additional contributions to the integral in Eq. 2.72. Then, this fit function can be extrapolated to the physical region. In calculating the sum rules for $B \to K_1(1270, 1400)\ell^+\ell^-$ decays, this method is used.

CHAPTER 3

PROPERTIES OF AXIAL VECTOR K_1 MESONS

In this chapter, the properties of the K_1 axial vector mesons are analyzed. To understand the behaviors of light axial vector mesons, first the quark model is reviewed following references[52, 53]. The quantum numbers and classifications of the mesons are then summarized. Then the axial vector $K_1(1270)$ and $K_1(1400)$ states, and their mixings in terms of G-parity eigenstates, which are also orbital angular momentum eigen states are analyzed.

3.1 The Quark Model

According to quark model, all hadrons are formed of more basic entities, called quarks, bound together in different ways. In the fundamental representation of $SU(3)$, all multiplets can be formed from a triplet. Basic quark multiplet is a triplet formed from light quarks, i.e. u, d, s. The basic quark and anti-quark multiplet are presented in figure 3.1. All of the quarks in figure 3.1 have spin $s = \frac{1}{2}$ and baryon number $B = \frac{1}{3}$. The quantum numbers of u, d, s quarks are listed in table 3.1. The hypercharge is used rather then strangeness and it is defined as

$$Y \equiv B + S. \tag{3.1}$$

This choice is made to center the triplet in figure 3.1 to origin. The charge is

$$Q = I_3 + \frac{Y}{2}. \tag{3.2}$$

In quark model, mesons are $q\bar{q}$ states and baryons are qqq states bound together. In QCD, nuclear interaction does not distinguish neutron and proton, so isospin symmetry ($SU(2)$ symmetry as the carbon copy of spin) is introduced as intrinsic symmetry of nucleon. For $q\bar{q}$ states,the wave functions for isospin triplet and singlet states can be written as:

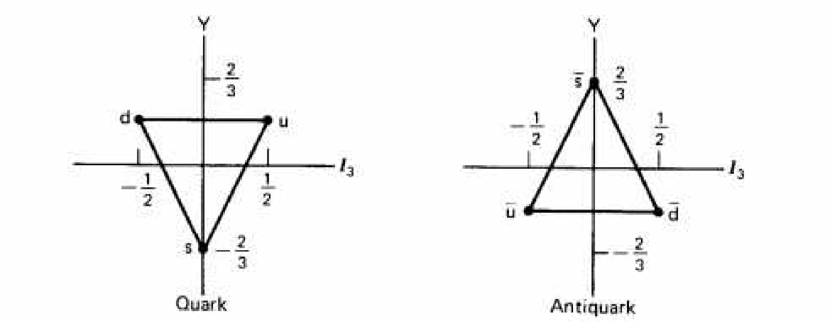

Figure 3.1: $SU(3)$ quark and anti-quark triplets in Y-I_3 plane[52].

Table 3.1: The quantum numbers of the members of basic quark triplet.

Quark	Spin(s)	Baryon(B)	Charge (Q)	Strangeness(S)	Isospin(I_3)	Hypercharge(Y)
u	$\frac{1}{2}$	$\frac{1}{3}$	$\frac{2}{3}$	0	$\frac{1}{2}$	$\frac{1}{3}$
d	$\frac{1}{2}$	$\frac{1}{3}$	$\frac{-1}{3}$	0	$\frac{-1}{2}$	$\frac{1}{3}$
s	$\frac{1}{2}$	$\frac{1}{3}$	$\frac{-1}{3}$	-1	0	$\frac{-2}{3}$

$$
\begin{aligned}
&\text{triplet} \quad \begin{cases} |I = 1, I_3 = 1\rangle = -u\bar{d} \\ |I = 1, I_3 = 0\rangle = \frac{1}{\sqrt{2}}(u\bar{u} - d\bar{d}) \\ |I = 1, I_3 = -1\rangle = d\bar{u} \end{cases} \\
&\text{singlet} \quad |I = 0, I_3 = 0\rangle = \frac{1}{\sqrt{2}}(u\bar{u} + d\bar{d}).
\end{aligned} \tag{3.3}
$$

For three flavors of quarks (u, d, s), the nine $q\bar{q}'$ states divide into an $SU(3)$ octet and an $SU(3)$ singlet. The $SU(3)$ representation of meson nonet is given in figure 3.2.

In quark model, besides isospin symmetry, there are other three $SU(2)$ subgroups, in which the doublets are:

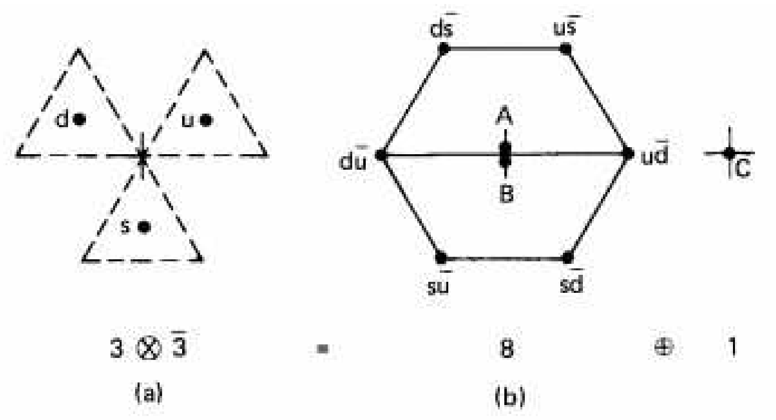

Figure 3.2: $SU(3)$ decomposition of meson nonet, where $A = \sqrt{\frac{1}{3}}(u\bar{u}+d\bar{d}+\bar{s}s)$, $B = \sqrt{\frac{1}{2}}(u\bar{u}-d\bar{d})$ and $C = \sqrt{\frac{1}{6}}(u\bar{u} + d\bar{d} - 2s\bar{s})$ are $Y = I_3 = 0$ states.[52].

$$\begin{pmatrix} u \\ d \end{pmatrix}, \quad \begin{pmatrix} d \\ s \end{pmatrix} \quad \text{and} \quad \begin{pmatrix} u \\ s \end{pmatrix}. \tag{3.4}$$

The symmetry due to first $SU(2)$ doublet in Eq. 3.4 is called I-spin, due to second $SU(2)$ doublet in Eq. 3.4 is called U-spin, and third $SU(2)$ doublet in Eq. 3.4 is called V-spin. These symmetries are important when considering hadrons. The wave functions of the I-spin triplet and singlet states can be written as

$$\begin{aligned} \text{triplet} \quad & \begin{cases} |I = 1, I_3 = 1\rangle = uu \\ |I = 1, I_3 = 0\rangle = \frac{1}{\sqrt{2}}(ud + du) \\ |I = 1, I_3 = -1\rangle = dd \end{cases} \\ \text{singlet} \quad & |I = 0, I_3 = 0\rangle = \frac{1}{\sqrt{2}}(ud - du). \end{aligned} \tag{3.5}$$

The wave functions of the U-spin triplet and singlet states can be written as

$$
\begin{aligned}
&\text{triplet} \quad \begin{cases} |U=1, U_3=1\rangle = dd \\ |U=1, U_3=0\rangle = \frac{1}{\sqrt{2}}(ds+sd) \\ |U=1, U_3=-1\rangle = ss \end{cases} \\
&\text{singlet} \quad |U=0, U_3=0\rangle = \frac{1}{\sqrt{2}}(ds-sd).
\end{aligned} \tag{3.6}
$$

The wave functions of the V-spin triplet and singlet states can be written as

$$
\begin{aligned}
&\text{triplet} \quad \begin{cases} |V=1, V_3=1\rangle = uu \\ |V=1, V_3=0\rangle = \frac{1}{\sqrt{2}}(us+su) \\ |V=1, V_3=-1\rangle = ss \end{cases} \\
&\text{singlet} \quad |V=0, V_3=0\rangle = \frac{1}{\sqrt{2}}(us-su).
\end{aligned} \tag{3.7}
$$

The generators of both $SU(2)$ subgroups are the usual Pauli matrices, satisfying the commutation relation

$$
[\sigma_i, \sigma_j] = i\epsilon_{ijk}\sigma_k. \tag{3.8}
$$

In addition to symmetries mentioned, there is an additional symmetry for the $q\bar{q}$ meson states, i.e. for the mesons which have anti-quark pair of same quark. These states are the eigen states of the charge conjugation (alternatively C-parity) operator C which is defined as

$$
Cq = \bar{q}. \tag{3.9}
$$

In other words charge conjugation takes the particle to its anti-particle. So the $q\bar{q}$ states are the eigen states of C. Thus

$$
Cq_{(x)}\bar{q}_{(1-x)} = \pm q_{(1-x)}\bar{q}_{(x)}, \tag{3.10}
$$

where the subscripts x and $1-x$ denote the momentum fractions carried by each quark. For instance, for the pion triplet

$$
\begin{aligned}
C\begin{pmatrix} \pi^+ \\ \\ \pi^0 \\ \\ \pi^- \end{pmatrix} &= C\begin{pmatrix} u\bar{d} \\ \\ \frac{1}{\sqrt{2}}(u\bar{u} - d\bar{d}) \\ \\ d\bar{u} \end{pmatrix} \\
&= \begin{pmatrix} d\bar{u} \\ \\ \frac{1}{\sqrt{2}}(u\bar{u} - d\bar{d}) \\ \\ u\bar{d} \end{pmatrix} \\
&= \begin{pmatrix} \pi^- \\ \\ \pi^0 \\ \\ \pi^+ \end{pmatrix}.
\end{aligned} \tag{3.11}
$$

Notice that while π^0 remains same under C, π^+ and π^- are exchanged among themselves. Therefore all members of the the pion triplet are not C-parity eigen states.

For $q\bar{q}'$ states, the C-parity is generalized to G-parity. Under G-parity, the wave functions of the $q\bar{q}'$ states is either symmetric or anti-symmetric under the exchange of momentum fractions carried by each quark, thus they have either $+1$ or -1 eigenvalues respectively. G-parity operator($\mathcal{G}$) is defined due to $q\bar{q}'$ structure of the mesons as

$$
\mathcal{G} \equiv O^{(q\leftrightarrow q')}C \tag{3.12}
$$

where $O^{(q\leftrightarrow q')} = e^{i\pi I_2}$ is the operator interchanging q and q' quarks, and it is formulated as π radian of rotation about 2 axis of I(U)[V]-spin space for $ud(sd)[us]$ quarks, and $I_2(U_2)[V_2] = \frac{\sigma_2^{I(U)[V]}}{2}$ are the generators of $SU(2)$ subgroups. In $SU(3)$ symmetry, $m_u = m_d = m_s$, thus G-parity is conserved.

3.2 Classification of Mesons

In quark model[53], mesons are valence quark anti-quark pairs, i.e., $|q'\bar{q}\rangle$ states, and they are classified according to their quantum numbers. Some of these quantum numbers can be listed as

$$
\begin{array}{cccc}
\mathbf{S} & = & \mathbf{S}_{q'} + \mathbf{S}_{\bar{q}} & : & \text{spin,} \\
\mathbf{L} & & & : & \text{orbital angular momentum,} \\
\mathbf{J} & = & \mathbf{L} + \mathbf{S} & : & \text{total angular momentum,} \\
n & & & : & \text{radial quantum number,} \\
P & & (-1)^{L+1} & : & \text{parity number(for mesons),} \\
C & & (-1)^{L+S} & : & \text{charge conjugation(for neutral mesons),} \\
I(U)[V] - spin & & & : & SU(2) \text{ symmetries,} \\
G & & (-1)^{L+S}C = (-1)^{L+S+I} & : & \text{G-parity number,}
\end{array}
$$

where the values of spin for mesons are either of $0, 1$, due to the half integer spin of quarks, and the value of total angular momentum number lay in the region: $L - S \leq J \leq L + S$. The parity number depends on the spatial wave function of the meson and so on the orbital angular momentum, and $(-1)^{+1}$ in the definition of parity number comes from the intrinsic properties of the quark anti-quark pair, i.e., due to Dirac equation they should have opposite intrinsic parities. In the previous listing C denotes the charge conjugation and I is the isospin.

In terms of J^P notation, mesons are classified as

$$
\begin{array}{ccc}
0^+ & : & \text{scalar mesons,} \\
0^- & : & \text{pseudoscalar mesons,} \\
1^- & : & \text{vector mesons,} \\
1^+ & : & \text{axial vector mesons ,} \\
2^- & : & \text{pseudotensor mesons .}
\end{array}
\tag{3.13}
$$

On the other hand mesons can also be classified in terms of spectroscopic notation, i.e., $n^{2S+1}L_j$, in terms of orbital momentum eigenstates, where $L = S, P, D, F, ...$ are the names given to orbits with $L = 0, 1, 2, 3, ...$ respectively. The classification of mesons in terms of spectroscopic notation are given in table 3.2.

From the mesons listed in table 3.2, states $^1P_1$ and $^3P_1$ will be analyzed, since they are axial vector states with $J^{PC} = 1^{+-}$ and $J^{PC} = 1^{++}$.

3.3 Properties of K_1 Mesons

In QCD, two lowest nonets of axial vector mesons $J^P = 1^+$ are expected as the orbitally excited $q'\bar{q}$ states. As summarized in table 3.2, there are two types of P-wave axial vector mesons, namely 1^3P_1 and 1^1P_1, which are G-even and G-odd respectively. The $1^3P_1(1^{++})$ states are: $a_1(1260)$, $f_1(1285)$, $f_1(1420)$ and K_{1A}, and the $1^1P_1(1^{+-})$ states are $b_1(1235)$, $h_1(1170)$, $h_1(1380)$ and K_{1B}. Among those states, $a_1(1260)$ and $b_1(1235)$ are pure mass eigenstates. The 1^3P_1 states $f_1(1285)$ and $f_1(1420)$, and the 1^1P_1 states $h_1(1170)$ and $h_1(1380)$ are mixed among themselves in terms of pure singlet and octet states like $\eta - \eta'$ mixing[54]. For K_{1A} and K_{1B} states, the situation is more complicated. In QCD language, a real hadron should be represented in terms of mass eigen states. K_{1A} and K_{1B} are not mass eigen states, however they mix to form $K_1(1270)$ and $K_1(1400)$ states which are physical[37, 38]. Although K_{1A} and K_{1B} are not physical, while studying any process involving $K_1(1270)$ and $K_1(1400)$, one might consider K_{1A} and K_{1B} and their properties.

The $K_1(1270)$ and $K_1(1400)$ states can be written in terms of $1^3P_1(K_{1A})$ and $1^1P_1(K_{1B})$ orbital angular momentum (G-parity) eigen states as follows:

$$\begin{pmatrix} |K_1(1270)\rangle \\ |K_1(1400)\rangle \end{pmatrix} = \mathcal{M}_\theta \begin{pmatrix} |K_{1A}\rangle \\ |K_{1B}\rangle \end{pmatrix}, \tag{3.14}$$

where

Table 3.2: Quantum numbers of mesons.

	L	singlet	triplet
s-wave	0	$^1S_0$ (0^{-+})	$^3S_1$ (1^{--})
p-wave	1	$^1P_1$ (1^{+-})	$^3P_{0,1,2}$ $(0^{++}, 1^{++}, 2^{++})$
d-wave	2	$^1D_2$ (2^{-+})	$^3D_{1,2,3}$ $(1^{--}, 2^{--}, 3^{--})$
f-wave	3	$^1F_3$ (3^{+-})	$^3F_{2,3,4}$ $(2^{++}, 3^{++}, 4^{++})$

$$\mathcal{M}_\theta = \begin{pmatrix} \sin\theta_{K_1} & \cos\theta_{K_1} \\ \cos\theta_{K_1} & -\sin\theta_{K_1} \end{pmatrix} \tag{3.15}$$

is the mixing matrix, and θ_{K_1} is the mixing angle[55, 56]. The magnitude of the mixing angle is estimated to be $34^\circ \le |\theta_{K_1}| \le 58^\circ$ [55, 56, 57, 58]. To estimate the sign of the θ_{K_1} the following analysis is performed[38]. In the covariant light front approach, the ratio of the branching fractions of radiative B decays to $K_1(1270)$ and $K_1(1400)$ are calculated as

$$\frac{\mathcal{B}(B \to K_1(1270)\gamma)}{\mathcal{B}(B \to K_1(1400)\gamma)} = \begin{cases} 10.1 \pm 6.2 & : \text{ for } \theta_{K_1} = -58^\circ , \\ 280 \pm 200 & : \text{ for } \theta_{K_1} = -37^\circ , \\ 0.02 \pm 0.02 & : \text{ for } \theta_{K_1} = 58^\circ , \\ 0.05 \pm 0.05 & : \text{ for } \theta_{K_1} = 37^\circ . \end{cases} \tag{3.16}$$

Since for the radiative decays of B meson into $K_1(1270, 1400)$ axial vector meson states, Belle reported the following branching fractions[33, 27]:

$$\begin{aligned} \mathcal{B}(B^+ \to K_1(1270)^+\gamma) &= (4.28 \pm 0.94 \pm 0.43) \times 10^{-5}, \\ \mathcal{B}(B^+ \to K_1(1400)^+\gamma) &< 1.44 \times 10^{-5}, \end{aligned} \tag{3.17}$$

the negative values for θ_{K_1} are favored. The window for θ_{K_1} is determined as[38]

$$\theta_{K_1} = -(34 \pm 13)^\circ. \tag{3.18}$$

When the interpolating currents of K_1 states are considered, the K_{1A} and K_{1B} can be distinguished using G-parity. While the wave function of K_{1A} state is G-even, the wave function of K_{1B} state is G-odd. Due to G-parity, K_{1A} and K_{1B} states couple to different interpolating currents. These currents are given as

$$\begin{aligned} J^A_\mu &= \bar{s}\gamma_\mu\gamma_5 d \\ J^T_{\mu\nu} &= \bar{s}\sigma_{\mu\nu}\gamma_5 d, \end{aligned} \tag{3.19}$$

where J_μ^A is the G-even axial vector current, and $J_{\mu\nu}^T$ is the G-odd tensor current. These currents are used in studying QCD sum rules analysis of $B \to K_1(1270, 1400)\ell^+\ell^-$ decays in the next chapter.

CHAPTER 4

SUM RULES ANALYSIS OF $B \to K_1(1270, 1400)\ell^+\ell^-$ DECAYS

4.1 Introduction

In this chapter, semileptonic $B \to K_1(1270)\ell^+\ell^-$ and $B \to K_1(1400)\ell^+\ell^-$ decays are analyzed in the frame work of QCD sum rules reviewed in chapter 2. Considering the K_1 mixing, the sum rules for $B \to K_1(1270, 1400)\ell^+\ell^-$ transitions are found as explained in chapter 3. From the result of these sum rules, the form factors of $B \to K_{1(A,B)}\ell^+\ell^-$ and $B \to K_1(1270, 1400)\ell^+\ell^-$ transitions are obtained.

4.2 Defining $B \to K_1(1270, 1400)\ell^+\ell^-$ transitions

In SM the $B \to K_1\ell^+\ell^-$ transitions occur via $b \to s\ell^+\ell^-$ loop transition, due to penguin and box diagrams shown in Fig. 4.1. The effective Hamiltonian for $b \to s\ell^+\ell^-$ transition is written as[39]

$$
\begin{aligned}
\mathcal{H} = \frac{G_F\alpha}{2\sqrt{2}\pi}V_{tb}V_{ts}^* \quad & \times \quad \Big\{C_9^{eff}\bar{s}\gamma_\mu(1-\gamma_5)b\bar{l}\gamma_\mu l \\
& + \quad C_{10}\bar{s}\gamma_\mu(1-\gamma_5)b\bar{l}\gamma_\mu\gamma_5 l \\
& - \quad 2C_7^{eff}\frac{m^b}{q^2}\bar{s}\sigma_{\mu\nu}q^\nu(1+\gamma_5)b\bar{l}\gamma_\mu l\Big\}, \qquad (4.1)
\end{aligned}
$$

where C_7^{eff}, C_9^{eff} and C_{10} are the Wilson coefficients, G_F is the Fermi constant, α is the fine structure constant at the Z scale, V_{ij} are the elements of the CKM matrix and $q = p - p'$ is the momentum transferred to leptons. By sandwiching the effective Hamiltonian in Eq. 4.1

between initial and final meson states, the transition amplitude for $B \to K_1\ell^+\ell^-$ decays is obtained as

$$\begin{aligned} \mathcal{M} = \frac{G_F\alpha}{2\sqrt{2}\pi}V_{tb}V_{ts}^* \quad &\times \quad \Big\{C_9^{eff}\langle K_1(p',\epsilon)|\bar{s}\gamma_\mu(1-\gamma_5)b|B(p)\rangle\bar{l}\gamma_\mu l \\ &+ \quad C_{10}\langle K_1(p',\epsilon)|\bar{s}\gamma_\mu(1-\gamma_5)b|B(p)\rangle\bar{l}\gamma_\mu\gamma_5 l \\ &- \quad 2C_7^{eff}\frac{m^b}{q^2}\langle K_1(p',\epsilon)|\bar{s}\sigma_{\mu\nu}q^\nu(1+\gamma_5)b|B(p)\rangle\bar{l}\gamma_\mu l\Big\}, \end{aligned} \tag{4.2}$$

where $p(p')$ is the momentum of the $B(K_1)$ meson, and ϵ is the polarization vector of the axial vector K_1 meson. In order to calculate the amplitude, the matrix elements in Eq. 4.2 should be found. These matrix elements are parameterized in terms of the form factors as

$$\begin{aligned} \langle K_1(p',\epsilon)|\bar{s}\gamma_\mu(1-\gamma_5)b|B(p)\rangle &= \frac{2iA(q^2)}{M+m}\varepsilon_{\mu\nu\alpha\beta}\epsilon^{*\nu}p^\alpha p'^\beta - V_1 q^2(M+m)\epsilon_\mu^* \\ &+ \frac{V_2(q^2)}{M+m}(\epsilon^*.p)P_\mu + \frac{V_3(q^2)}{M+m}(\epsilon^*.p)q_\mu \ , \end{aligned} \tag{4.3}$$

$$\begin{aligned} \langle K_1(p',\epsilon)|\bar{s}\sigma_{\mu\nu}q^\nu(1+\gamma_5)b|B(p)\rangle &= 2T_1(q^2)\varepsilon_{\mu\nu\alpha\beta}\epsilon^{*\nu}p^\alpha p'^\beta \\ &- iT_2(q^2)[(M^2-m^2)\epsilon_\mu^* - (\epsilon^*.p)P_\mu] \\ &- iT_3(q^2)(\epsilon^*.p)\left[q_\mu - \frac{q^2P_\mu}{M^2-m^2}\right] \ , \end{aligned} \tag{4.4}$$

where $P = p + p'$, $M \equiv M_B$, the mass of the B meson and $m \equiv m_{K_1}$ is the mass of the K_1 meson. The Dirac identity

$$\sigma_{\mu\nu}\gamma_5 = \frac{-i}{2}\varepsilon_{\mu\nu\alpha\beta}\sigma_{\alpha\beta} \tag{4.5}$$

with the convention $\gamma_5 = \gamma_0\gamma_1\gamma_2\gamma_3$ and $\varepsilon_{0123} = -1$ requires that $T_1(0) = T_2(0)$. The relation of the chosen form factors with the ones in the literature [38, 39, 55] are presented in table 4.1.

4.3 Sum rules for $B \to K_1(1270, 1400)\ell^+\ell^-$ transitions

In this section the sum rules for the form factors of $B \to K_1(1270, 1400)\ell^+\ell^-$ transitions are found. In QCD sum rules approach, to obtain the matrix elements in Eqs. 4.3 and 4.4, one should calculate the three-point correlation functions

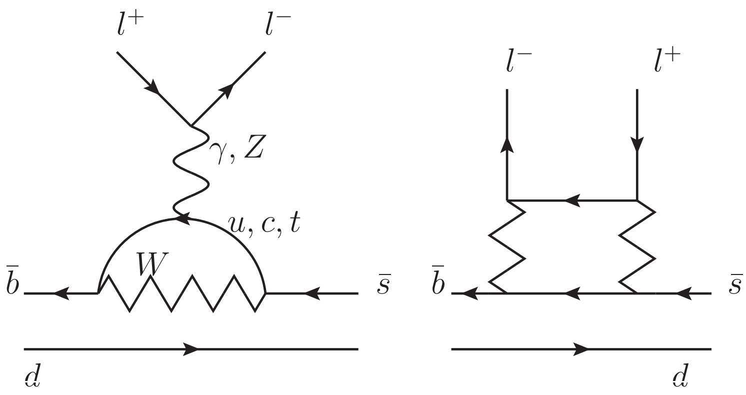

Figure 4.1: The loop penguin and box diagrams contributing to semileptonic B to K_1 transitions.

$$
\begin{aligned}
\Pi^{A,a}_{\mu\nu}(p^2, p'^2) &= i^2 \int dx^4 dy^4 e^{-ipx} e^{ip'y} \langle 0|T[J^A_\nu(y) J^a_\mu(0) J^\dagger_B(x)]|0\rangle, \\
\Pi^{T,a}_{\mu\nu\rho}(p^2, p'^2) &= i^2 \int dx^4 dy^4 e^{-ipx} e^{ip'y} \langle 0|T[J^T_{\nu\rho}(y) J^a_\mu(0) J^\dagger_B(x)]|0\rangle,
\end{aligned}
\tag{4.6}
$$

where $J^A_\nu = \bar{s}\gamma_\nu\gamma_5 d$ and $J^T_{\nu\rho} = \bar{s}\sigma_{\nu\rho}\gamma_5 d$ are axial vector and tensor interpolating currents creating K_1 states, $J_B = \bar{b}\gamma_5 d$ is the interpolating current of B mesons, and $J^a_\mu = J^{V-A,T+PT}_\mu$ are the vector and tensor parts of the transition currents with $J^{V-A}_\mu = \bar{b}\gamma_\mu(1-\gamma_5)s$ and $J^{T+PT} = \bar{b}\sigma_{\mu\varrho}q^\varrho(1+\gamma_5)s$.

The correlators in the phenomenological side are calculated in terms of the matrix elements of $K_1(1270)$ and $K_1(1400)$ states. The phenomenological parts of the correlators (Eq. 2.54) can be written as

Table 4.1: The relation of form factors used in this work, and used in literature[38, 39, 55].

this work	[38]	[39]	[55]
A	A	$g(M+m)$	
V_1	V_1	$f/(M+m)$	
V_2	V_2	$-a_+(M+m)$	
V_3	$\frac{-2m(M+m)}{q^2}(V_3 - V_0)$	$-a_-(M+m)$	
T_1	T_1	$-g_+$	$-Y_1/2$
T_2	T_2	$-g_+ - g_- \frac{q^2}{M+m}$	Y_2
T_3	T_3	$g_- + h(M+m)$	Y_2

$$\begin{aligned}
\Pi^{A,a}_{\mu\nu}(p^2, p'^2) &= -\frac{\langle 0|J^A_\nu|K_1(1270)(p',\epsilon)\rangle\langle K_1(1270)(p',\epsilon)|J^a_\mu|B(p)\rangle\langle B(p)|J_B|0\rangle}{R_1 R} \\
&- \frac{\langle 0|J^A_\nu|K_1(1400)(p',\epsilon)\rangle\langle K_1(1400)(p',\epsilon)|J^a_\mu|B(p)\rangle\langle B(p)|J_B|0\rangle}{R_2 R} \\
&+ \text{ higher resonances and continuum states,} \\
\Pi^{T,a}_{\mu\nu\rho}(p^2, p'^2) &= -\frac{\langle 0|J^T_{\nu\rho}|K_1(1270)(p',\epsilon)\rangle\langle K_1(1270)(p',\epsilon)|J^a_\mu|B(p)\rangle\langle B(p)|J_B|0\rangle}{R_1 R} \\
&- \frac{\langle 0|J^T_{\nu\rho}|K_1(1400)(p',\epsilon)\rangle\langle K_1(1400)(p',\epsilon)|J^a_\mu|B(p)\rangle\langle B(p)|J_B|0\rangle}{R_2 R} \\
&+ \text{ higher resonances and continuum states,}
\end{aligned} \quad (4.7)$$

where $R = p^2 - M^2$, $R_1 = p'^2 - m^2_{K_1(1270)}$ and $R_B = p'^2 - m^2_{K_1(1400)}$. The matrix elements for the B meson is defined as

$$\langle B(p)|J_B|0\rangle = -i\frac{F_B M^2}{m_b + m_d}. \quad (4.8)$$

In QCD sum rules, each correlator function has its own continuum. Due to this fact, obtaining the matrix elements $\langle K_1(1270)(p',\epsilon)|J^a_\mu|B(p)\rangle$ and $\langle K_1(1400)(p',\epsilon)|J^a_\mu|B(p)\rangle$ from two correlator reduces the reliability of the sum rules. An alternative way to obtain the transition matrix elements is to express $K_1(1400)$ and $K_1(1400)$ states in terms of K_{1A} and K_{1B} which are G-parity eigenstates as defined in Eq. 3.14[37, 38].

The matrix elements $\langle K_1(1270)|J_\mu|B\rangle$ and $\langle K_1(1400)|J_\mu|B\rangle$ in Eq. 4.2 can be written in terms of matrix elements $\langle K_{1A}|J_\mu|B\rangle$ and $\langle K_1(1400)|J_\mu|B\rangle$ states as[59]

$$\begin{pmatrix} \langle K_1(1270)|J_\mu|B\rangle \\ \\ \langle K_1(1400)|J_\mu|B\rangle \end{pmatrix} = \mathcal{M}_\theta \begin{pmatrix} \langle K_{1A}|J_\mu|B\rangle \\ \\ \langle K_{1B}|J_\mu|B\rangle \end{pmatrix} \tag{4.9}$$

where J_μ is any of the transition currents. Due to this relation, the form factors parameterizing $\langle K_1(1270, 1400)|J_\mu|B\rangle$ matrix elements can be expressed in terms of the form factors parameterizing $\langle K_{1(A,B)}|J_\mu|B\rangle$ matrix elements as follows

$$\begin{pmatrix} \xi f_i^{1270} \\ \\ \xi' f_i^{1400} \end{pmatrix} = \mathcal{M}_\theta \begin{pmatrix} \varsigma f_{i,A} \\ \\ \varsigma' f_{i,B} \end{pmatrix} \tag{4.10}$$

where f_i is defined as the form factors $\{A, V_1, V_2, V_3, T_1, T_2, T_3\}$ respectively for $i = 1, 2, ..., 7$, and f_i^{1270}, f_i^{1400}, $f_{i,A}$ and $f_{i,B}$ denotes the form factors parameterizing $\langle K_1(1270)|J_\mu|B\rangle$, $\langle K_1(1400)|J_\mu|B\rangle$, $\langle K_{1A}|J_\mu|B\rangle$ and $\langle K_{1B}|J_\mu|B\rangle$ matrix elements respectively. The values for factors ξ, ξ', ς and ς' are given in table 4.2, where $m_1 \equiv m_{K_1(1270)}$, $m_2 \equiv m_{K_1(1400)}$, $m_A \equiv m_{K_{1A}}$ and $m_B \equiv m_{K_{1B}}$. The masses of K_{1A} and K_{1B} states are defined as[38]

$$\begin{aligned} m_{K_{1A}}^2 &= m_{K_1(1400)}^2 \cos^2\theta_K + m_{K_1(1270)}^2 \sin^2\theta_K \\ m_{K_{1B}}^2 &= m_{K_1(1400)}^2 \sin^2\theta_K + m_{K_1(1270)}^2 \cos^2\theta_K. \end{aligned} \tag{4.11}$$

Table 4.2: The values for factors ξ, ξ', ς and ς' for the form factors.

f_i	ξ	ξ'	ς	ς'
A, V_2, V_3	$1/(M+m_1)$	$1/(M+m_2)$	$1/(M+m_A)$	$1/(M+m_B)$
V_1	$(M+m_1)$	$(M+m_2)$	$(M+m_A)$	$(M+m_B)$
T_1, T_3	1	1	1	1
T_2	$(M^2-m_1^2)$	$(M^2-m_2^2)$	$(M^2-m_A^2)$	$(M^2-m_B^2)$

Inserting Eqs. 3.14 and 4.9 in Eq. 4.7, and applying double Borel transformations(Eq. 2.68) with respect to the variables p^2 and p'^2 ($p^2 \to M_1^2, p'^2 \to M_2^2$), the phenomenological parts of the correlators are found in terms of G-parity eigen states as

$$
\begin{aligned}
\hat{\Pi}^{A,a}_{\mu\nu}(p^2,p'^2) &= -e^{\frac{-M^2}{M_1^2}} e^{\frac{-m_1^2}{M_2^2}} \Bigg\{ \langle 0|J^A_\nu \Bigg[s^2|K_{1A}(p',\epsilon)\rangle\langle K_{1A}(p',\epsilon)| + c^2|K_{1B}(p',\epsilon)\rangle\langle K_{1B}(p',\epsilon)| \\
&+sc\Bigg(|K_{1A}(p',\epsilon)\rangle\langle K_{1B}(p',\epsilon)| + |K_{1B}(p',\epsilon)\rangle\langle K_{1A}(p',\epsilon)|\Bigg)\Bigg] J^a_\mu |B(p)\rangle\langle B(p)|J_B|0\rangle \Bigg\} \\
&-e^{\frac{-M^2}{M_1^2}} e^{\frac{-m_2^2}{M_2^2}} \Bigg\{ \langle 0|J^A_\nu \Bigg[c^2|K_{1A}(p',\epsilon)\rangle\langle K_{1A}(p',\epsilon)| + s^2|K_{1B}(p',\epsilon)\rangle\langle K_{1B}(p',\epsilon)| \\
&-sc\Bigg(|K_{1A}(p',\epsilon)\rangle\langle K_{1B}(p',\epsilon)| + |K_{1B}(p',\epsilon)\rangle\langle K_{1A}(p',\epsilon)|\Bigg)\Bigg] J^a_\mu |B(p)\rangle\langle B(p)|J_B|0\rangle \Bigg\} \\
\hat{\Pi}^{T,a}_{\mu\nu\rho}(p^2,p'^2) &= -e^{\frac{-M^2}{M_1^2}} e^{\frac{-m_1^2}{M_2^2}} \Bigg\{ \langle 0|J^T_{\nu\rho} \Bigg[s^2|K_{1A}(p',\epsilon)\rangle\langle K_{1A}(p',\epsilon)| + c^2|K_{1B}(p',\epsilon)\rangle\langle K_{1B}(p',\epsilon)| \\
&+sc\Bigg(|K_{1A}(p',\epsilon)\rangle\langle K_{1B}(p',\epsilon)| + |K_{1B}(p',\epsilon)\rangle\langle K_{1A}(p',\epsilon)|\Bigg)\Bigg] J^a_\mu |B(p)\rangle\langle B(p)|J_B|0\rangle \Bigg\} \\
&-e^{\frac{-M^2}{M_1^2}} e^{\frac{-m_2^2}{M_2^2}} \Bigg\{ \langle 0|J^T_{\nu\rho} \Bigg[c^2|K_{1A}(p',\epsilon)\rangle\langle K_{1A}(p',\epsilon)| + s^2|K_{1B}(p',\epsilon)\rangle\langle K_{1B}(p',\epsilon)| \\
&-sc\Bigg(|K_{1A}(p',\epsilon)\rangle\langle K_{1B}(p',\epsilon)| + |K_{1B}(p',\epsilon)\rangle\langle K_{1A}(p',\epsilon)|\Bigg)\Bigg] J^a_\mu |B(p)\rangle\langle B(p)|J_B|0\rangle \Bigg\},
\end{aligned}
\tag{4.12}
$$

where $s \equiv \sin\theta_{K_1}$ and $c \equiv \cos\theta_{K_1}$. M_1^2 and M_2^2 appearing in Eq. 4.12 are Borel mass parameters and $\hat{\Pi}$ denotes the Borel transformation of Π.

The matrix elements $\langle K_{1(A,B)}|J_\mu|B\rangle$ of $K_{1(A,B)}$ states are defined in terms of both G parity conserving and violating decay constants discussed in [59]. The G parity conserving decay constants are given as

$$
\begin{aligned}
\langle K_{1A}(p',\epsilon)|\bar{s}\gamma_\mu\gamma_5 d|0\rangle &= i f_{K_{1A}} m_A \epsilon^*_\mu, \\
\langle K_{1B}(p',\epsilon)|\bar{s}\sigma_{\mu\nu}\gamma_5 d|0\rangle &= f^\perp_{K_{1B}}[\epsilon^*_\mu p'_\nu - \epsilon^*_\nu p'_\mu],
\end{aligned}
\tag{4.13}
$$

and the G parity violating decay constants are given as

$$
\begin{aligned}
\langle K_{1A}(p',\epsilon)|\bar{s}\sigma_{\mu\nu}\gamma_5 d|0\rangle &= i f_{K_{1A}} a_0^{\perp K_{1A}}[\epsilon^*_\mu p'_\nu - \epsilon^*_\nu p'_\mu], \\
\langle K_{1B}(p',\epsilon)|\bar{s}\gamma_\mu\gamma_5 d|0\rangle &= i f^\perp_{K_{1B}} m_B (1GeV) a_0^{\parallel K_{1B}} \epsilon^*_\mu,
\end{aligned}
\tag{4.14}
$$

where $f_{K_{1A}}(\equiv f_A)$ and $f^{\perp}_{K_{1B}}(\equiv f_B)$ are the decay constants of K_{1A} and K_{1B} mesons, and $a_0^{\perp K_{1A}}$ and $a_0^{\parallel K_{1B}}$ are the zeroth Gagenbauer moments. Since the Gagenbauer moments are zero in $SU(3)$ limit[37], the G parity violating matrix elements are expected to be small. In [59], their values are predicted as

$$\begin{aligned} a_0^{\perp K_{1A}} &= 0.08 \pm 0.09 \ , \\ a_0^{\parallel K_{1B}} &= 0.14 \pm 0.15 \ , \end{aligned} \tag{4.15}$$

which are consistent with zero. In this thesis, they are neglected. After defining the matrix elements $\langle K_{1(A,B)}|J_\mu|B\rangle$ and inserting in Eq. 4.12 the following assumptions are made.

$$\begin{aligned} &e^{\frac{-m_1^2}{M_2^2}} s^2|K_{1A}(p',\epsilon)\rangle\langle K_{1A}(p',\epsilon)| + e^{\frac{-m_2^2}{M_2^2}} c^2|K_{1A}(p',\epsilon)\rangle\langle K_{1A}(p',\epsilon)| \sim e^{\frac{-m_A^2}{M_2^2}}|K_{1A}(p',\epsilon)\rangle\langle K_{1A}(p',\epsilon)| \\ &e^{\frac{-m_1^2}{M_2^2}} c^2|K_{1B}(p',\epsilon)\rangle\langle K_{1B}(p',\epsilon)| + e^{\frac{-m_2^2}{M_2^2}} s^2|K_{1B}(p',\epsilon)\rangle\langle K_{1B}(p',\epsilon)| \sim e^{\frac{-m_B^2}{M_2^2}}|K_{1B}(p',\epsilon)\rangle\langle K_{1B}(p',\epsilon)| \\ &(e^{\frac{-m_1^2}{M_2^2}} - e^{\frac{-m_2^2}{M_2^2}})sc\Big(|K_{1A}(p',\epsilon)\rangle\langle K_{1B}(p',\epsilon)| + |K_{1B}(p',\epsilon)\rangle\langle K_{1A}(p',\epsilon)|\Big) \sim 0. \end{aligned} \tag{4.16}$$

The numerical values of the masses of K_1 states given in numerical discussions satisfy $m_1 < m_A < m_B < m_2$. And also the minimum value of the Borel mass parameter M_2^2 guarantees $e^{\frac{-m_1^2+m_2^2}{M_2^2}} > 0.94$. Due to this considerations the assumptions made in Eq. 4.16 effects the results of the form factors by less than 5%. After employing the assumptions defined in Eq. 4.16, the phenomenological parts of the correlators are written in terms of G-parity eigenstates as

$$\begin{aligned} \hat{\Pi}^{A,a}_{\mu\nu}(p^2,p'^2) &= -e^{\frac{-M^2}{M_1^2}} e^{\frac{-m_A^2}{M_2^2}} \langle 0|J^A_\nu|K_{1A}(p',\epsilon)\rangle\langle K_{1A}(p',\epsilon)|J^a_\mu|B(p)\rangle\langle B(p)|J_B|0\rangle \\ \hat{\Pi}^{T,a}_{\mu\nu\rho}(p^2,p'^2) &= -e^{\frac{-M^2}{M_1^2}} e^{\frac{-m_B^2}{M_2^2}} \langle 0|J^T_{\nu\rho}|K_{1B}(p',\epsilon)\rangle\langle K_{1B}(p',\epsilon)|J^a_\mu|B(p)\rangle\langle B(p)|J_B|0\rangle. \end{aligned} \tag{4.17}$$

Using equations 4.8, 4.13 and 4.17 and summing over the polarizations of the $K_{1(A,B)}$ mesons, the so called phenomenological parts of the correlation functions are found and expressed in terms of selected structures as

$$
\begin{aligned}
\hat{\Pi}^{A(V-A)}_{\mu\nu} &= \frac{F_B M^2}{m_b+m_c} f_A m_A e^{\frac{-M^2}{M_1^2}} e^{\frac{-m_A^2}{M_2^2}} \Bigg[g_{\mu\nu} A_A (M+m_A) \\
&\quad + \frac{1}{2} V_{2A} (M+m_A)(p_\mu p_\nu + p'_\mu p_\nu) \\
&\quad + \frac{1}{2} V_{3A} (M+m_A)(p_\mu p_\nu - p'_\mu p_\nu) \\
&\quad + i \frac{V_{1A} \varepsilon_{\mu\nu\rho\varrho} p^\rho p'^\varrho}{(M+m_A)} \Bigg], \\
\hat{\Pi}^{A(T+PT)}_{\mu\nu} &= \frac{F_B M^2}{m_b+m_c} f_A m_A e^{\frac{-M^2}{M_1^2}} e^{\frac{-m_A^2}{M_2^2}} \Bigg[i T_{1A} \varepsilon_{\mu\nu\rho\varrho} p^\rho p'^\varrho \\
&\quad + \frac{T_{2A} g_{\mu\nu}}{M^2 - m_A^2} + T_{3A} (p_\mu p_\nu + p'_\mu p_\nu)/2 \Bigg],
\end{aligned} \tag{4.18}
$$

and

$$
\begin{aligned}
\hat{\Pi}^{T(V-A)}_{\mu\nu\rho} &= i \frac{F_B M^2}{m_b+m_c} f_B e^{\frac{-M^2}{M_1^2}} e^{\frac{-m_B^2}{M_2^2}} \Bigg[A_B (M+m_B) g_{\mu\nu} p'_\rho \\
&\quad + \frac{1}{2} V_{2B} (M+m_B)(p_\mu p_\nu + p'_\mu p_\nu) p_\rho \\
&\quad + \frac{1}{2} V_{3B} (M+m_B)(p_\mu p_\nu - p'_\mu p_\nu) p_\rho \\
&\quad + i \frac{V_{1B} \varepsilon_{\mu\nu\alpha\varrho} p^\alpha p'^\varrho p_\rho}{(M+m_B)} \Bigg], \\
\hat{\Pi}^{T(T+PT)}_{\mu\nu\rho} &= \frac{F_B M^2}{m_b+m_c} f_B e^{\frac{-M^2}{M_1^2}} e^{\frac{-m_B^2}{M_2^2}} \Bigg[i \frac{1}{2} T_{1B} \varepsilon_{\mu\nu\alpha\varrho} p^\alpha p'^\varrho p_\rho \\
&\quad + \frac{T_{2B} g_{\mu\nu} p_\rho}{(M^2 - m_B^2)} \\
&\quad + \frac{1}{2} T_{3B} (p_\mu p_\nu + p'_\mu p_\nu) p_\rho \Bigg].
\end{aligned} \tag{4.19}
$$

In QCD sum rules, the correlation functions are also calculated theoretically using the operator product expansion (OPE) in the space-like region where $p'^2 \ll (m_s + m_d)^2$ and $p^2 \ll (m_b + m_d)^2$ in the so called deep Euclidean region as described in chapter 2. The contributions to the correlation functions in the QCD side of sum rules come from bare-loop (perturbative) diagrams and also quark condensates (nonperturbative).

The correlators in the QCD side are obtained by taking $\Gamma_1 \to \gamma_5$, $\Gamma_2 \to \gamma_\nu \gamma_5$ for K_{1A} and $\Gamma_2 \to \sigma_{\nu\rho}\gamma_5$ for K_{1B}, $\Gamma_3 \to \gamma_\mu(1-\gamma_5)$ for V-A interpolating currents, $\Gamma_3 \to \sigma_{\mu\rho} q^\rho (1+\gamma_5)$ for T+PT interpolating currents, $(Q, q', q) \to (b, s, d)$, $H_1 \to B$ and $H_2 \to K_{1A}(K_{1B})$ in equations 2.60, 2.61 and 2.62 given in section 2.3.

In QCD side of the calculations, in terms of the selected Lorentz structures, the correlators are written as

$$\begin{aligned}
\hat{\Pi}^{A(V-A)}_{\mu\nu} &= \hat{\Pi}_{A_A} g_{\mu\nu} \\
&+ \frac{\hat{\Pi}_{V_{2A}}(p_\mu p_\nu + p'_\mu p_\nu)}{2} + \frac{\hat{\Pi}_{V_{3A}}(p_\mu p_\nu - p'_\mu p_\nu)}{2} \\
&+ i\hat{\Pi}_{V_{1A}} \varepsilon_{\mu\nu\rho\varrho} p^\rho p'^\varrho, \\
\hat{\Pi}^{A(T+PT)}_{\mu\nu} &= \hat{\Pi}_{T_{1A}} \varepsilon_{\mu\nu\rho\varrho} p^\rho p'^\varrho + \hat{\Pi}_{T_{2A}} g_{\mu\nu} \\
&+ \hat{\Pi}_{T_{3A}} \frac{(p_\mu p_\nu + p'_\mu p_\nu)}{2},
\end{aligned} \tag{4.20}$$

and

$$\begin{aligned}
\hat{\Pi}^{T(V-A)}_{\mu\nu\rho} &= i\hat{\Pi}_{V_{2B}} \frac{(p_\mu p_\nu + p'_\mu p_\nu) p_\rho}{2} \\
&+ \frac{\hat{\Pi}_{V_{3B}}(p_\mu p_\nu - p'_\mu p_\nu) p_\rho}{2} \\
&+ \hat{\Pi}_{A_B} g_{\mu\nu} p'_\rho + i\hat{\Pi}_{V_{1B}} \varepsilon_{\mu\nu\alpha\varrho} p^\alpha p'^\varrho p_\rho, \\
\hat{\Pi}^{T(T+PT)}_{\mu\nu\rho} &= i\frac{\hat{\Pi}_{T_{1B}} \varepsilon_{\mu\nu\alpha\varrho} p^\alpha p'^\varrho p_\rho}{2} \\
&+ \hat{\Pi}_{T_{2B}} g_{\mu\nu} p_\rho \\
&+ \frac{\hat{\Pi}_{T_{3B}}(p_\mu p_\nu + p'_\mu p_\nu) p_\rho}{2}.
\end{aligned} \tag{4.21}$$

Each of $\hat{\Pi}_{f_{i(A,B)}}$ are expressed in terms of perturbative and nonperturbative contributions as

$$\hat{\Pi}_{f_{i(A,B)}} = \hat{\Pi}^{pert}_{f_{i(A,B)}} + \hat{\Pi}^{nonpert}_{f_{i(A,B)}}. \tag{4.22}$$

The perturbative parts of the correlators are written in terms of double dispersion relation for the coefficients of the selected Lorentz structures, as

$$\hat{\Pi}^{per}_{f_i} = \int ds \int ds' \rho_{f_i}(s, s', q^2) e^{\frac{-s}{M_1^2}} e^{\frac{-s'}{M_2^2}}, \tag{4.23}$$

where $\rho_{f_i}(s, s', q^2)$ are the spectral densities defined as

$$\rho_{f_i}(s, s'; q^2) = \frac{Im_s Im_{s'} \Pi^{OPE}_{f_i}(s, s'; q^2)}{\pi^2}. \tag{4.24}$$

The spectral densities in Eq. 4.23 are calculated by using the usual Feynman integral for the loop diagrams, with the help of Cutkovsky rules as discussed in chapter 2. The physical region in s, s' plane is described by the following inequality

$$-1 \le f(s, s') = \frac{2ss' + (m_b^2 - s - m_d^2)(s + s' - q^2) + 2s(m_b^2 - m_d^2)}{\lambda^{1/2}(m_b^2, s, m_d^2)\lambda^{1/2}(s, s', q^2)} \le +1, \tag{4.25}$$

where $\lambda(a,b,c) = a^2 + b^2 + c^2 - 2(ab + bc + ca)$.

The calculations lead to the following results for the spectral densities. For the $\langle K_{1A}|J_\mu|B\rangle$ matrix elements, the spectral densities are calculated as

$$\rho_{A_A} = 2(M+m)I_0\{m_d + (-m_b + m_d)A_1 + (m_d + m_s)B_1\}, \tag{4.26}$$

$$\begin{aligned}\rho_{V_{1A}} = {} & \frac{2}{M+m}I_0\{m_d[(m_d - m_b)(m_d + m_s) - q^2 + s + s'] \\ & +[2m_s s + m_b(q^2 - s - s') + m_d(-q^2 + 3s + s')]A_1 + 4(m_b - m_d)A_2 \\ & +[(m_d + m_s)(s - q^2) + (m_s + 3m_d - 2m_b)]B_1\},\end{aligned} \tag{4.27}$$

$$\begin{aligned}\rho_{V_{2A}} = {} & 2(M+m)I_0\{m_d - (m_b - 3m_d)A_1 + (m_d + m_s)B_1 \\ & -2(m_b - m_d)(B_2 + D_2)\},\end{aligned} \tag{4.28}$$

$$\begin{aligned}\rho_{V_{3A}} = {} & -2(M+m)I_0\{m_d - (m_b + m_d)A_1 + (m_d + m_s)B_1 \\ & +2(m_b - m_d)(B_2 - D_2)\},\end{aligned} \tag{4.29}$$

$$\begin{aligned}\rho_{T_{1A}} = {} & -4e^{\frac{-s}{M_1^2}}e^{\frac{-s'}{M_2^2}}I_0\{m_d(m_s - m_b) + 6A_2 \\ & +[s + (m_d - m_s)(m_s + m_d)]A_1 + [s' + (m_d - m_s)(m_s + m_d)]B_1 \\ & +2sB_2 - (q^2 - s)(C_2 + D_2) + s'(C_2 + D_2 + 2F_2)\}\end{aligned} \tag{4.30}$$

$$\begin{aligned}\rho_{T_{2A}} = {} & \frac{2}{M^2 - m^2}I_0\{-m_d[2m_d(s - s') \\ & +m_s(q^2 + s - s') + m_b(q^2 - s + s')] \\ & +[-m_d^2(q^2 + s - s') - m_d m_s(q^2 + s - s') + m_b(m_d + m_s)(q^2 + s - s') + s(q^2 - s + s')]A_1 \\ & +2(q^2 + s - s')A_2 + [(m_d - m_b)(m_d + m_s)(q^2 - s + s') - (q^2 + s - s')s']B_1\},\end{aligned} \tag{4.31}$$

$$\begin{aligned}\rho_{T_{3A}} = {} & 2I_0\{m_d(2m_d - m_b + m_s) + [s + (m_d - m_b)(m_d + m_s)]A_1 \\ & -2A_2 + [s' + (m_d - m_b)(m_d + m_s)]B_1 + 2q^2 D_2\}.\end{aligned} \tag{4.32}$$

For the $\langle K_{1B}|J_\mu|B\rangle$ matrix elements, the spectral densities are calculated as

$$\begin{aligned}
\rho_{A_B} &= -8(M+m)I_0(s,s',q^2)\{B_1+D_2+F_2\}, && (4.33)\\
\rho_{V_{1B}} &= \frac{4}{M+m}I_0(s,s',q^2)\{(m_b-m_d)m_d - sA_1 && (4.34)\\
&\quad +[(m_b-m_d)(m_d+m_s)+q^2-s-s']B_1\\
&\quad -2sD_2+(q^2-s-s')F_2\},\\
\rho_{V_{2B}} &= -4(M+m)I_0(s,s',q^2)\{B_1+D_2+F_2\}, && (4.35)\\
\rho_{V_{3B}} &= 4(M+m)I_0(s,s',q^2)\{B_1-D_2+F_2\}, && (4.36)\\
\rho_{T_{1B}} &= 8I_0(s,s',q^2)\{(m_b-m_s)(B_1+D_2+F_2)\}, && (4.37)\\
\rho_{T_{2B}} &= \frac{-4}{M^2-m^2}I_0(s,s',q^2)\{[s'+(m_d-m_b)(m_d+m_s)-4(m_b-m_d)A_2] && (4.38)\\
&\quad +[sm_s+s'm_b+m_d(q^2-2s')]A_1+s'(m_b-2m_d+m_s)B_1\\
&\quad +(m_d-m_b)(q^2+s-s')B_2+(m_b-m_d)(q^2-s+s')C_2\},\\
\rho_{T_{3B}} &= -4I_0(s,s',q^2)\{m_d-(m_b-2m_d)A_1-2(m_b-2m_d)B_1 && (4.39)\\
&\quad -(m_b-m_d)(B_2+2D_2+F_2)\},
\end{aligned}$$

where

$$\begin{aligned}
I_0(s,s',q^2) &= \frac{1}{\lambda^{\frac{1}{2}}(s,s',q^2)}, && (4.40)\\
A_1 &= \frac{s'(q^2+s-s'-2m_b^2)+m_d^2(q^2-s+s')+m_s^2(s+s'-q^2)}{q^4-(s-s')^2-2q^2(s+s')}, && (4.41)\\
B_1 &= \frac{s(q^2-s+s'-2m_s^2)+m_d^2(q^2+s-s')+m_b^2(-s-s'+q^2)}{q^4-(s-s')^2-2q^2(s+s')}, && (4.42)\\
A_2 &= \frac{1}{2(q^4-(s-s')^2-2q^2(s+s'))} && (4.43)\\
&\quad \{m_d^4q^2+m_b^4s'+s(m_s^4+q^2s'-m_s^2(q^2-s+s'))\\
&\quad -m_b^2[s'(q^2+s-s')+m_d^2(q^2-s+s')+m_s^2(s+s'-q^2)]\\
&\quad -m_d^2[m_s^2(q^2+s-s')+q^2(-q^2+s+s')]\}
\end{aligned}$$

$$
\begin{aligned}
B_2 &= \frac{1}{(q^4-(s-s')^2-2q^2(s+s'))^2} && (4.44)\\
&\{m_s^4[q^4+s^2+4ss'+s'^2-2q^2(s+s')]\\
&+s'^2[6m_b^4+q^4+4sq^2+s^2\\
&-6m_b^2(q^2+s-s')-2(q^2+s)s'+s'^2]\\
&+m_d^4[(q^2-s)^2+4q^2s'-2ss'+s'^2]\\
&-2m_s^2s'[q^4-2s^2+q^2(s-2s')\\
&+ss'+s^{prime2}+3m_b^2(s+s'-q^2)]\\
&-2m_d^2[m_s^2((s-q^2)^2+(s+q^2)s'-2s'^2)\\
&+s'(-2q^4+(s-s')^2\\
&\quad+3m_b^2(q^2-s+s')+q^2(s+s'))]\},\\
C_2 &= \frac{1}{(q^4-(s-s')^2-2q^2(s+s'))^2} && (4.45)\\
&\{3m_b^4(q^2-s-s')s'\\
&-2m_b^2[(m_d^2-m_s^2)(q^2-s)^2+2m_s^2s'(q^2-2s)\\
&+s(m_d^2(q^2+s)+(q^2-s)(q^2+2s))\\
&\quad-s'^2(2m_d^2+m_s^2+2q^2-s)+s'^3]\\
&+m_d^4[2q^4-(s-s')^2-q^2(s+s')]\\
&-m_d^2[-q^6+q^4(s+s')-(s-s')^2(s+s')+q^2(s^2-6ss'+s'^2)\\
&\quad+2m_s^2(q^4-2s^2+q^2(s-2s')+ss'+s'^2)]\\
&-s[3m_s^4(s+s'-q^2)+2m_b^2((q^2-s)^2+(q^2-s)s'-2s'^2)\\
&\quad+s'(-2q^4+s-s'^2+q^2(s+s'))]\},\\
D_2 &= C_2, && (4.46)\\
F_2 &= \frac{1}{(q^4-(s-s')^2-2q^2(s+s'))^2} && (4.47)\\
&\{m_d^4[q^4+q^2s+s^2-2s'(q^2-s)+s'^2]\\
&+s^2[6m_s^4+(q^2-s)^2+4q^2s'-2ss'\\
&+s'^2-6m_s^2(q^2-s+s')]\\
&+m_b^4[q^4+s^2+4ss'+s'^2-2q^2(s+s')]\\
&-2m_d^2s[-2q^4+(s-s')^2+3m_s^2(q^2+s-s')+q^2(s+s')]\\
&-2m_b^2[m_d^2(q^4-2s^2+q^2(s-2s')+ss'+s'^2)\\
&\quad+s((q^2-s)^2+(q^2+s)q^2-2s'^2+3m_s^2(s+s'-q^2))]\}.
\end{aligned}
$$

The nonperturbative contributions to the correlators are calculated by taking the operators with dimensions $d = 3(\langle\bar{q}q\rangle)$, $d = 4(m_d\langle\bar{q}q\rangle)$ and $d = 5(m_0^2\langle\bar{q}q\rangle)$ into account. For the $\langle K_{1A}|J_\mu|B\rangle$ matrix elements nonperturbative parts of the correlators are calculated as

$$\begin{aligned}
\Pi_{A_A} &= (M+m)\langle\bar{q}q\rangle\{\frac{1}{rr'}\} + m_0^2(M+m)\langle\bar{q}q\rangle\{\frac{1}{8rr'^2} - \frac{m_s^2}{2rr'^3} \\
&\quad -\frac{m_b^2}{2r^3r'} + \frac{1}{8r^2r'} + \frac{m_b^2+m_d^2-q^2}{r^2r'^2}\},
\end{aligned} \tag{4.48}$$

$$\begin{aligned}
\Pi_{V_{1A}} &= \frac{\langle\bar{q}q\rangle}{M+m}\{\frac{(m_b-m_s)^2-q^2}{2rr'}\} \\
&\quad +\frac{m_0^2\langle\bar{q}q\rangle}{M+m}\{\frac{(q^2-(m_b-m_s)^2)m_s^2}{4rr'^3} + \frac{(q^2-(m_b-m_s)^2)m_b^2}{4r^3r'} \\
&\quad +\frac{m_b^2+7m_bm_s-q^2}{8rr'^2} + \frac{m_s^2+7m_bm_s-q^2}{8r^2r} \\
&\quad +\frac{((m_b-m_s)^2-q^2)(m_b^2+m_s^2-q^2)}{r^2r'^2}\},
\end{aligned} \tag{4.49}$$

$$\begin{aligned}
\Pi_{V_{2A}} &= (M+m)\langle\bar{q}q\rangle\{\frac{1}{2rr'}\} \\
&\quad -m_0^2(M+m)\langle\bar{q}q\rangle\{\frac{m_s}{4rr'^3} - \frac{1}{16rr'^2} \\
&\quad +\frac{1}{16r'r^2} + \frac{m_b}{4r^3r'} \\
&\quad +\frac{q^2-m_s^2-m_b^2}{16r^2r'^2}\},
\end{aligned} \tag{4.50}$$

$$\begin{aligned}
\Pi_{V_{3A}} &= -(M+m)\langle\bar{q}q\rangle\{\frac{1}{2rr'}\} \\
&\quad m_0^2(M+m)\langle\bar{q}q\rangle\{\frac{m_s}{4rr'^3} - \frac{1}{16rr'^2} + \frac{3}{16r'r^2} \\
&\quad +\frac{m_b}{4r^3r'} + \frac{q^2-m_s^2-m_b^2}{16r^2r'^2}\},
\end{aligned} \tag{4.51}$$

$$\begin{aligned}
\Pi_{T_{1A}} &= -\langle\bar{q}q\rangle\{\frac{(m_b-m_d)}{16rr'}\} - m_0^2\langle\bar{q}q\rangle\{\frac{m_s^2(m_b-m_s)}{rr'^3} + \frac{m_b^2(m_b-m_s)}{r^3r'} \\
&\quad -\frac{(m_b+8m_s)}{8rr'^2} + \frac{(m_b+m_s)}{8r^2r'} - \frac{(m_b-m_s)(m_b^2+m_d^2-q^2)}{8r^2r'^2}\},
\end{aligned} \tag{4.52}$$

$$\Pi_{T_{2A}} = -\frac{\langle\bar{q}q\rangle}{M^2-m^2}\{\frac{(m_b+m_d)(8m_b^2-9m_s^2+8m_b(m_b-2m_s)-8q^2)}{rr'}\} \quad (4.53)$$
$$-\frac{m_0^2\langle\bar{q}q\rangle}{M^2-m^2}\{\frac{m_b^2(m_b+m_s)(m_b^2+m_d^2-2m_bm_s-q^2)}{4r^3r'}$$
$$-\frac{[2m_b^3+7m_b^2m_s-m_s(7m_b^2-2m_s^2+7q^2)+2m_b(m_d^2-m_s^2-q^2)]}{16rr'^2}$$
$$+\frac{[9m_b^3-2m_s(m_d^2-q^2)+m_b(7m_d^2-14m_s^2+7q^2)]}{16r^2r'}$$
$$-\frac{(m_b+m_s)(m_b^2+m_d^2-q^2)(m_b^2+m_d^2-2m_bm_s-q^2)}{16r^2r'^2}$$
$$+\frac{m_s^2(m_b+m_s)(m_b^2+m_d^2-2m_bm_s-q^2)}{4rr'^3}\},$$
$$\Pi_{T_{3A}} = \langle\bar{q}q\rangle\{\frac{(m_b-m_d)}{16rr'}\}+m_0^2\langle\bar{q}q\rangle\{\frac{m_s^2(m_b-m_s)}{4rr'^3}+\frac{m_b^2(m_b-m_s)}{4r^3r'} \quad (4.54)$$
$$+\frac{(8m_b+m_s)}{16r^2r'}-\frac{(m_b-m_s)(m_b^2+m_d^2-q^2)}{16r^2r'^2}+-\frac{(m_b+8m_s)}{8rr'^2}\}.$$

For the $\langle K_{1B}|J_\mu|B\rangle$ matrix elements the nonperturbative parts of the correlators are calculated as

$$\Pi_{A_B} = 0, \quad (4.55)$$
$$\Pi_{V_{1B}} = \frac{\langle\bar{q}q\rangle}{M+m}\{\frac{m_b}{rr'}\}-\frac{m_0^2\langle\bar{q}q\rangle}{M+m}\{\frac{m_s^2m_b}{2r'^3r}+\frac{m_sm_b^2}{2r^3r} \quad (4.56)$$
$$+\frac{(m_b+m_s)}{8r'^2r}+\frac{7m_b}{8r'r^2}+\frac{m_b(q^2-m_b^2-m_s^2)}{8r^2r'^2}\},$$
$$\Pi_{V_{2B}} = 0, \quad (4.57)$$
$$\Pi_{V_{3B}} = 0, \quad (4.58)$$
$$\Pi_{T_{1B}} = 0, \quad (4.59)$$
$$\Pi_{T_{2B}} = -\frac{\langle\bar{q}q\rangle}{M^2-m^2}\{\frac{m_s(m_b+m_s)}{rr'}\}+\frac{m_0^2\langle\bar{q}q\rangle}{M^2-m^2}\{\frac{m_s^3(m_b+m_s)}{2r'^3r}+\frac{m_b^3(m_b+m_s)}{2r^3r'} \quad (4.60)$$
$$-\frac{m_s(m_b+m_s)(m_b^2+m_d^2-q^2)}{8r^2r'^2}+\frac{7m_bm_s}{8r'^2r}-\frac{m_b^2+m_s^2-7m_bm_s}{8r'r^2}\},$$
$$\Pi_{T_{3B}} = m_0^2\langle\bar{q}q\rangle\{\frac{1}{8r^2r'}-\frac{1}{8rr'^2}\}. \quad (4.61)$$

In the expressions of non-perturbative contributions to correlator (Eqs. 4.48 to 4.61), the first terms in brackets which are proportional to $\langle\bar{q}q\rangle$ are $d=3$ dimensional, and the second terms in brackets which are proportional to $m_0^2\langle\bar{q}q\rangle$ are $d=5$ dimensional contributions corresponding to operators $\langle\bar{q}q\rangle$ and $\langle\bar{q}\sigma Gq\rangle$.

To obtain the final expression for the sum rules of the form factors, the quark hadron duality assumption, which states that the phenomenological and perturbative spectral densities give the same result when integrated over an appropriate interval, is used. The quark hadron duality is expressed as[66]

$$\left[\int_{s_0}^{\infty}\int_{s_0'}^{\infty}+\int_{s_0}^{\infty}\int_{0}^{s_0'}+\int_{0}^{s_0}\int_{s_0'}^{\infty}\right]dsds'\{\rho^h_{f_i}(s,s',q^2)-\rho_{f_i}(s,s',q^2)\}=0, \tag{4.62}$$

where s_0 and s_0' are the continuum thresholds in s and s' channels, and $\rho^h(s,s',q^2)$ is the spectral density of the continuum in the phenomenological part.

After calculating all spectral densities and nonperturbative contributions to correlators, by equating the coefficients of the selected structures from the phenomenological side (Eqs. 4.18 and 4.19) and the theoretical side (Eqs. 4.20 and 4.21), the QCD sum rules for the form factors parameterizing $\langle K_{1(A,B)}|J_\mu|B\rangle$ matrix elements are found as

$$\begin{aligned} f_{i,A}(q^2) &= \frac{m_b+m_d}{f_A m_A F_B M^2} e^{\frac{M^2}{M_1^2}} e^{\frac{m^2}{M_2^2}} \\ &\quad \{\frac{-1}{4\pi}\int_0^{s_0} ds \int_0^{s_0'} ds' \Theta \rho_{f_{i,A}}(s,s',q^2) e^{\frac{-s}{M_1^2}} e^{\frac{-s'}{M_2^2}} + \hat{\Pi}^{nonpert}_{f_{i,A}}\}, \end{aligned} \tag{4.63}$$

and

$$\begin{aligned} f_{i,B}(q^2) &= -i\frac{m_b+m_d}{f_B(1\mathrm{GeV}) F_B M^2} e^{\frac{M^2}{M_1^2}} e^{\frac{m^2}{M_2^2}} \\ &\quad \{\frac{-1}{4\pi}\int_0^{s_0} ds \int_0^{s_0'} ds' \Theta \rho_{f_{i,B}}(s,s',q^2) e^{\frac{-s}{M_1^2}} e^{\frac{-s'}{M_2^2}} + \hat{\Pi}^{nonpert}_{f_{i,B}}\}. \end{aligned} \tag{4.64}$$

where $\Theta \equiv \Theta(1-f(s,s')^2)$ is the unit step function determining the integration region and $f(s,s')$ is the function defined in Eq. 4.25. The expressions for the form factors of $B \to K_1(1270,1400)\ell^+\ell^-$ transitions are obtained by using Eq. 4.10.

In this thesis the branching fractions of $B \to K_1(1270,1400)\ell^+\ell^-$ transitions are also estimated. The partial decay width of the B meson is found by squaring the amplitude in Eq. 4.2, and by multiplying with the phase space factors as

$$\frac{d\Gamma}{d\hat{q}} = \frac{G_F^2\alpha^2 M}{2^{14}\pi^5}|V_{tb}V_{ts}^*|^2\lambda^{1/2}(1,\hat{r},\hat{q})v\Delta(\hat{q})\ , \tag{4.65}$$

where $\hat{q}=q^2/M^2$ and

$$
\begin{aligned}
\Delta(\hat{q}) &= \frac{2}{3\hat{r}\hat{q}}M^2 Re\Big[-12M^2\hat{m}_l\hat{q}\lambda(1,\hat{r},\hat{q})\Big\{(\mathcal{E}_3-\mathcal{D}_2-\mathcal{D}_3)\mathcal{E}_1^*\\
&- (\mathcal{E}_2+\mathcal{E}_3-\mathcal{D}_3)\mathcal{D}_1^*\Big\} + 12M^4\hat{m}_l\hat{q}(1-\hat{r})\lambda(1,\hat{r},\hat{q})(\mathcal{E}_2-\mathcal{D}_2)(\mathcal{E}_3^*-\mathcal{D}_3^*)\\
&+ 48\hat{m}_l\hat{r}\hat{q}\Big\{3\mathcal{E}_1\mathcal{D}_1^* + 2M^4\lambda(1,\hat{r},\hat{q})\mathcal{E}_0\mathcal{D}_0^*\Big\} - 16M^4\hat{r}\hat{q}(\hat{m}_l-\hat{q})\lambda(1,\hat{r},\hat{q})\Big\{|\mathcal{E}_0|^2+|\mathcal{D}_0|^2\Big\}\\
&- 6M^4\hat{m}_l\hat{q}\lambda(1,\hat{r},\hat{q})\Big\{2(2+2\hat{r}-\hat{q})\mathcal{E}_2\mathcal{D}_2^* - \hat{q}|(\mathcal{E}_3-\mathcal{D}_3)|^2\Big\}\\
&- 4M^2\lambda(1,\hat{r},\hat{q})\Big\{\hat{m}_l(2-2\hat{r}+\hat{q})+\hat{q}(1-\hat{r}-\hat{q})\Big\}(\mathcal{E}_1\mathcal{E}_2^*+\mathcal{D}_1\mathcal{D}_2^*)\\
&+ \hat{q}\Big\{6\hat{r}\hat{q}(3+v^2)+\lambda(1,\hat{r},\hat{q})(3-v^2)\Big\}\Big\{|\mathcal{E}_1|^2+|\mathcal{D}_1|^2\Big\}\\
&- 2M^4\lambda(1,\hat{r},\hat{q})\Big\{\hat{m}_l[\lambda(1,\hat{r},\hat{q})-3(1-\hat{r})^2]-\hat{q}\Big\}\Big\{|\mathcal{E}_2|^2+|\mathcal{D}_2|^2\Big\}\Big], \qquad (4.66)
\end{aligned}
$$

and $\hat{r} = m^2/M^2$, $\hat{m}_l = m_l^2/M^2$ and $v = \sqrt{1-4\hat{m}_l/\hat{q}}$ is the final lepton velocity. The following definitions are also used.

$$
\begin{aligned}
\mathcal{D}_0 &= (C_9^{eff}+C_{10})\frac{A(q^2)}{M+m} + (2m_bC_7^{eff})\frac{T_1(q^2)}{q^2},\\
\mathcal{D}_1 &= (C_9^{eff}+C_{10})(M+m)V_1(q^2) + (2m_bC_7^{eff})(M^2-m^2)\frac{T_2(q^2)}{q^2},\\
\mathcal{D}_2 &= \frac{C_9^{eff}+C_{10}}{M+m}V_2(q^2) + (2m_bC_7^{eff})\frac{1}{q^2}\left[T_2(q^2)+\frac{q^2}{M^2-m^2}T_3(q^2)\right],\\
\mathcal{D}_3 &= (C_9^{eff}+C_{10})\frac{V_3(q^2)}{M+m} - (2m_bC_7^{eff})\frac{T_3(q^2)}{q^2},\\
\mathcal{E}_0 &= (C_9^{eff}-C_{10})\frac{A(q^2)}{M+m} + (2m_bC_7^{eff})\frac{T_3(q^2)}{q^2},\\
\mathcal{E}_1 &= (C_9^{eff}-C_{10})(M+m)V_1(q^2) + (2m_bC_7^{eff})(M^2-m^2)\frac{T_2(q^2)}{q^2},\\
\mathcal{E}_2 &= \frac{C_9^{eff}-C_{10}}{M+m}V_2(q^2) + (2m_bC_7^{eff})\frac{1}{q^2}\left[T_2(q^2)+\frac{q^2}{M^2-m^2}T_3(q^2)\right],\\
\mathcal{E}_3 &= (C_9^{eff}-C_{10})\frac{V_3(q^2)}{M+m} - (2m_bC_7^{eff})\frac{T_3(q^2)}{q^2}.
\end{aligned}
\qquad (4.67)
$$

4.4 Numerical results and discussions

In this section, the numerical results for the $B \to K_1\ell^+\ell^-$ transitions are presented. The expressions of form factors and the effective Hamiltonian depend on the parameters M_1^2, M_2^2, s_0, s_0', on the masses and decay constants of the K_1 and B states, on the values of V_{ij}, and on the values of the Wilson coefficients C_7^{eff}, C_9^{eff} and C_{10}. The values of the input parameters are presented in table 4.3.

The explicit expressions of the form factors in Eqs. 4.63 and 4.64 contain four auxiliary parameters: Borel parameters M_1^2 and M_2^2, as well as the continuum thresholds s_0 and s_0'. These are not physical quantities, hence the physical quantities , form factors, must be independent of these auxiliary parameters. The working region of M_1^2 and M_2^2 is determined by requiring that the higher state and continuum contributions are suppressed and the contribution of the highest order operator must be small. These conditions are both satisfied in the following regions; $12\, GeV^2 \leq M_1^2 \leq 20\, GeV^2$ and $4\, GeV^2 \leq M_2^2 \leq 8\, GeV^2$. The dependence of form factors T_{1A} and T_{1B} on Borel masses at $q^2 = 0$ are plotted in figures 4.2 and 4.3. From the figures it is found that the results are stable in the working region of Borel mass parameters.

The continuum thresholds s_0 and s_0' are determined by two-point QCD sum rules and related to the energy of the excited states. The form factors which are the physical quantities defining the transitions, should be stable with respect to the small variations of these parameters. In general, the continuum thresholds are taken to be $(m_{hadron} + 0.5)^2$ [64, 65, 1]. The dependence of form factors T_{1A} and T_{1B} on continuum thresholds at $q^2 = 0$ are plotted in figures 4.4 and 4.5. From the figures it is found that the results are stable for variations of s_0 and s_0'.

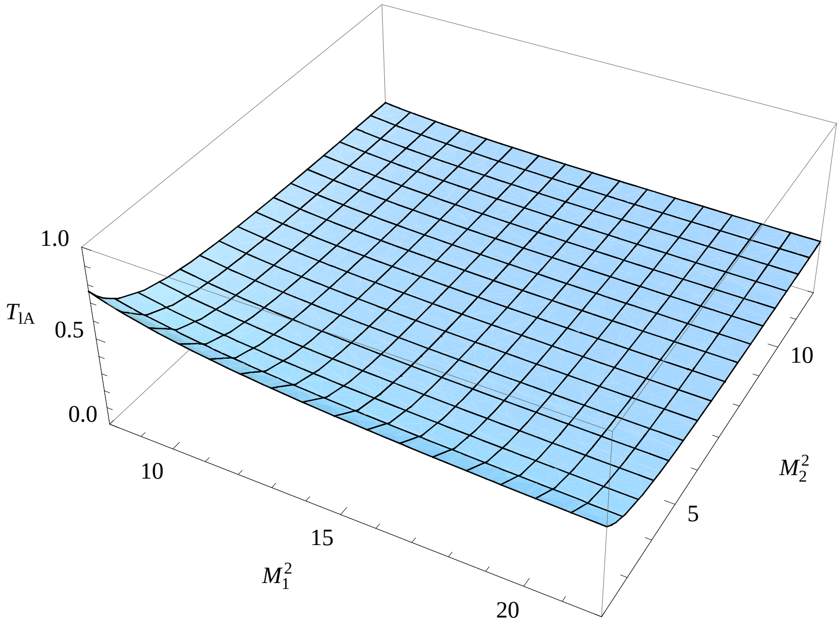

Figure 4.2: The dependence of the form factor T_{1A} on Borel mass parameters M_1^2 and M_2^2 at $q^2 = 0$ for $s_0 = 34 GeV^2$ and $s_0' = 4 GeV^2$.

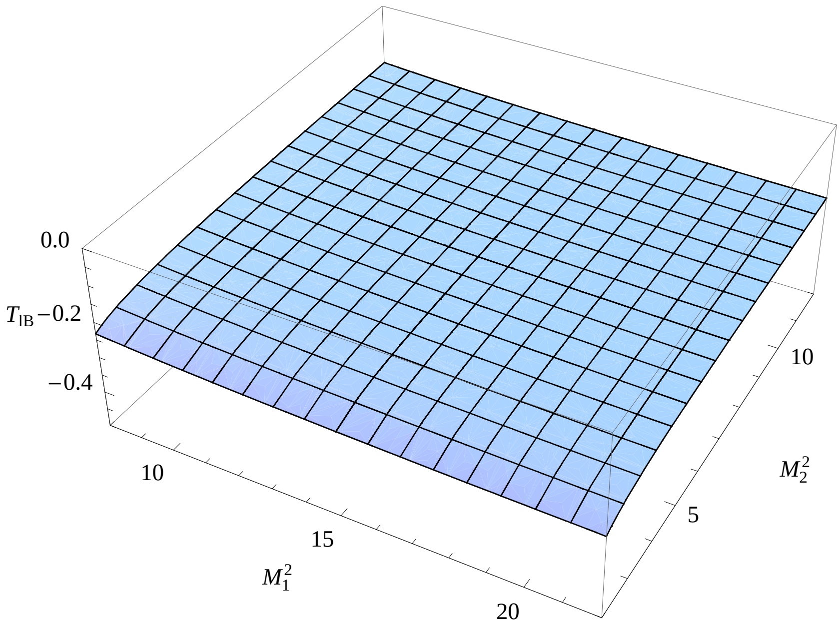

Figure 4.3: The dependence of the form factor T_{1B} on Borel mass parameters M_1^2 and M_2^2 at $q^2 = 0$ for $s_0 = 34 GeV^2$ and $s_0' = 4 GeV^2$.

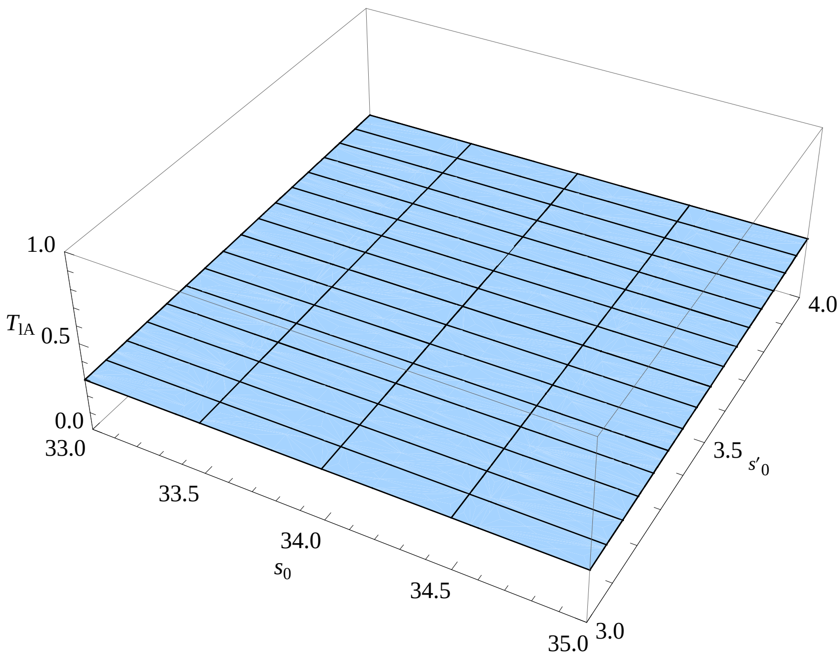

Figure 4.4: The dependence of the form factor T_{1A} on continuum thresholds s_0 and s'_0 at $q^2 = 0$ for $M_1^2 = 16GeV^2$ and $M_2^2 = 6GeV^2$.

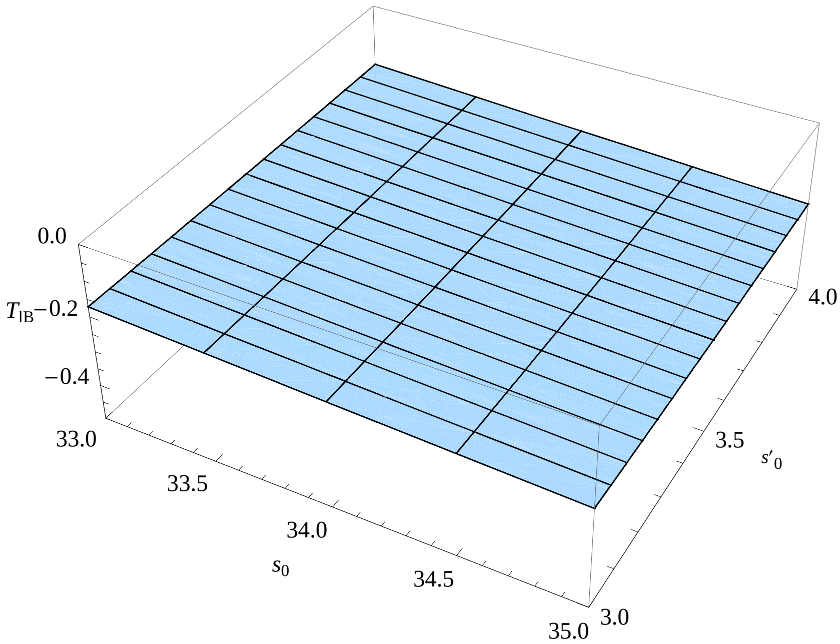

Figure 4.5: The dependence of the form factor T_{1B} on continuum thresholds s_0 and s'_0 at $q^2 = 0$ for $M_1^2 = 16GeV^2$ and $M_2^2 = 6GeV^2$.

The sum rules expressions for the form factors are truncated at 7 GeV^2. In order to extend our results to the whole physical region, i.e., $0 \leq q^2 < (m_B - m_{K_1})^2$ and for the reliability of the sum rules in the full physical region, a fit parametrization is applied such that in the region $-10GeV^2 \leq q^2 \leq -2\ GeV^2$, where the spectral integrals can be handled safely by applying Cutkovsky rules as discussed at the end of chapter 2, and this parametrization coincides with the sum rules predictions. To find the extrapolation of the form factors in the whole physical region, the fit function is chosen as

$$f_i(q^2) = \frac{f_i(0)}{1 - a\hat{q} + b\hat{q}^2}. \tag{4.68}$$

The values for a, b and $f_i(0)$ are given in Table 4.4 and 4.5 for the form factors of $B \to K_{1A}\ell^+\ell^-$ and $B \to K_{1B}\ell^+\ell^-$ transitions respectively. The errors in the values of $f_i(0)$ in tables 4.4 and 4.5 are due to uncertainties in sum rule calculations and also due to errors in input parameters.

Table 4.3: The values of the input parameters for numerical analysis.

INPUT PARAMETERS
$M_B = 5279$ MeV $\quad \tau_B = (1.525 \pm 0.002) \times 10^{-12}$s. $\quad F_B = 0.14 \pm 0.01\ GeV$[61]
$m_s = 95 \pm 25\ MeV \quad m_b = (4.7 \pm 0.07)\ GeV \quad m_d = (3 - 7)\ MeV$ [61] $\quad \langle \bar{q}q \rangle \equiv \langle \bar{d}d \rangle = -(240 \pm 10 MeV)^3$[63]
$m_{K_1}(1270) = 1.27\ GeV \quad m_{K_1}(1400) = 1.40\ GeV$ $f_A = (250 \pm 13)\ MeV \quad f_B = (190 \pm 10)\ MeV$ $m_A = (1.31 \pm 0.06)\ GeV \quad m_B = (1.34 \pm 0.08)\ MeV$ [45, 59, 61]
$V_{tb} \mid = 0.77^{+0.18}_{-0.24} \quad \mid V_{ts} \mid = (40.6 \pm 2.7) \times 10^{-3}$ [60]
$C_{10} = -4.669 \quad C_9^{eff} = 4.344 \quad C_7^{eff} = -0.313$ [62]
$G_F = 1.17 \times 10^{-5} GeV^{-2} \quad \alpha = 1/129$ [61]
$M_1^2 = 16 \pm 2\text{GeV}^2 \quad M_2^2 = 6 \pm 1\text{GeV}^2 \quad s_0 = 34 \pm 4\text{GeV}^2 \quad s_0' = 4 \pm 1\text{GeV}^2$

Table 4.4: The fit parameters and coupling constants of $B \to K_{1A}\ell^+\ell^-$ decay.

f_i	$f_i(0)$	a	b
A_A	0.47 ± 0.08	0.55	-1.3
V_{1A}	0.35 ± 0.07	0.23	-0.80
V_{2A}	0.36 ± 0.07	0.47	-0.28
V_{3A}	$-(0.39 \pm 0.08)$	0.39	-0.99
T_{1A}	0.38 ± 0.08	1.4	0.37
T_{2A}	0.38 ± 0.09	0.97	0.14
T_{3A}	0.36 ± 0.07	0.54	-0.18

Table 4.5: The fit parameters and coupling constants of $B \to K_{1B}\ell^+\ell^-$ decay.

f_i	$f_i(0)$	a	b
A_B	-0.31 ± 0.06	0.19	-0.11
V_{1B}	-0.40 ± 0.08	0.11	-0.18
V_{2B}	-0.34 ± 0.06	1.3	0.37
V_{3B}	0.39 ± 0.08	1.5	0.46
T_{1B}	-0.22 ± 0.05	1.31	0.37
T_{2B}	-0.21 ± 0.07	1.3	0.079
T_{3B}	-0.26 ± 0.04	1.41	0.41

The q^2 dependance of $f_{i,A}$ and $f_{i,B}$, the sum rules predictions and also the fit results, are plotted in the range $-10 \le q^2 \le M^2 - m^2$ in figures 4.6 to 4.19. It is seen from tables 4.4 and 4.5, and from figures 4.6 to 4.19 that the form factors of $B \to K_{1A}\ell^+\ell^-$ transition, i.e. $f_{i,A}$, and the form factors of $B \to K_{1B}\ell^+\ell^-$ transition, i.e. $f_{i,B}$ are opposite in sign.

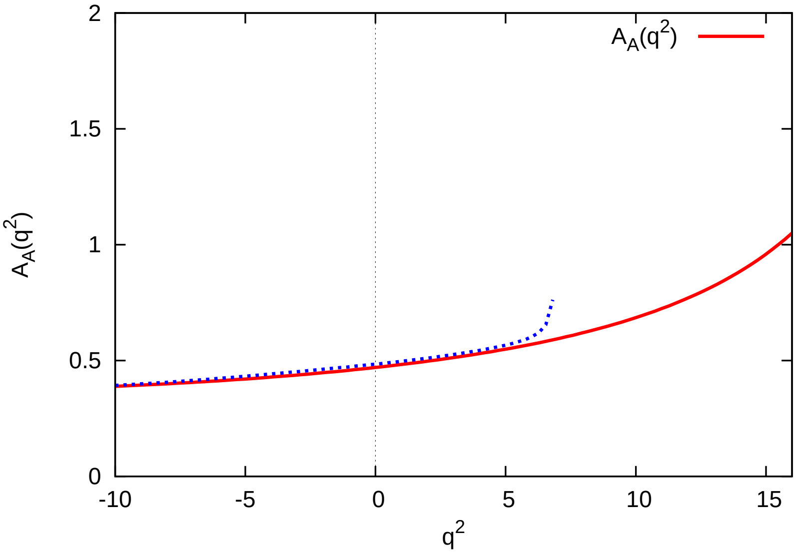

Figure 4.6: The q^2 dependence of the form factor A_A, sum rules prediction(blue-dashed) and fitted(red-solid) for $M_1^2 = 16GeV^2$, $M_2^2 = 6GeV^2$ and $s_0 = 34GeV^2$, $s_0' = 4GeV^2$.

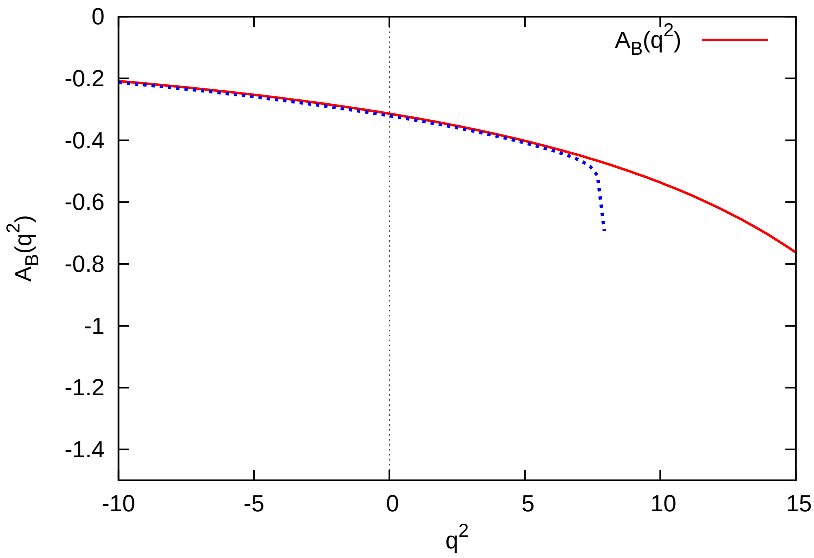

Figure 4.7: The q^2 dependence of the form factor A_B, sum rules prediction(blue-dashed) and fitted(red-solid) for $M_1^2 = 16GeV^2$, $M_2^2 = 6GeV^2$ and $s_0 = 34GeV^2$, $s_0' = 4GeV^2$.

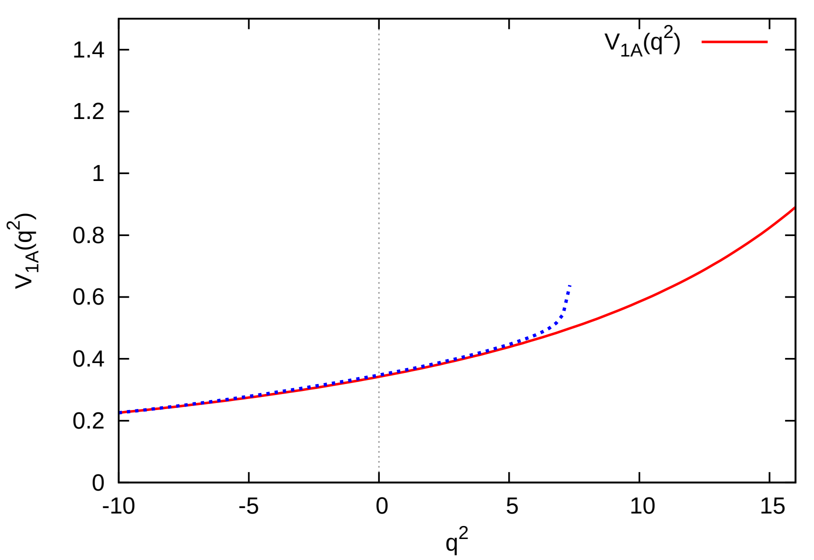

Figure 4.8: The q^2 dependence of the form factor V_{1A}, sum rules prediction(blue-dashed) and fitted(red-solid) for $M_1^2 = 16GeV^2$, $M_2^2 = 6GeV^2$ and $s_0 = 34GeV^2$, $s_0' = 4GeV^2$.

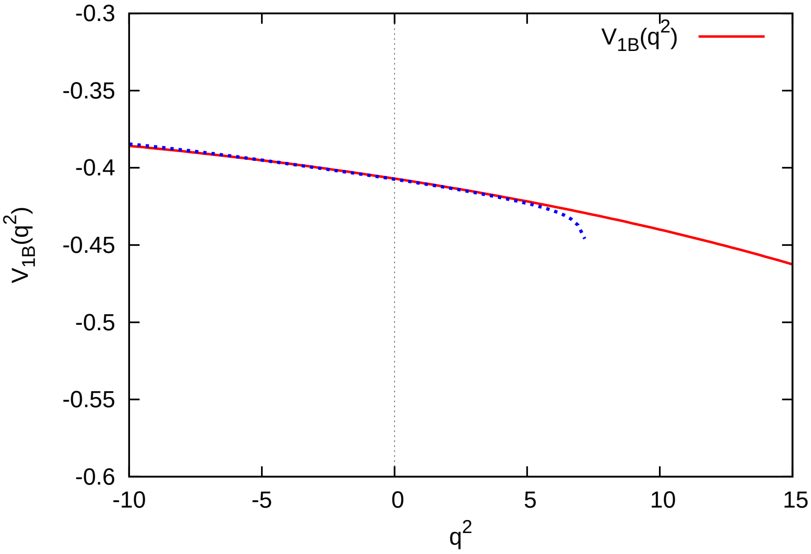

Figure 4.9: The q^2 dependence of the form factor V_{1B}, sum rules prediction(blue-dashed) and fitted(red-solid) for $M_1^2 = 16GeV^2$, $M_2^2 = 6GeV^2$ and $s_0 = 34GeV^2$, $s_0' = 4GeV^2$.

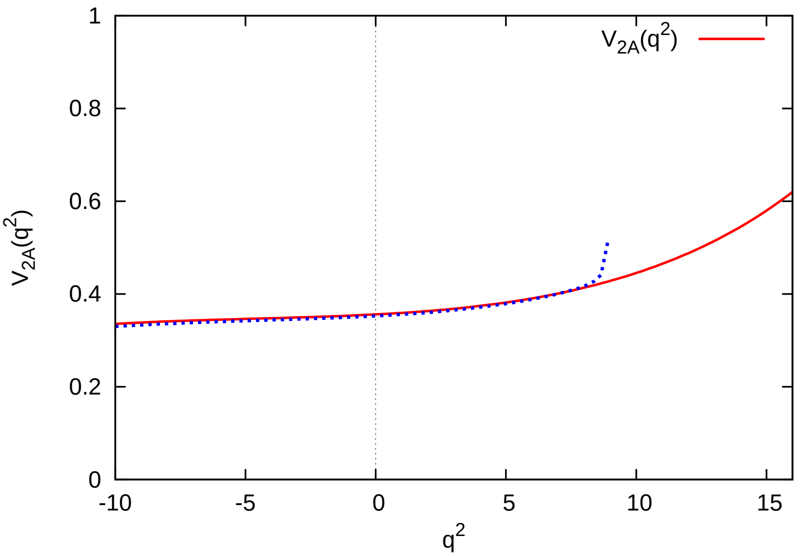

Figure 4.10: The q^2 dependence of the form factor V_{2A}, sum rules prediction(blue-dashed) and fitted(red-solid) for $M_1^2 = 16GeV^2$, $M_2^2 = 6GeV^2$ and $s_0 = 34GeV^2$, $s_0' = 4GeV^2$.

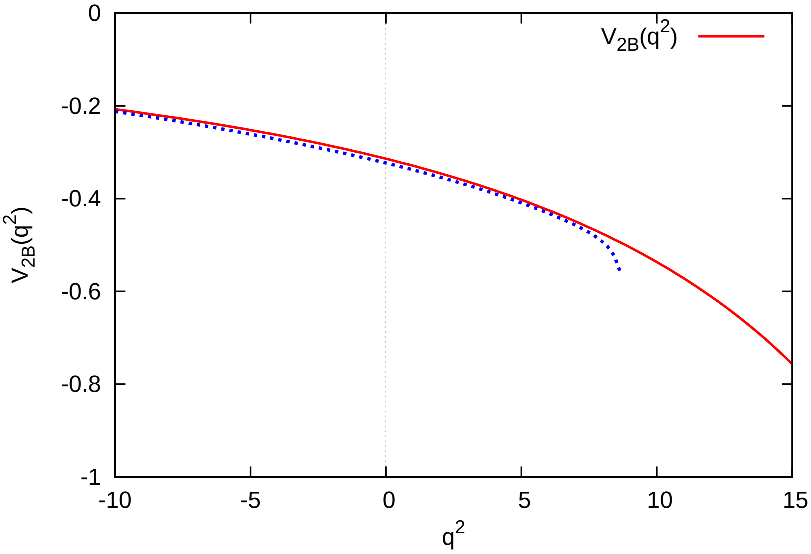

Figure 4.11: The q^2 dependence of the form factor V_{2B}, sum rules prediction(blue-dashed) and fitted(red-solid) for $M_1^2 = 16GeV^2$, $M_2^2 = 6GeV^2$ and $s_0 = 34GeV^2$, $s_0' = 4GeV^2$.

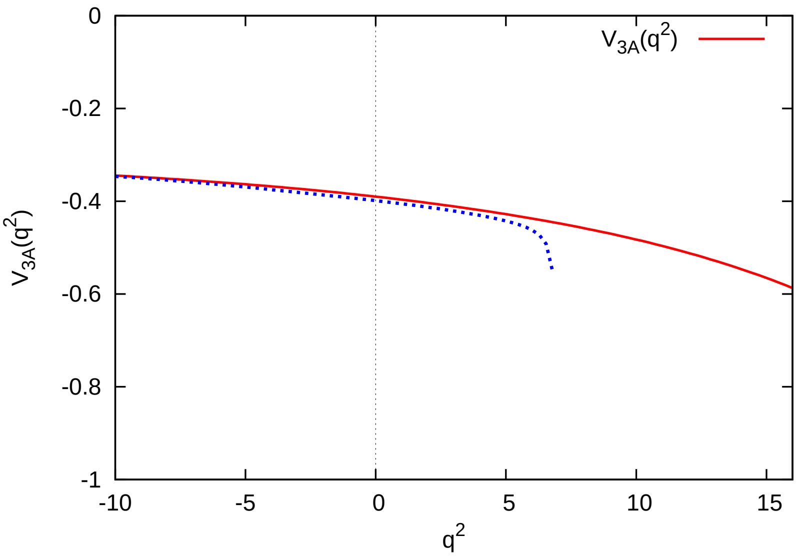

Figure 4.12: The q^2 dependence of the form factor V_{3A}, sum rules prediction(blue-dashed) and fitted(red-solid) for $M_1^2 = 16GeV^2$, $M_2^2 = 6GeV^2$ and $s_0 = 34GeV^2$, $s_0' = 4GeV^2$.

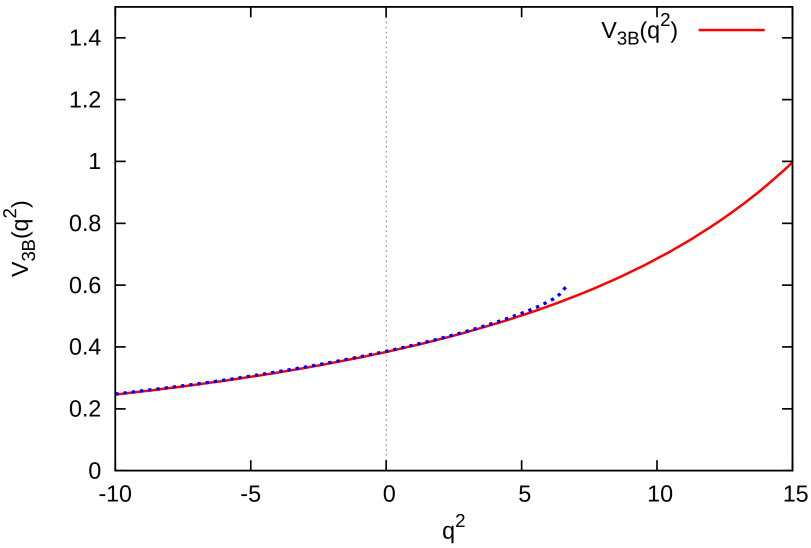

Figure 4.13: The q^2 dependence of the form factor V_{3B}, sum rules prediction(blue-dashed) and fitted(red-solid) for $M_1^2 = 16GeV^2$, $M_2^2 = 6GeV^2$ and $s_0 = 34GeV^2$, $s_0' = 4GeV^2$.

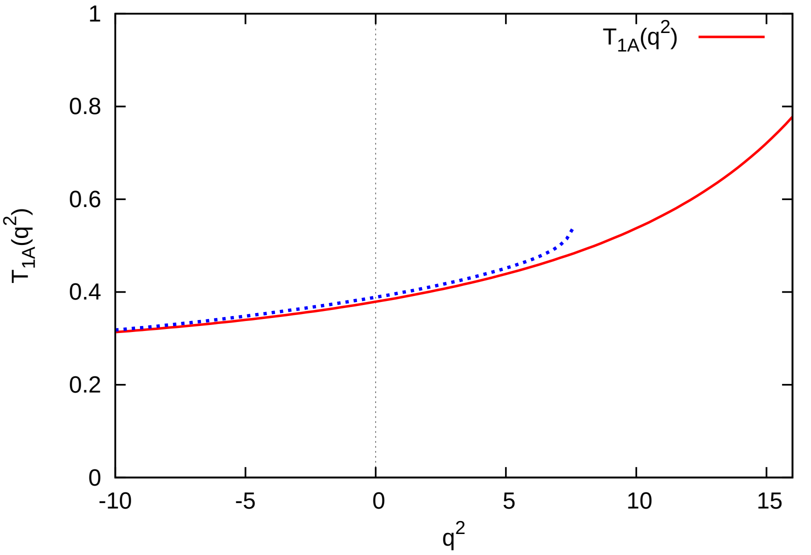

Figure 4.14: The q^2 dependence of the form factor T_{1A}, sum rules prediction(blue-dashed) and fitted(red-solid) for $M_1^2 = 16GeV^2$, $M_2^2 = 6GeV^2$ and $s_0 = 34GeV^2$, $s_0' = 4GeV^2$.

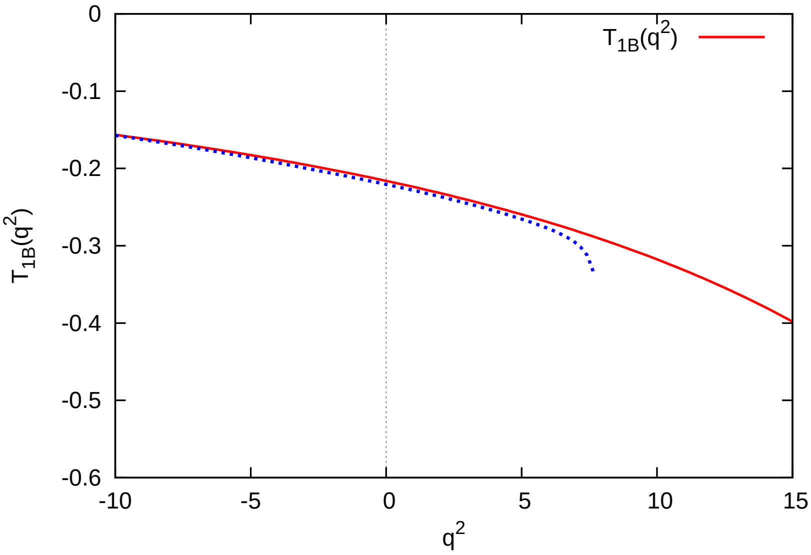

Figure 4.15: The q^2 dependence of the form factor T_{1B}, sum rules prediction(blue-dashed) and fitted(red-solid) for $M_1^2 = 16GeV^2$, $M_2^2 = 6GeV^2$ and $s_0 = 34GeV^2$, $s_0' = 4GeV^2$.

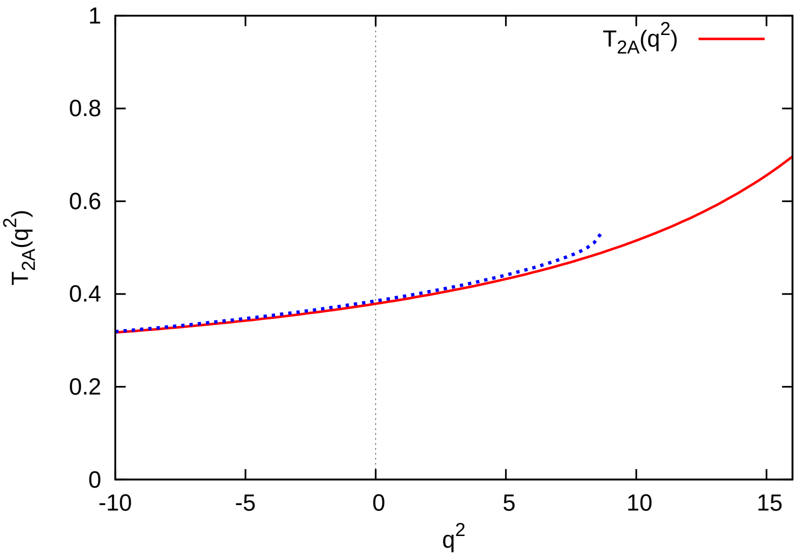

Figure 4.16: The q^2 dependence of the form factor T_{2A}, sum rules prediction(blue-dashed) and fitted(red-solid) for $M_1^2 = 16GeV^2$, $M_2^2 = 6GeV^2$ and $s_0 = 34GeV^2$, $s_0' = 4GeV^2$.

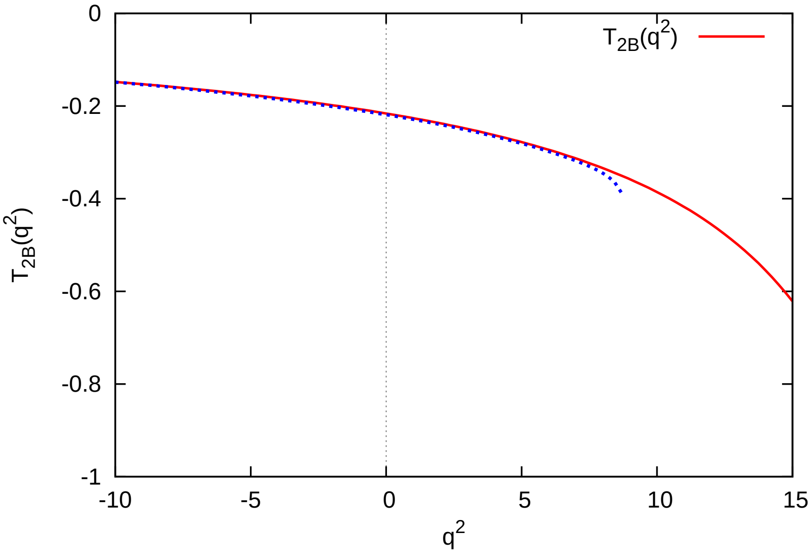

Figure 4.17: The q^2 dependence of the form factor T_{2B}, sum rules prediction(blue-dashed) and fitted(red-solid) for $M_1^2 = 16GeV^2$, $M_2^2 = 6GeV^2$ and $s_0 = 34GeV^2$, $s_0' = 4GeV^2$.

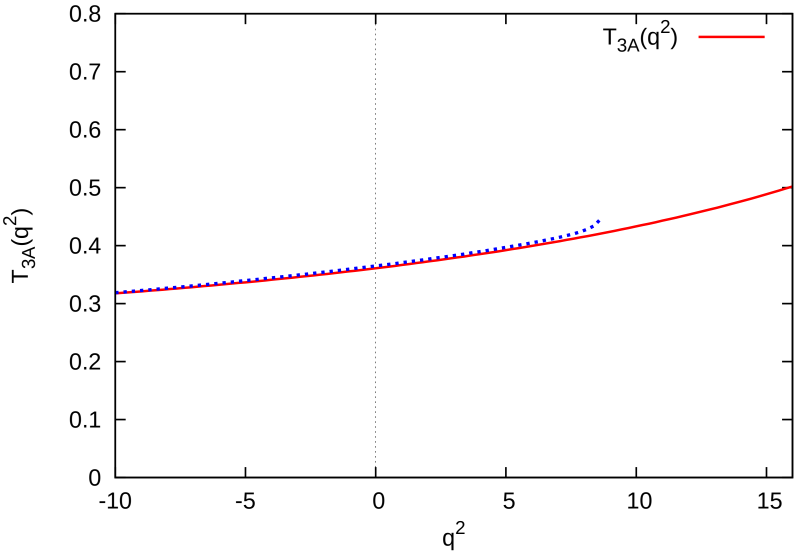

Figure 4.18: The q^2 dependence of the form factor T_{3A}, sum rules prediction(blue-dashed) and fitted(red-solid) for $M_1^2 = 16GeV^2$, $M_2^2 = 6GeV^2$ and $s_0 = 34GeV^2$, $s_0' = 4GeV^2$.

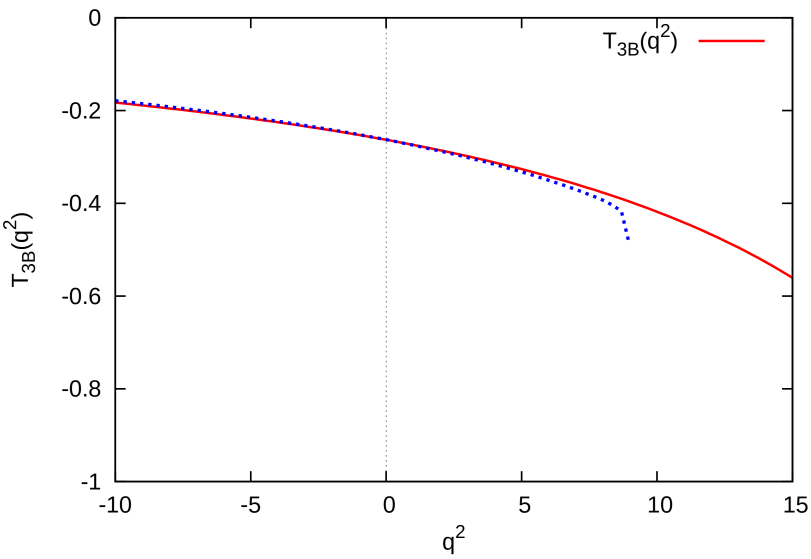

Figure 4.19: The q^2 dependence of the form factor T_{3B}, sum rules prediction(blue-dashed) and fitted(red-solid) for $M_1^2 = 16GeV^2$, $M_2^2 = 6GeV^2$ and $s_0 = 34GeV^2$, $s_0' = 4GeV^2$.

For the transitions to physical states, i.e. for $B \to K_1(1270, 1400)\ell^+\ell^-$ transitions, the dependance of the form factors of $B \to K_1(1270)\ell^+\ell^-$ on the mixing angle θ_{K_1} are plotted in figures 4.20 and 4.22, and the dependance of form factors of $B \to K_1(1400)\ell^+\ell^-$ on the mixing angle θ_{K_1} are plotted in figures 4.21 and 4.23 at $q^2 = 0$. The region between two black dashed vertical lines is the region estimated as $\theta_{K_1} = (-34 \pm 13)^\circ$[38]. It is seen from figures 4.20 and 4.22 that the absolute values the form factors of $B \to K_1(1270)\ell^+\ell^-$ transition are maximum at $\theta_{K_1} = -(45 \pm 5)^\circ$, and their values are zero at $\theta_{K_1} = 42 \pm 5^\circ$. For the form factors of $B \to K_1(1400)\ell^+\ell^-$ transitions, it is seen from figures 4.21 and 4.23 that the absolute values of the form factors are maximum at $\theta_{K_1} = 40 \pm 5^\circ$, their values are zero at $\theta_{K_1} = -(47 \pm 7)^\circ$. Since the region $\theta_{K_1} = -(47 \pm 7)^\circ$ in which form factors are zero coincides with the region $\theta_{K_1} = (-34 \pm 13)^\circ$, to obtain a precise prediction of the form factors, the mixing angle should be determined more precisely.

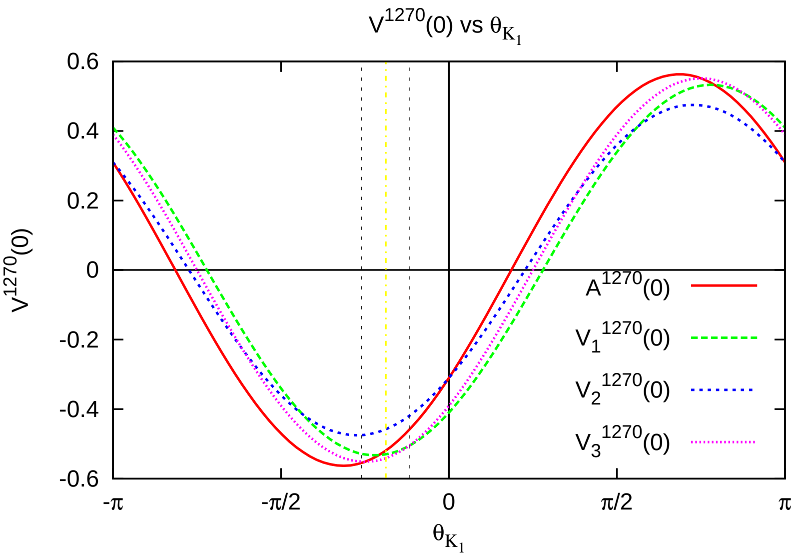

Figure 4.20: The θ_{K_1} dependence of the vector form factors of $B \to K_1(1270)\ell^+\ell^-$ at $q^2 = 0$.

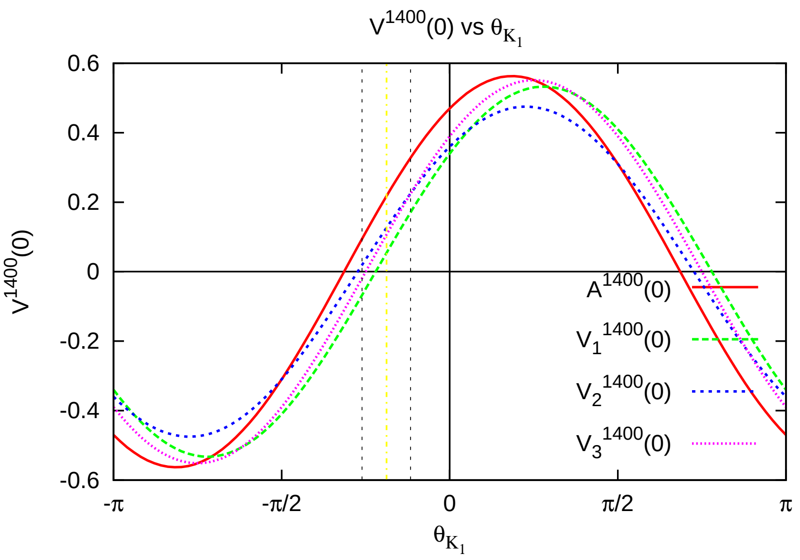

Figure 4.21: The θ_{K_1} dependence of the vector form factors of $B \to K_1(1400)\ell^+\ell^-$ at $q^2 = 0$.

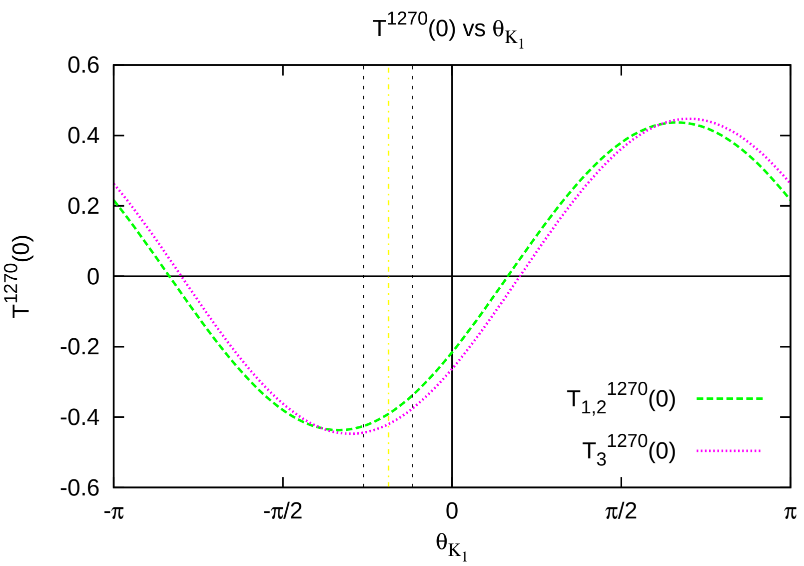

Figure 4.22: The θ_{K_1} dependence of the tensor form factors of $B \to K_1(1270)\ell^+\ell^-$ at $q^2 = 0$.

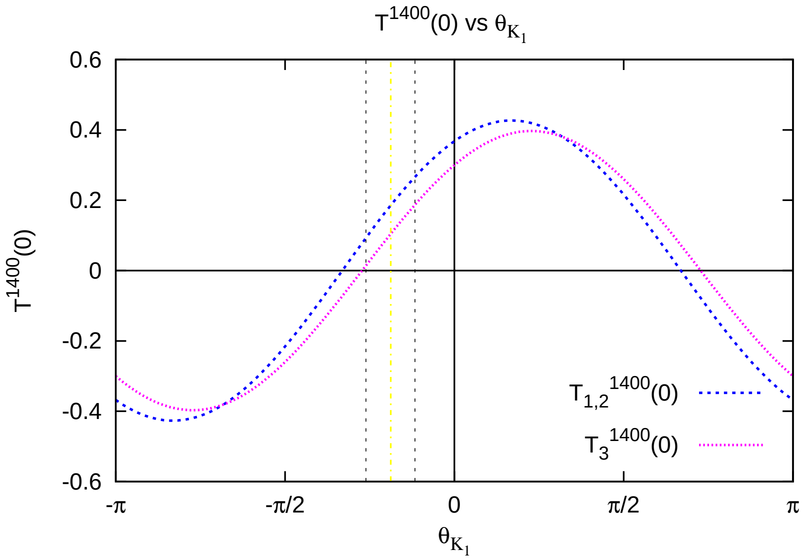

Figure 4.23: The θ_{K_1} dependence of the tensor form factors of $B \to K_1(1400)\ell^+\ell^-$ at $q^2 = 0$.

Finally, the branching fractions to leptonic final states e^+e^-, $\mu^+\mu^-$ and $\tau^+\tau^-$ for $\theta_{K_1} = -34^\circ$ are also estimated by integrating the partial width in Eq. 4.65. The results are presented in table 4.6 in comparison with the results found in [38]. The first errors in our results are due to uncertainties from sum rule calculations and input parameters, and the second errors are due to uncertainty in the mixing angle θ_{K_1}. Our results are in good agreement with the results found in [38].

In table 4.7, the inclusive branching ratios of $B \to X_s \ell^+\ell^-$ channels are presented. The first values in table 4.7 are the published averages by Heavy Flavor Averaging Group(HFAG)[67], and the second values are the recent values[68]. The results found in this thesis (table 4.6) are also in good agreement with this average values. Only when the new averages for the inclusive branching ratios[68] are considered, for $B \to K_1(1270)\mu^+\mu^-$ channel, the branching fraction is about the value inclusive branching ratio of $B \to X_s\mu^+\mu^-$ leaving no room for other semileptonic decays appearing quark level $b \to s\mu^+\mu^-$. But since the other decay channels have smaller width compared to $B \to X_s\mu^+\mu^-$, and when the errors in the values are considered, this result can also be acceptable. But this results implies that a new window for the value of θ_{K_1} should be searched.

The θ_{K_1} dependance of branching fractions and the ratios

$$R = \frac{\mathcal{B}(B \to K_1(1270)\ell^+\ell^-)}{\mathcal{B}(B \to K_1(1270)\ell^+\ell^-)} \tag{4.69}$$

in e^+e^- and $\mu^+\mu^-$ channels are also plotted in figures 4.24 and 4.25 respectively. According to our results, the value of θ_{K_1} is smaller then zero, but due to new limit from inclusive $B \to X_s\mu^+\mu^-$, the recent window for the value of θ_{K_1} should be reconsidered. Since the errors in the values are a bit higher, it is not possible to estimate a new window using branching ratios.

Table 4.6: The branching fractions of $B \to K_1(1270, 1400)\ell^+\ell^-$ decays for $\theta_{K_1} = -34°$.

mode	this work	[38]
$\mathcal{B}(K_1(1270)e^+e^-)$	$(2.11 \pm 0.82^{+0.42}_{-0.52}) \times 10^{-6}$	$(2.5^{+1.4+0.0}_{-1.1-0.3}) \times 10^{-6}$
$\mathcal{B}(K_1(1270)\mu^+\mu^-)$	$(2.10 \pm 0.81^{+0.41}_{-0.49}) \times 10^{-6}$	$(2.1^{+1.2+0.0}_{-0.9-0.2}) \times 10^{-6}$
$\mathcal{B}(K_1(1270)\tau^+\tau^-)$	$(0.42 \pm 0.21^{+0.11}_{-0.15}) \times 10^{-7}$	$(0.8^{+0.4+0.0}_{-0.3-0.1}) \times 10^{-7}$
$\mathcal{B}(K_1(1400)e^+e^-)$	$(1.1 \pm 0.4^{+0.4}_{-0.5}) \times 10^{-7}$	$(0.9^{+0.3+2.3}_{-0.3-0.4}) \times 10^{-7}$
$\mathcal{B}(K_1(1400)\mu^+\mu^-)$	$(1.0 \pm 0.4^{+0.4}_{-0.5}) \times 10^{-7}$	$(0.6^{+0.2+1.8}_{-0.1-0.2}) \times 10^{-7}$
$\mathcal{B}(K_1(1400)\tau^+\tau^-)$	$(0.3 \pm 0.2^{+0.1}_{-0.1}) \times 10^{-8}$	$(0.1^{+0.0+0.5}_{-0.0-0.1}) \times 10^{-8}$

Table 4.7: Experimental values of the inclusive branching fractions of $B \to s\ell^+\ell^-$ obtained from HFAG. The first values are the published averages from reference [67], and the second values are the preliminary averages[68].

mode	[67]	[68]
$\mathcal{B}(B \to X_s e^+e^-)$	$(4.7 \pm 1.3) \times 10^{-6}$	$(4.56 \pm 1.15^{+0.33}_{-0.40}) \times 10^{-6}$
$\mathcal{B}(B \to X_s \mu^+\mu^-)$	$(4.3 \pm 1.2) \times 10^{-6}$	$(1.91 \pm 1.02^{+0.16}_{-0.18}) \times 10^{-6}$
$\mathcal{B}(B \to X_s \ell^+\ell^-)$	$(4.5 \pm 1.0) \times 10^{-6}$	$(3.33 \pm 0.80^{+0.19}_{-0.24}) \times 10^{-6}$

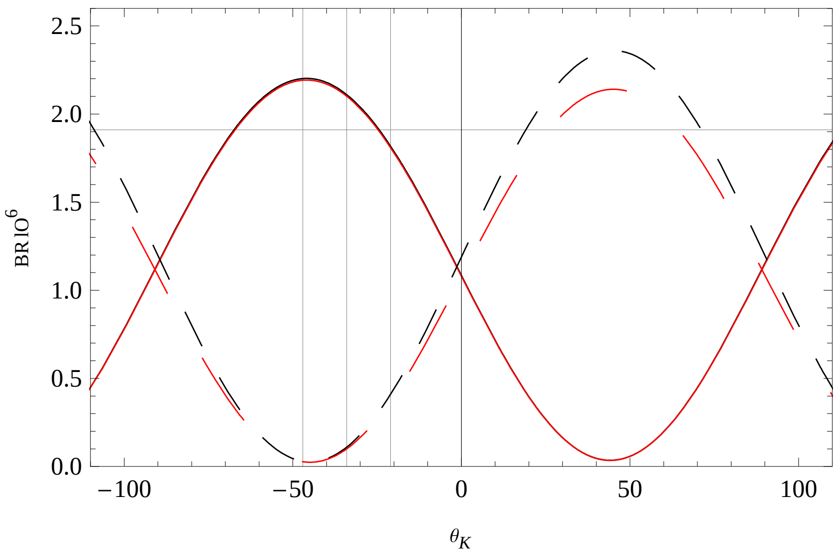

Figure 4.24: The θ_{K_1} dependence of the branching ratios of $B \to K_1(1270)e^+e^-$(black-solid), $B \to K_1(1270)\mu^+\mu^-$(red-solid), $B \to K_1(1400)e^+e^-$(black-dashed) and $B \to K_1(1270)\mu^+\mu^-$(red-dashed) channels. The horizontal line at 1.91 is the new average for inclusive $B \to X_s\mu^+\mu^-$ decays[68].

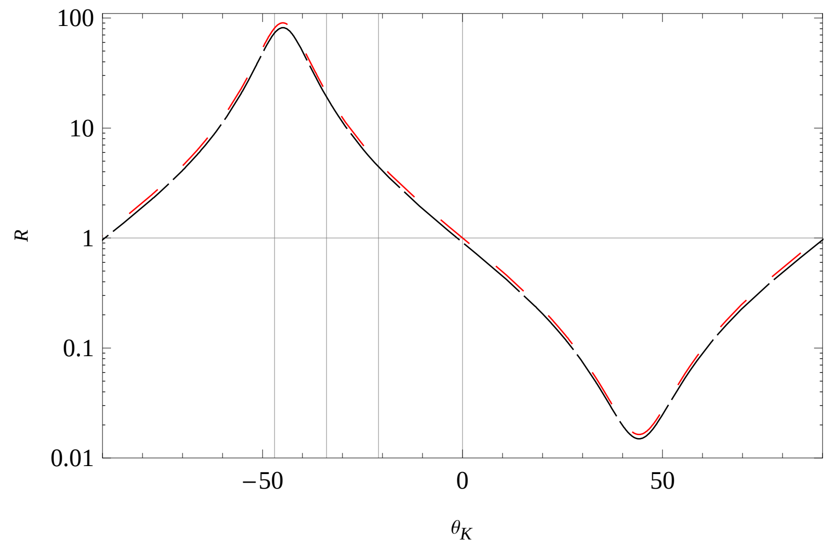

Figure 4.25: The θ_{K_1} dependance of the ratios(R) of branching fractions $R = \frac{\mathcal{B}(B\to K_1(1270)e^+e^-)}{\mathcal{B}(B\to K_1(1400)e^+e^-)}$(black-dashed) and $R = \frac{\mathcal{B}(B\to K_1(1270)\mu^+\mu^-)}{\mathcal{B}(B\to K_1(1400)\mu^+\mu^-)}$(red-dashed).

In conclusion, the form factors of $\langle K_{1(A,B)}|J_\mu|B\rangle$ matrix elements are calculated using three point QCD sum rules approach. The q^2 behaviors of the form factors of $B \to K_{1(A,B)}\ell^+\ell^-$ transitions are analyzed. Considering the axial vector mixing angle θ_{K_1}, the form factors of $B \to K_1(1270,1400)\ell^+\ell^-$ transitions, i.e. transitions into physical states are analyzed, and their dependance on the mixing angle θ_{K_1} at $q^2 = 0$ are obtained. Using these results, the branching fractions into final leptonic states are estimated. It is concluded that the transitions $B \to K_1(1270,1400)\ell^+\ell^-$ can be observed at LHC and further B factories and measurements on the mixing angle θ_{K_1} can be performed.

CHAPTER 5

CONCLUSION

In this thesis, the QCD sum rules approach, which is one of the powerful non-perturbative methods, is discussed and reviewed, and then applied to semileptonic $B \to K_1(1270)\ell^+\ell^-$ and $B \to K_1(1400)\ell^+\ell^-$ decays.

To study the semileptonic decay of B meson to $K_1(1270, 1400)$ states, using the definition of $K_{1A}(1^3P_1)$-$K_{1B}(1^1P_1)$ mixing, or alternatively the so called K_1 mixing, the method to apply sum rules to axial vector K_1 states is discussed.

Instead of decays into physical states, starting with the decays into ideal states (G-parity eiegen states), the form factors of $\langle K_{1(A,B)}|J_\mu|B\rangle$ matrix elements are defined. The matrix elements are re parameterized and their connections to the ones in literature are also presented. Starting with axial vector and tensor interpolating currents, which only couple to K_{1A} and K_{1B} states respectively in $SU(3)$ limit, the transition form factors of the matrix elements $\langle K_{1A}|J_\mu|B\rangle$ and $\langle K_{1B}|J_\mu|B\rangle$ are found. The results for these form factors are fitted to functions coinciding in the region $-10GeV^2 \leq q^2 \leq -2GeV^2$. The results for form factors are explored to physical region and their q^2 dependencies are shown explicitly. Hence contributions of non-Landau type singularities in the region $q^2 > 0$ to spectral densities are eliminated. It is shown that the form factors of $\langle K_{1A}|J_\mu|B\rangle$ and $\langle K_{1B}|J_\mu|B\rangle$ matrix elements are opposite in sign, in agreement with the ones found by applying light-cone QCD sum rules in literature.

Then, the form factors of $B \to K_1(1270)\ell^+\ell^-$ and $B \to K_1(1400)\ell^+\ell^-$ transitions are obtained following the definition for $\mathcal{M}_\theta$, the K_1-mixing matrix. For the form factors of

$B \to K_1(1270, 1400)\ell^+\ell^-$ decays, the θ_{K_1} dependance of the form factors are analyzed. It is shown that for some regions in the predicted θ_{K_1} region, some of the form factors are changing their signs. As a result it is concluded that the mixing angle θ_{K_1} should be more investigated.

Finally, the branching fractions $B \to K_1(1270)\ell^+\ell^-$ transitions with final lepton pairs being e^+e^-, $\mu^+\mu^-$ and $\tau^+\tau^-$ are estimated. It is found that branching fractions of $B \to K_1(1270)\ell^+\ell^-$ decays are bigger than $B \to K_1(1400)\ell^+\ell^-$ decays, as expected. The results found for branching ratios can be confirmed in forthcoming B experiments like LHCb in LHC and SuperB in ILC.

The results found in chapter 4 are published in:

- Hüseyin Dağ, Altuğ Özpineci and Mehmet T. Zeyrek, *"The Semileptonic B to* $K_1(1270, 1400)$ *in QCD Sum Rules"*, submitted to PRD, arXiv:1001.0939 [hep-ph].

REFERENCES

[1] M. A. Shifman, A. I. Vainshtein, V. I. Zakharov, Nucl. Phys. **B147** (1979) 385.

[2] V.A. Novikov, L. B. Okun, M. A. Shifman, A. I. Vainshtein, M. B. Voloshin and V. I. Zakharov, Phys. Rept. **41** (1978) 1.

[3] V.A. Novikov, M. A. Schifman, A. I. Vainshtein, V. I. Zakharov, *Fortsch. Phys.***32**, 585, 1985.

[4] M. A. Shifman, "Vacuum structure and QCD sum rules", North-Holland, 1992.

[5] B. L. Ioffe, in "The spin structure of nucleon", edited by B. Frois, V. W. Hughes, N. de Groot, World Scientific (1997), arXiv/hep-ph:9511401.

[6] V. M. Braun, Plenary talk given at " 4th International Workshop on Progress in Heavy Quark Physics", Rostock, Germany, 20-22 Sep 1997, arXiv: hep-ph/9801222 (1998).

[7] G. P. Lapage, Proceedings of HUGS 98, edited by J.L. Goity, World Scientific (2000).

[8] B. Holdom, M. Sutherland, Phys.Rev. **D47** (1993) 5067-5074.

[9] H-Y Cheng, C-K Chua, C-W Hwang, Phys.Rev. **D69** (2004) 074025.

[10] M. Beneke, G. Buchalla, M. Neubert, C.T. Sachrajda, Phys.Rev.Lett.**83** (1999)1914-1917.

[11] M. Jamil Aslam, Riazuddin, Phys.Rev. **D72** (2005) 094019.

[12] Gilberto Colangelo, Gino Isidori, Lectures given at at the 2000 LNF Spring School, Frascati, Italy, 15-20 May 2000,[arXiv:hep-ph/0101264].

[13] S. Hong, S. Yoo, M. J. Strassler, JHEP 0604 (2006) 003.

[14] M. A. Shifman, Prog. Theor. Phys. Suppl. **131**,1,1998.

[15] A.V. Radyushkin, Published in " Strong Interactions at Low and Intermediate Energies", Proceedings of the 13th Annual HUGS at CEBAF, 26May-12 June 1998; Edited by J.L. Goity, World Scientific (2000) pp. 91-150, arXiv:hep-ph/0101227.

[16] E. D. Rafael, Published in " Les Houches 1997, Probing the standard model of particle interactions", Pt. 2 1171-1218, arXiv:hep-ph/9802448.

[17] D. B. Leinweber, Annals of Physics **254**,328(1997).

[18] L. J. Reinders, H. Rubinstein and S. Yazaki, Phys.Rept. **41**1(1985).

[19] S. Narison and E. de Rafael, Phys. Lett. **B 103**, 57(1981).

[20] P. Colangelo, A. Khodjamirian, "At the Frontier of Particle Physics: Handbook of QCD" ed. by M. Shifman (World Scientific, Singapore, 2001), V. 3,1995.

[21] A. Ozpineci, Ph.D. thesis, Submitted to the Graduate School of Natural and Applied Sciences of the Middle East Technical University, September (2001).

[22] A. Ozpineci, Lectures given in ”Lectures on QCD sum rules”, September 2009, Feza Gursey Institiute, Istanbul Turkey.

[23] K. Azizi, Ph.D. thesis, Submitted to the Graduate School of Natural and Applied Sciences of the Middle East Technical University, March (2009).

[24] B. Aubert *et al.* [BABAR Collaboration], Phys. Rev. D **70**, 112006 (2004) [arXiv:hep-ex/0407003].

[25] M. Nakao *et al.* [Belle Collaboration], Phys. Rev. D **69**, 112001 (2004) [arXiv:hep-ex/0402042].

[26] T. E. Coan *et al.* [CLEO Collaboration], Phys. Rev. Lett. **84**, 5283 (2000) [arXiv:hep-ex/9912057].

[27] H. Yang, *et al*, Belle Collaboration, Phys. Rev. Lett. **94**, 111802 (2005).

[28] A. Ishikawa *et al.* [Belle Collaboration], Phys. Rev. Lett. **91**, 261601 (2003) [arXiv:hep-ex/0308044].

[29] B. Aubert *et al.* [BABAR Collaboration], Phys. Rev. D **73**, 092001 (2006) [arXiv:hep-ex/0604007].

[30] A. Ishikawa *et al.* [Belle Collaboration], Phys. Rev. Lett. **96**, 251801 (2006) [arXiv:hep-ex/0603018].

[31] B. Aubert *et al.* [BABAR Collaboration], arXiv:0804.4412 [hep-ex].

[32] B. Aubert *et al.* [BABAR Collaboration], arXiv:0807.4119 [hep-ex].

[33] K. Abe *et al.*, [BELLE Collaboration], BELLE-CONF-0411, arXiv:0408138[hep-ex].

[34] A Augusto Alves Jr *et al*, The LHCb Collaboration, JINST **3** S08005(2008).

[35] M-O Bettler *et al*, for the LHCb collabaration, CERN-LHCB-CONF-2009-038, LPHE-2009-05, arXiv:0910.0942[hep-ex].

[36] SuperB Collabaration, *SuperB: A High-Luminosity Asymmetric e^+e^- Super Flavor Factory. Conceptual Design Report*, INFN/AE - 07/2, SLAC-R-856, LAL 07-15, arXiv:0709.0451v2[hep-ex].

[37] K.-C. Yang, Phys.Rev.**D**78 (2008) 034018.

[38] H. Hatanaka, K.-C. Yang, Phys. Rev. **D 77** (2008) 094023.

[39] S. R. Choudnury, A. S. Cornell, N. Gaur, Eur.Phys.J.**C58**(2008)251-259, arXiv:0707.0446[hep-ph].

[40] V. Basihry, JHEP 0906(2009)062, arXiv:0902.2578[hep-ph].

[41] V. Bashiry, K. Azizi, arXiv:0903.1505[hep-ph]

[42] M. A. Paracha, I. Ahmed and M. J. Aslam, Eur. Phys. J. C **52**, 967 (2007), arXiv:0707.0733 [hep-ph].

[43] I. Ahmed, M. A. Paracha and M. J. Aslam, Eur. Phys. J. C **54**, 591 (2008), arXiv:0802.0740 [hep-ph].

[44] A. Saddique, M. J. Aslam and C. D. Lu, arXiv:0803.0192 [hep-ph].

[45] J. P. Lee, Phys. Rev. **D 74** (2006) 074001.

[46] Y. Sarac, H. Kim and S. H. Lee, Phys.Rev. D73 (2006) 014009.

[47] Z-G. Wang, Z-C. Liu and X-H. Zhang, Eur.Phys.J.C64:373-386,2009.

[48] J-R. Zhang and M-Q. Huang, arXiv/hep-ph:0905.4672, arXiv/hep-ph:0905.4178.

[49] W. Lucha, D. Melikhov, S. Simula, Phys.Rev. **D76**(2007)036002.

[50] W. Lucha, D. Melikhov, Phys.Rev. **D73** (2006) 054009.

[51] P. Ball, V. M. Braun, H. G. Dosch, Phys. Rev. D **44** (1991) 3567.

[52] F. Hanzel and A. D. Martin, *"Quarks and Leptons:An Introductory Course in Modern Particle Physics"*, John Wiley & Sons, 1984.

[53] J. F. Donoghue, E. Golowich and B. R. Holstein, *"Dynamics of the Standard Model"*, Cambridge University Press, Great Britain 1992.

[54] H. Hatanaka, K.-C. Yang, arXiv/hep-ph:0805.0329v3.

[55] H. Y. Cheng, C. K. Chua, Phys. Rev. **D 69** (2004) 094007.

[56] M. Suzuki, Phys. Rev. D **47**, 1252 (1993).

[57] H. Y. Cheng, C. K. Chua, Phys. Rev. **D 69** (2004) 074025.

[58] L. Burakovsky and T. Goldman, Phys. Rev. D **57**, 2879 (1998), arXiv:9703271[hep-ph].

[59] K.-C. Yang, Nucl.Phys.B776(2007)187-257.

[60] A. Ceccucci, Z. Ligeti, Y. Sakai, PDG, J. Phys. **G 33** (2006) 139.

[61] C. Amsler et al., Particle Data Group, Phys. Lett. B 667 1 (2008).

[62] A. J. Buras, M. Munz, Phys. Rev. **D 52** (1995) 186.

[63] B.L. Ioffe, Prog. Part. Nucl. Phys. **56**, 232(2006).

[64] T. M. Aliev, M. Savci, Phys. Lett. **B 434** (1998) 358.

[65] P. Colangelo, F. De Fazio, A. Ozpineci, Phys. Rev. **D72**, (2005) 074004.

[66] P. Colangelo, F. De Fazio, P. Santorelli and E. Scrimieri, Phys.Rev. **D53** (1996) 3672-3686.

[67] E. Barberio *et al*, HFAG(Heavy Flavor Averaging Group), arXiv:0809.1297v3[hep-ex]

[68] T. Iijima, *"Rare B decays"*, Talk given in *Lepton-Photon 2009: XXIV. International Symposium on Lepton Photon Interactions at High Energies*, August 2009, Hamburg, Germany;
Also the results appear at HFAG website,
"`http://www.slac.stanford.edu/xorg/hfag`".

VITA

Hüseyin Dağ was born in Sakarya, Turkey, in 1979. He received his BS degree in physics at Midle East Echnical University(METU) in Ankara, Turkey, in 2001. Having completed the BS program, he started MS studies at physics department of METU, Ankara, Turkey and received his MS degree in mathematical physics in 2003. He started his Ph.D. studies in high energy physics at METU, in 2003.